

SCALE-UP STUDIES FOR PHOTOBIOLOGICAL PRODUCTION OF
HYDROGEN

A THESIS SUBMITTED TO
THE GRADUATE SCHOOL OF NATURAL AND APPLIED SCIENCES
OF
MIDDLE EAST TECHNICAL UNIVERSITY

BY

DİLAN SAVAŞTÜRK

IN PARTIAL FULFILLMENT OF THE REQUIREMENTS
FOR
THE DEGREE OF MASTER OF SCIENCE
IN
CHEMICAL ENGINEERING

JULY 2019

Approval of the thesis:

**SCALE-UP STUDIES FOR PHOTOBIOLOGICAL PRODUCTION OF
HYDROGEN**

submitted by **DİLAN SAVAŞTÜRK** in partial fulfillment of the requirements for
the degree of **MASTER OF SCIENCE in CHEMICAL ENGINEERING**
Department, Middle East Technical University by,

Prof. Dr. Halil Kalıpçılar
Dean, Graduate School of **Natural and Applied Sciences**

Prof. Dr. Pınar Çalık
Head of Department, **Chemical Engineering**

Assist. Prof. Dr. Harun Koku Harun Koku
Supervisor, **Chemical Engineering, METU**

Examining Committee Members:

Prof. Dr. Pınar Çalık
Chemical Engineering Dept., METU

Assist. Prof. Dr. Harun Koku Harun Koku
Chemical Engineering, METU

Assoc. Prof. Dr. Eda Çelik-Akdur
Chemical Engineering Dept., Hacettepe University

Assoc. Prof. Dr. Can Özen
Biotechnology Dept., METU

Assist. Prof. Dr. Bahar İpek-Torun
Chemical Engineering Dept., METU

Date: 25.07.2019

I hereby declare that all information in this document has been obtained and presented in accordance with academic rules and ethical conduct. I also declare that, as required by these rules and conduct, I have fully cited and referenced all material and results that are not original to this work.

Name, Surname: Dilan Savařtürk

Signature:

ABSTRACT

SCALE-UP STUDIES FOR PHOTOBIOLOGICAL PRODUCTION OF HYDROGEN

Savaştürk, Dilan
MASTER OF SCIENCE, CHEMICAL ENGINEERING
Supervisor: Assist. Prof. Dr Harun Koku

July 2019, 140 pages

Photofermentative hydrogen production was performed with sugar sources (glucose, fructose or sucrose) utilized by *Rhodobacter capsulatus hup⁻* bacteria in both small-scale (indoor) and large-scale (outdoor) reactors. In small-scale experiments, the effect of carbon-to-nitrogen ratio (20, 50 and 80) on photofermentative hydrogen production was investigated with 10, 20 and 30mM glucose and fructose feedings. The highest production rates were obtained from 10 mM glucose and 10 mM fructose as 0.45 mol.m⁻³.h⁻¹ and 0.40 mol.m⁻³.h⁻¹, respectively. In the pilot-scale outdoor experiment, stacked tubular photobioreactor (20 L) with manifolds was used. The temperature was maintained around 30°C by a temperature controller. Molasses, side-product of sugar factory, was utilized as a sustainable and renewable feedstock by adjusting to 5 mM sucrose by dilution. The maximum productivity and conversion efficiency were found as 0.52 mol H₂.m⁻³.h⁻¹ and 54%, respectively. Compared to a previous study of our laboratory, photobioreactor design was improved and scaled-up to 20 L for an economically feasible hydrogen production. The decreased carbon to nitrogen ratio (C/N=13) reduced lag-period for hydrogen production and adaptation period, as observed in small-scale experiments. However,

low C/N ratio promoted cell-growth and thus light transmission was limited. Still, maximum productivity was found significantly higher ($0.47 \text{ mol H}_2\cdot\text{m}^{-3}\cdot\text{h}^{-1}$) than a similar study with a smaller reactor volume and this indicates that scale-up was successful. To the best of our knowledge, this study is the lowest C/N ratio applied in pilot-scale photofermentative hydrogen production.

Keywords: Photofermentation, *Rhodobacter Capsulatus*, Carbon-to-Nitrogen Ratio, Molasses, Scale-up

ÖZ

HİDROJENİN FOTOBİYOLOJİK ÜRETİMİ İÇİN ÖLÇEKLENDİRME ÇALIŞMALARI

Savaşürk, Dilan
Yüksek Lisans, Kimya Mühendisliği
Tez Danışmanı: Dr. Öğr. Üyesi Harun Koku

Temmuz 2019, 140 sayfa

Rhodobacter capsulatus hup⁻ bakterisinin kullandığı şeker kaynaklarıyla (glukoz, fruktoz veya sukroz) fotofermentatif hidrojen üretimi, hem küçük ölçekli (iç mekan) hem de büyük ölçekli (dış mekan) reaktörlerle yapıldı. Küçük ölçekli deneylerde, karbon-azot oranının (20, 50 ve 80) fotofermentatif hidrojen üretimi üzerindeki etkisi 10, 20 ve 30mM glukoz ve fruktoz beslemeleri ile incelendi. En yüksek üretim oranları 10 mM glukoz ve 10 mM fruktoz ile sırasıyla 0.45 mol.m⁻³.h⁻¹ ve 0.40 mol.m⁻³.h⁻¹ olarak elde edildi. Pilot ölçekli dış mekan deneyinde, manifoldlu istiflenmiş tübüler fotobiyoreaktör (20 L) kullanıldı. Sıcaklık, sıcaklık kontrol cihazı ile 30 ° C civarında tutuldu. Şeker fabrikasının yan ürünü olan melas, seyreltme ile 5 mM sukroza ayarlanarak sürdürülebilir ve yenilenebilir bir hammadde olarak kullanıldı. Maksimum üretkenlik ve verim sırasıyla 0.52 mol H₂.m⁻³.h⁻¹ ve % 54 olarak bulundu. Laboratuvarımızın önceki bir çalışmasına kıyasla, ekonomik olarak uygulanabilir hidrojen üretimi için fotobiyoreaktör tasarımı iyileştirildi ve 20 litreye ölçek büyütüldü. Azaltılmış karbon/azot oranı (C/N = 13), küçük ölçekli deneylerde gözlemlendiği gibi, hidrojen üretimi ve adaptasyon süresi için gecikme periyodunu azalttı. Ancak, düşük C/N oranı hücre çoğalmasını destekledi ve bu yüzden ışık geçirgenliği kısıtlandı. Yine de, maksimum üretkenlik daha küçük bir reaktör

hacmine sahip benzer çalışmadan önemli ölçüde olarak daha yüksek bulundu ($0.47 \text{ mol H}_2 \cdot \text{m}^{-3} \cdot \text{h}^{-1}$) bu, ölçek büyütmenin başarılı olduğunu gösterir. Bildiğimiz kadarıyla bu çalışma pilot ölçekli fotofermentatif hidrojen üretiminde uygulanan en düşük C/N oranıdır.

Anahtar Kelimeler: Fotofermentasyon, *Rhodobacter Capsulatus*, Karbon-Azot Oranı, Melas, Ölçek Büyütme

To my family,

ACKNOWLEDGEMENTS

I would like to gratitude to my supervisor Asst. Prof. Dr. Harun Koku for his support, guidance, suggestions and motivation throughout this research.

I am thankful to Prof. Dr. İnci Eroğlu and Prof. Dr. Meral Yücel for their recommendations on biological systems.

I would like to give my special thanks to Emine Kayahan and Emrah Sağır who contributed considerably to this study with their support and advice. Especially, I am grateful to Emrah Sağır for his help in small-scale experiments and to Emine Kayahan for her help in large-scale experiments.

I would like to thank to Muazzez Gürkan and Siamak Alipour for their help and advices in this study. I am thankful to my labmate Betül Oflaz for her help and friendship. I thank to Ayhan İldam and Kazım Yılmaz who work in İldam Cam for their help on the glass reactor. I also thank to İsa Çağlar, who works in the Chemical Engineering Workshop.

Lastly, I am grateful to my family, Hakan Savaştürk and Saliha Savaştürk, for their endless support, faith and love. I also thank to Çağdaş Ata for his motivation, support and love.

This study was supported by the Scientific and Technological Research Council of Turkey (TUBITAK) as project numbered ‘114M436’.

TABLE OF CONTENTS

ABSTRACT	v
ÖZ	vii
ACKNOWLEDGEMENTS	x
TABLE OF CONTENTS	xi
LIST OF TABLES	xv
LIST OF FIGURES	xvii
CHAPTERS	
INTRODUCTION	1
2.1. Hydrogen as an Energy Carrier	7
2.2. Biohydrogen Production Methods.....	12
2.2.1. Biophotolysis	13
2.2.1.1. Direct Biophotolysis	13
2.2.1.2. Indirect Biophotolysis	14
2.2.2. Photofermentation.....	14
2.2.3. Dark fermentation	17
2.2.4. Sequential dark and photofermentation	20
2.2.5. Combined dark and photofermentation	22
2.3. General Characteristics of Purple non-sulphur Bacteria	23
2.4. Parameters Affecting Photofermentative Hydrogen Production.....	24
2.4.1. Temperature	24
2.4.2. pH.....	26
2.4.3. Substrate Type and Concentration.....	26

2.4.4. C/N Ratio.....	27
2.4.5. Light Intensity and Distribution	30
2.4.6. Metal Ion Addition	32
2.4.7. Inoculum age of PNS bacteria in hydrogen production media	33
2.5. Photobioreactors for Hydrogen Production	34
2.5.1. Immobilized-cell Photobioreactors	35
2.5.2. Suspended-cell Photobioreactors	36
2.5.2.1. PanelPhotobioreactors	36
2.5.2.2. TubularPhotobioreactors.....	38
3.1. The Bacterial Strain	43
3.2. Culture Media	43
3.2.1. Solid Media	43
3.2.2. Growth Media.....	44
3.2.3. Sucrose Adaptation Media for Pilot-scale Outdoor Experiment.....	44
3.2.4. Hydrogen Production Media for Small-scale Indoor Experiments	44
3.2.5. Hydrogen Production Media for the Pilot-scale Outdoor Experiment.....	44
3.2.6. Storage Media.....	45
3.3. Experimental Set-up and Procedure.....	45
3.3.1. Pretreatment Procedure	45
3.3.2. Small-scale Indoor Experiments	47
3.3.3. Pilot-scale Outdoor Experiments.....	48
3.3.3.1. Construction: Stacked U-tube Photobioreactor	49
3.3.3.2. Start-up: Leakage Test, Sterilization and Inoculation	52
3.3.3.3. Operation: Feeding and Sampling	53

3.4. Analyses and Measurements	53
3.4.1. Temperature	53
3.4.2. Light Intensity	54
3.4.3. pH.....	54
3.4.4. Cell Concentration	54
3.4.5. Molasses.....	55
3.4.6. Sugar and Organic Acids	55
3.4.7. Gas Composition.....	56
3.5. Data Analysis and Calculations	56
3.5.1. Substrate Conversion Efficiency (Yield)	56
3.5.2. Hydrogen Productivity	57
4. RESULTS AND DISCUSSION	59
4.1. Indoor Small-Scale Photobioreactors	59
4.1.1. Experiments with <i>R. capsulatus</i> hup ⁻ on 10, 30 and 50 mM Glucose	60
4.1.1.1. Glucose and Organic Acid Concentrations	60
4.1.1.2. Growth and Hydrogen Productivity	67
4.1.2. Experiments with <i>R. capsulatus</i> hup ⁻ on 10, 30 and 50 mM Fructose	69
4.1.2.1. Fructose and Organic Acid Concentrations	70
4.1.2.2. Growth and Hydrogen Productivity	74
4.1.3. Comparison of Productivities with Other Small-scale Studies.....	78
4.2. Outdoor Pilot-Scale Stacked U-Tube Photobioreactor	79
4.2.1. C/N Ratio Selection	79
4.2.2. Diameter Selection.....	80
4.2.3. Solar Irradiation and Temperatures	83

4.2.4. Light Distribution in the Photobioreactor	84
4.2.5. Sucrose Concentration and Feeding Strategy.....	87
4.2.6. Organic Acid Concentrations and pH	88
4.2.7. Growth and Hydrogen Productivity	91
4.2.8. Comparison of Productivities with Other Outdoor Studies.....	96
5. CONCLUSION	99
REFERENCES	103
A. Composition of the Growth Media.....	117
B. Molasses Analyses	119
C. HPLC Calibration Curve of Sucrose	122
D. Sample HPLC and GC Chromatogram	123
E. Indoor and Outdoor Experimental Data	125
a. HPLC DATA.....	125
b. UV Spectrophotometer Data	127
c. pH Data.....	130
d. Gas Chromatography Data	133
e. Weather Station Data.....	135

LIST OF TABLES

TABLES

Table 2.1. CO ₂ generation from various fuels [42].	9
Table 2.2. Classification of hydrogen production methods [44].	11
Table 2.3. The advantages and disadvantages of biophotolysis, photofermentation and dark fermentation processes [45].	19
Table 3.1. Carbon-to-nitrogen (C/N) ratios of the runs for the small-scale experiments.	48
Table 4.1. C/N ratio, sugar type and concentrations of the runs.	60
Table 4.2. Substrate conversion efficiencies (% yields) for 10mM (R2g), 30mM (R4g) and 50mM (R6g) glucose feedings at start-up.	61
Table 4.3. The carbon balance for 30 mM glucose (C/N=50).	64
Table 4.4. Substrate conversion efficiencies (yields) for 10mM (R1f), 30mM (R3f) and 50mM (R5f) fructose feedings at start-up.	70
Table 4.5. Comparison of productivities with other small-scale studies (in glass bottles) with <i>R. capsulatus</i> hup- in batch mode.	78
Table 4.8. Summary of results and comparison with the 9L volume study.	96
Table 4.9. Comparison of the outdoor studies conducted with <i>R. capsulatus</i> hup-bacteria.	97
Table 0.1. Growth Media Component	117
Table 0.2. Vitamin Solution Component	117
Table 0.3. Trace Element Solution.	118
Table 0.4. Iron Citrate Solution (50X)	118
Table 0.5. Molasses analysis produced in Ankara Sugar Factory in 2013.	119
Table 0.6. The content of amino acid in molasses	120
Table 0.7. Analysis of the some elements in molasses.	121

Table 0.8. Daily variation in total and individual organic acids and sugar (glucose, fructose or sucrose) concentrations for indoor and outdoor experiments.....	125
Table 0.9. Daily variation in OD and cell concentration for indoor and outdoor experiments.....	127
Table 0.10. Daily variation in pH for indoor and outdoor experiments	130
Table 0.11. Biogas production during (a) indoor and (b) outdoor experiments.....	133
Table 0.12. Data taken from the weather station for the outdoor experiment (8/13/2016).	135

LIST OF FIGURES

FIGURES

Figure 2.1. The distribution of energy sources in 1973 and 2016 [37]. 1.Including solar, geothermal, wind, wave, heat and other 2.Oil shale and peat are aggregated with coal.	7
Figure 2.2. Carbon dioxide in the atmosphere according to a base case scenario[42].	9
Figure 2.3. World energy consumption by different energy sources (U. S. Energy Information Administration - IEO (2017)).	10
Figure 2.4. Photofermentative hydrogen production mechanism by PNS bacteria (Androga et al., 2012).	16
Figure 2.5. A immobilized-cell photobioreactor in A) indoor and B) outdoor conditions (Sagir et. al, 2017).	35
Figure 2.6. Panel type photobioreactors (4L) with internal cooling system in outdoor conditions.	37
Figure 2.7. The types of tubular photobioreactors (Dasgupta et al. 2010).....	39
Figure 2.8. A stacked U-tube photobioreactor with internal cooling by manifolds in outdoor conditions.....	40
Figure 3.1. The experimental procedures of small-scale and large-scale experiments.	46
Figure 3.2. A photograph of small-scale bioreactors for glucose runs.	47
Figure 3.3. Process flow diagram of the stacked U-tube photobioreactor. T1, T2, T3 and T4 are temperature probes. V1, V2 and V3 are ball valves. V4 and V5 are check valves (1/3 psi). CW-in and CW-out are cooling water inlet and outlet in manifolds, respectively.	49
Figure 3.4. A photograph of (a) stacked U-tube photobioreactor (b) inlet manifold performed with <i>R. capsulatus</i> hup- on molasses. CW-in and CW-out are coolant water inlet and outlet, respectively. The experiment started on August 7 th , 2016.	52

Figure 4.1.Daily change in glucose concentration for 10, 30 and 30 mM glucose feedings.....	61
Figure 4.2.(a) Daily variations of the total organic acids (b) pH change during biogas production for 10, 30 and 30 mM glucose feedings.	63
Figure 4.3.Daily change in organic acid concentrations for (a) R2g (10mM Glucose), (b) R4g (30mM Glucose) and (c) R6g (50mM Glucose).	66
Figure 4.4.Change in cell concentration in gram dry cell weight over liter culture (g/L) with respect to time for 10, 30 and 30 mM glucose feedings.....	67
Figure 4.5.Total produced hydrogen for 10, 30 and 50 mM glucose having C/N ratio of 20, 50 and 80, respectively.....	68
Figure 4.6.Daily change in fructose concentration for 10, 30 and 30 mM fructose feedings.....	70
Figure 4.7.Daily variations of the total organic acids (b) pH change during biogas production for 10, 30 and 30 mM fructose feedings.	71
Figure 4.8.Daily change in organic acid concentrations for (a) R1f (10mM Fructose) (b) R3f (30mM Fructose) and (c) R5f (50mM Fructose).	73
Figure 4.9.Change in cell concentration in gram dry cell weight over liter culture (g/L) with respect to time for 10, 30 and 30 mM fructose feedings	74
Figure 4.10.A simplified overall scheme of the carbon metabolism in PNS bacteria. (Koku et al., 2002).	76
Figure 4.11.Total produced hydrogen for 10, 30 and 50 mM fructose feedings.	77
Figure 4.13.(a) Schematic representation of the regions in the tubes.(b) The thickness of optimal, feasible and dark region (cm) in the tube during the experiment. Tube radius is 2 cm.	86
Figure 4.14.Sucrose concentration change during the experiment. Sucrose contained molasses were fed on the 7th, 11th and 16th days as shown by the arrows. On the feeding days, the sucrose concentration values measured approximately 3-4 hours after feeding.	87
Figure 4.15.Daily variation in (a) individual organic acid concentration and (b) total organic acid concentration and pH during the experiment.	90

Figure 4.16.Daily variation in cell concentration of this study and a previous study having higher C/N value (35) and a lower reactor volume (9L) [17].	91
Figure 4.17.Comparison of the hydrogen productivity of the current study with a previous study [17] with the smaller volume (9L) and higher C/N ratio (35).	92
Figure 4.18.Daily variation in the hydrogen productivity and average solar irradiance.....	94
Figure 4.19.Percent hydrogen in the produced gas during the experiment. The rest of the produced gas is carbon dioxide.	95
Figure 0.1.Calibration Curve for Sucrose	122
Figure 0.2.HPLC Chromatogram for organic acids. Retention times for lactic acid, acetic acid and formic acid are 21.6, 24.0 and 26.7 min, respectively (August 10 th , 2016).	123
Figure 0.3.HPLC Chromatogram for sucrose. Retention time for sucrose is 15.0 min (August 10 th , 2016).	123
Figure 0.4.GC Chromatogram for produced biogas (August 10 th , 2016)	124

CHAPTER 1

INTRODUCTION

Hydrogen as an energy carrier is a promising alternative to fossil fuels because it has the highest energy content per mass (142 kJ/g) of any fuel. The most environmental-friendly way of the hydrogen production is biological hydrogen production because renewable feedstock can be used and biodegradable wastes are produced as final products.

The main biological hydrogen production methods can be classified as biophotolysis, photofermentation and dark fermentation (Manish and Banerjee 2008; Wu et al. 2012; Sinha and Pandey 2011; Das, Nejat, and Glu 2001). Among these methods, photofermentation has advantages of utilizing sun as a renewable energy source and utilizing complex nutrient media due to variety of photofermentative organisms (Sakurai et al. 2013; Hallenbeck and Liu 2016). The critical parameters of photofermentative hydrogen production are temperature, substrate type and concentration, pH, C/N ratio, light intensity and distribution, metal ion addition and inoculum age of the bacteria. Higher hydrogen productivities can be obtained with optimization of these parameters (Androga, Özgür, et al. 2011; Uyar et al. 2007; Barbosa et al. 2001; Krujatz et al. 2015). Bacterial growth has been observed between pH values of 6 and 9 and the maximum hydrogen productivity was observed at pH= 7 (K. Sasikala, Ramana, and Raghuveer Rao 1991). In a previous study, the optimum temperature for photofermentative hydrogen production was suggested between 30°C - 40°C and the maximum hydrogen productivity was observed at 27.5 °C (Androga et al. 2014). Cell growth of *Rhodobacter sphaeroides* O.U. 001 bacteria was not observed below 20°C or above 45°C (Androga et al. 2014).

In photofermentative hydrogen production studies, various pure substrates such as organic acids (e.g. acetic acid, lactic acid) and sugars (i.e. sucrose, glucose and fructose) have been utilized (Barbosa et al. 2001; Sagir, Alipour, et al. 2017; Özgür, Afsar, et al. 2010). Previously, while the maximum hydrogen yields were obtained as 0.56 mol H₂/mol glucose with *R. sphaeroides* (Fang et al., 2006) and 0.9 mol H₂/mol glucose with *Rubrivivax gelatinosus* (Li and Fang, 2008), it was found as 3.3 mol H₂/mol glucose for *R. capsulatus* under similar conditions (Abo-Hashesh et al., 2011), which is significantly higher.

In a previous study, photobioreactor (PBR) operated with the photosynthetic *R. capsulatus* JP91 (*hup⁻*) bacteria and the highest yield was found as 9.0 ± 1.2 mol H₂ / mol glucose (Abo-Hashesh, Desaunay, and Hallenbeck 2013). According to these results, single-stage photofermentative hydrogen production by utilizing glucose was reported as more promising than co-culture or two stage photofermentation processes, because considerably high hydrogen yields were obtained. On the other hand, for the large-scale outdoor operations, wastes and side products are more preferable compared to pure substrates for sustainable and economically feasible processes. In particular, the by-products of sugar factories (e.g. molasses, thick juice dark fermenter effluent (DFE)) have been used in photofermentative biohydrogen production studies under outdoor conditions and have yielded promising results (Boran et al. 2012b). Molasses and thick juice DFE are mainly composed of sucrose that is around 30-60% by weight. DFE also contains short chain organic acid mixture (e.g. acetate, lactate), besides sucrose. By using molasses directly rather than DFE as feedstock, the complexity of two-stage biohydrogen production can be eliminated (dark fermentation of thick juice followed by photofermentation of DFE of thick juice) (Keskin and Hallenbeck 2012; Kayahan, Eroglu, and Koku 2017; Sagir, Ozgur, et al. 2017). Furthermore, sucrose allows higher theoretical hydrogen yield because sucrose has higher hydrogen content compared to short chain organic acids.

Biological hydrogen production by purple non-sulfur (PNS) bacteria is promising for large-scale operations because these bacteria are able to utilize various carbon

sources including waste products (Shi and Yu 2006). PNS bacteria are able to utilize sugars (e.g. glucose, fructose and sucrose) as carbon sources in photofermentative hydrogen production under anoxygenic conditions. Therefore, purple non-sulfur bacteria are commonly used in photofermentative biohydrogen production. There are various PNS bacteria used in photofermentative biohydrogen production and among them *Rhodobacter capsulatus hup⁻* (YO_3) bacteria, which was modified from wild type by deleting the hydrogen uptake enzyme, was found to result in higher hydrogen yields (Öztürk et al., 2006). In previous studies, *R. capsulatus hup⁻* was found to result in very stable and robust in outdoor experiments when molasses was utilized (Kayahan, Eroglu, and Koku 2017; Savasturk, Kayahan, and Koku 2018).

In photofermentative hydrogen production, nitrogenase enzyme is primary catalyst and thus the factors that affect the nitrogenase activity have a strong impact on biohydrogen production (Vignais et al. 1985). In the culture medium, presence of oxygen inactivates nitrogenase irreversibly and ammonium inhibits activity of nitrogenase (Jones and Monty 1979; Gest, Kamen, and Bregoffs 1949). Furthermore, nitrogen sources other than ammonium can also lead to ammonium inhibition indirectly such that when lactate is produced before glutamate in photofermentation of *R. capsulatus*, ammonia is formed inhibiting nitrogenase (H. Koku et al. 2002). The carbon-to-nitrogen (C/N) ratio is a critical parameter affecting the photofermentative hydrogen production because of the complex interactions between nitrogen sources and nitrogenase enzyme (Androga, Özgür, et al. 2011). While nitrogen leads hydrogen-producing populations to be formed earlier by promoting cell growth, high levels of nitrogen containing substrates (i.e. low C/N ratios) can inactivate nitrogenase leading a decrease in the hydrogen production. Because of these competing effects, the optimum C/N ratios found in literature varies between 13 and 35 depending on operational conditions such as bacterial cultures, carbon sources and illumination (Androga, Özgür, et al. 2011; Sagir, Alipour, et al. 2017; Avcioglu 2010; Boran et al. 2010). In literature, various types of carbon sources (e.g. organic acids and sugars) and nitrogen sources (e.g. glutamate, yeast extract,

ammonium chloride) have been used by PNS bacteria (Kayahan, Eroglu, and Koku 2017; Savasturk, Kayahan, and Koku 2018; Özgür, Mars, et al. 2010; Uyar et al. 2009). It was shown in the studies with *R. sphaeroides* that when the same C/N ratio were utilized with different substrates, although the maximum cell concentrations were nearly the same, the maximum productivities and lag times of hydrogen production were found different (Uyar et al. 2009). Therefore, the type of carbon source is a critical factor affecting the hydrogen productivity, even for the same C/N ratio. Previously, lactic acid, acetic acid and glutamate at different concentrations were utilized leading the C/N ratios of 13, 15.25, 21 and 56.25 (Avcioglu 2010). According to the results, the highest hydrogen yield and productivity were achieved as 32% and 0.12 mmol H₂/L.h for the lowest C/N ratio (C/N=13), respectively. In another previous study, hydrogen production from acetic acid by *R. capsulatus* was conducted at different C/N ratios (C/N=15,25, 35, 45 and 55) and the lag time of hydrogen production was found to be decreased at lower C/N ratios (Özgür, Uyar, et al. 2010). Therefore, utilizing lower C/N ratios can be tested in large-scale outdoor experiments to increase the hydrogen productivity and decrease lag time for the hydrogen production.

A continuous decrease in pH is a commonly observed trend during photofermentation of all bacteria types with simple and complex sugars utilized as carbon sources (Boran et al. 2012a; Sagir, Alipour, et al. 2017; Kayahan, Eroglu, and Koku 2017; Savasturk, Kayahan, and Koku 2018) due to organic acid secretion in the photofermentative metabolism (Keskin et. al, 2012). The recommended methods to compensate the subsequent pH drop are using buffer solutions and slightly increasing the initial pH of the liquid media. It was also recommended to keep the concentration of sucrose below 5mM in the feeding, because higher sucrose concentrations can result in rapid acidification (Kayahan, Eroglu, and Koku 2016). In a previous long-term outdoor study (75 days), the hydrogen production model was found as closely following the daily light intensity variation (Avcioglu et al. 2011). Furthermore, hydrogen production was found to increase with increasing light

intensity until reaching saturation at 270 W/m^2 in a controlled indoor study (Uyar et al. 2007).

Mainly, the photobioreactor (PBR) types are classified as suspended-cell PBRs and immobilized-cell PBRs (Zhang et al. 2010). Suspended-cell PBRs are more commonly used because they provide uniform light and mass distribution and it is easy to operate. Design of a photobioreactor is critical for hydrogen production to be sustainable and economically feasible in large-scale outdoor studies. An effective design should provide uniform light distribution and mixing, high illuminated surface area to ground area ratio, low hydrogen gas permeability and sufficient cooling system to maintain optimum temperature. To achieve the maximum illuminated surface area per ground area ratio, a reactor should be designed as compact (Gebicki et al. 2010). Previously, a compact tubular reactor meeting these demands was designed and called as “stacked U-tube photobioreactor” (Kayahan, Eroglu, and Koku 2016). With this design the ratio of illuminated surface area to the ground area was increased from 1:1 to 5:1 compared with typical horizontal tubular PBRs (Gebicki et. al, 2010). Furthermore, the cost of ground area, which may constitute up to 90% of the total photofermentative hydrogen production cost (Urbaniec and Grabarczyk 2014), was reduced. With further compact scale-up studies, the cost item can be reduced and more economical hydrogen production processes can be achieved. In a previous study of our laboratory, the light transmission for varying depths and different substrate (molasses) concentrations were analyzed with photon count and accordingly the tube radius was suggested as between 1.5-2 cm (Kayahan et. al, 2017).

The main objective of the present study was to scale-up a stacked U-tube PBR, improve the PBR design and test the pilot-scale PBR under outdoor conditions by utilizing molasses as feedstock. Compared to the previously designed reactor by our research group, the PBR liquid volume was scaled-up from 9 L to 20 L by increasing the radius of the reactor tubes from 1.5 cm to 2 cm. In addition, carbon to nitrogen (C/N) ratio was decreased from 35 to 13 to decrease the lag-time for hydrogen

production. This study enables a meaningful comparison with the results of the previous study, which was with 9 liters culture volume, because the same reactor type, bacterial culture and feedstock type were utilized by Kayahan et al. 2017. To the best of our knowledge, this is the largest pilot-scale outdoor study for photofermentative hydrogen production by utilizing molasses.

CHAPTER 2

LITERATURE SURVEY

2.1. Hydrogen as an Energy Carrier

The world energy demand is increasing due to increasing population and industrialization. Fossil fuels such as coal, oil and natural gas are the most common sources of energy used to meet this demand. As seen from Figure 2.1, 26.9%, 36.0% and 17.1% of energy is supplied from natural gas, oil and coal, respectively. That means 80% of the energy is supplied from fossil fuels in 2016. However, fossil fuels have limited reserves and may cause environmental and health problems due to the carbon emission, which causes greenhouse effect.

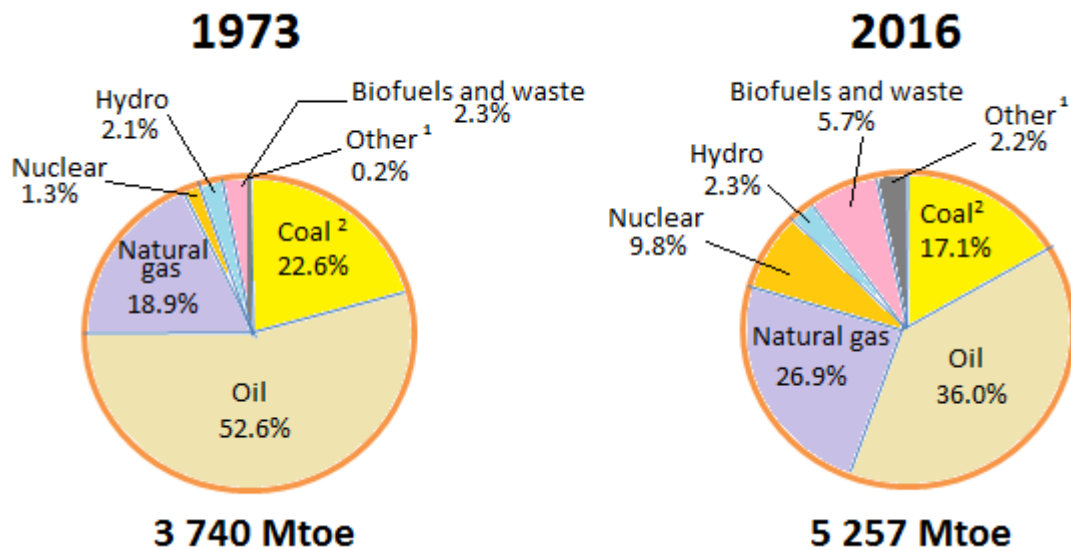


Figure 0.1. The distribution of energy sources in 1973 and 2016 (International Energy Agency 2017).

1. Including solar, geothermal, wind, wave, heat and other 2. Oil shale and peat are aggregated with coal.

Hydrogen, as an energy carrier, is promising due to its potential to be environmentally-friendly and sustainable. In addition, hydrogen as an energy carrier with the highest energy content per mass (142 kJ/g) of any fuel has 2.4, 2.8 and 4 times higher LHV (lower heating value) than methane, gasoline and coal, respectively (Marban and Valdes-Sois 2007).

Hydrogen can be separated from other substances containing hydrogen atoms, such as water, hydrocarbons and biomass. Hydrogen can be produced from fossil fuels (natural gas, oil and coal), renewable energy sources (such as solar, wind, hydro, biomass) and nuclear power (Holladay et al. 2009). Almost half of the hydrogen (48%) is produced from steam reforming of natural gas. The other main hydrogen production methods are partial oxidation of refinery oil (around 30%), coal gasification (18%) and water electrolysis (4%). Almost 96% of the total hydrogen production is from fossil fuels that produce greenhouse gases such as carbon dioxide, which causes global warming (Corbo, Migliardini, and Veneri 2011).

Although the main constituents of fossil fuels are carbon and hydrogen, combustion of fossil fuels produces various gases such as CO_x , SO_x and NO_x causing air pollution. The produced gases, which do not naturally exist in atmosphere or natural constituents of the atmosphere in extremely high concentrations, can be considered as air pollution. Air pollution caused by combustion of fossil fuels damages to human health, structures, animals and so on (Veziroğlu and Şahin 2008).

The amount of carbon dioxide generated from various fuels is shown in Table 2.1. While combustion of fossil fuels produces carbon dioxide, hydrogen from non-fossil energy does not. It has been predicted that with the introduction of hydrogen in 2000, maximum carbon dioxide in the atmosphere reaches at a maximum (520 ppm) before 2050 and then decreases (Figure 2.2). Otherwise, carbon dioxide continues to increase which indicates the importance of substituting hydrogen from non-fossil energy instead of fossil fuel (Momirlan and Veziroglu 2002).

Table 0.1. CO_2 generation from various fuels (Momirlan and Veziroglu 2002).

Fuel type	Chemical formula	Value (BTU/lb)	CO generated (lbs CO_2 /lb fuel)
Natural gas	CH_4	24000	2.75
Fuel oil and gasoline	$(CH_2)_n$	19600	3.14
Biomass (wood)	$(CH_2O)_n$	8000	1.47
H_2 from natural gas	H_2	61000	7.00
H_2 from coal liq.	H_2	61000	16.50
H_2 from non-fossil energy (Hydro, solar, nuclear)	H_2	61000	0

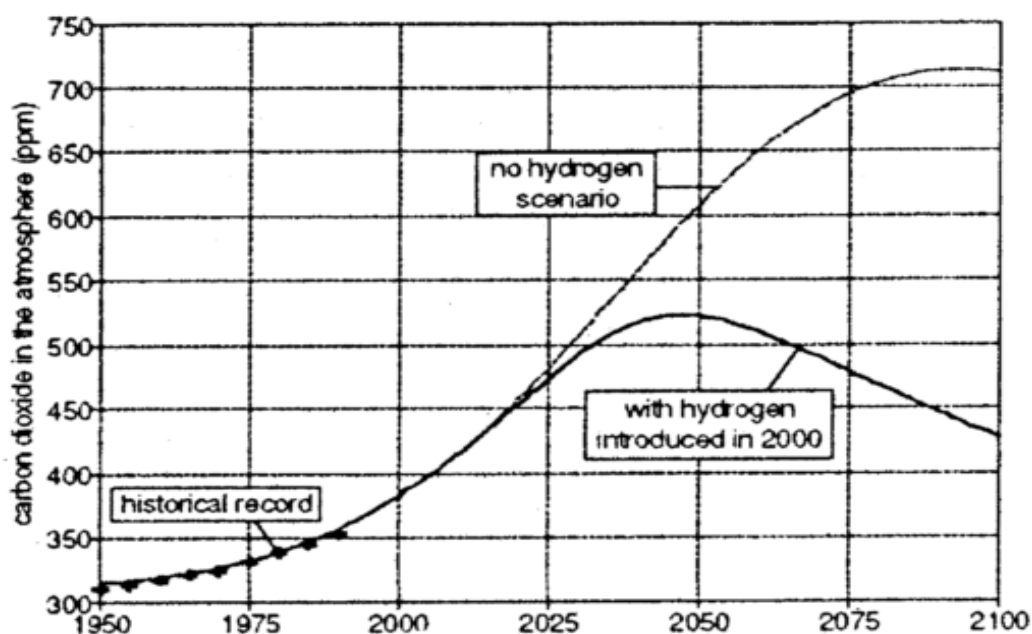


Figure 0.2. Carbon dioxide in the atmosphere according to a base case scenario (Momirlan and Veziroglu 2002).

Hydrogen can be produced using both renewable and non-renewable means. The interest in hydrogen production from renewable energy resources is increasing because it can be produced sustainably and in a clean manner, in contrast to fossil fuels. Renewable energy sources are promising alternatives to overcome the

problems of air pollution and global warming caused by fossil fuel combustion. The energy production from renewable sources is increasing in recent years and expected to continue to increase as seen from Figure 2.3.

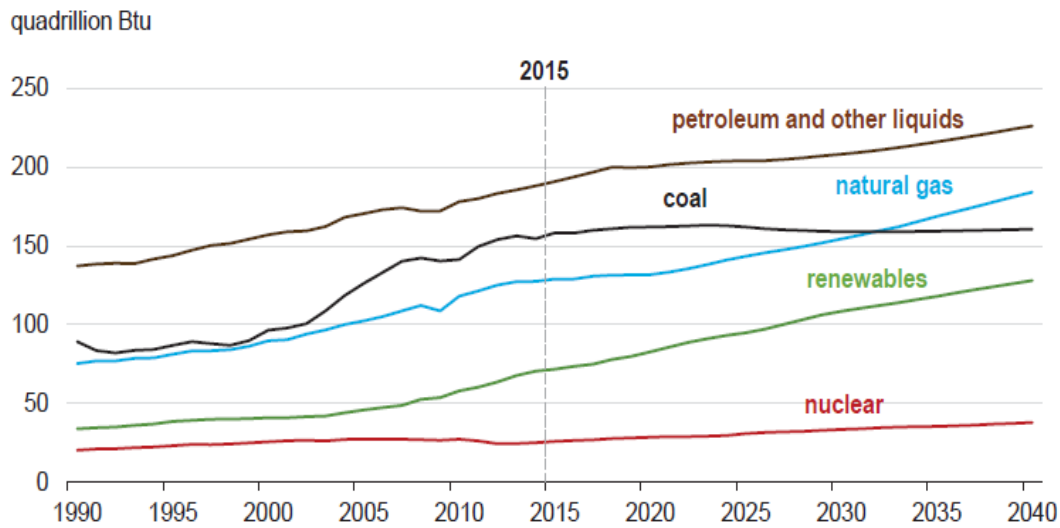


Figure 0.3. World energy consumption by different energy sources (EIA 2017).

Hydrogen is identified as one of the most promising fuels for future due to its potential to be clean and sustainable (Johnston, Mayo, and Khare 2005). Hydrogen production methods can be classified as electrical, thermal, hybrid and biological as shown in Table 2.2.

Table 0.2. *Classification of hydrogen production methods* (Dincer and Acar 2014).

Class	Method
Electrical	Plasma arc decomposition
	Electrolysis
Thermal	Thermolysis
	Thermochemical water splitting
	Biomass conversion
	Steam reforming
	Gasification
Hybrid	Photoelectrochemical
	Hybrid thermochemical water splitting cycles
	High temperature electrolysis
Biological	Biophotolysis
	Photofermentation
	Dark fermentation
	Sequential dark and photofermentation
	Combined dark and photofermentation

The most common biological hydrogen (biohydrogen) production methods can be classified as biophotolysis, photofermentation and dark fermentation (Table 2.2). Among these methods, photofermentation has the advantage of utilizing sun as a renewable source and various complex nutrient media can be utilized due to the metabolic variety of photofermentative organisms (Rahman et al. 2016).

2.2. Biohydrogen Production Methods

Biological hydrogen production is among the most environmental friendly way of hydrogen production because it allows the utilization of renewable feedstock and results in biodegradable waste.

Classification of biological hydrogen production processes is as follows (Rahman et al. 2016):

- Biophotolysis of water using green algae and blue-green algae (cyanobacteria)
 - Direct biophotolysis
 - Indirect biophotolysis
- Photofermentation
- Dark fermentation
- Sequential dark and photofermentation
- Combined dark and photofermentation

Biological hydrogen production methods substantially depend on the presence of hydrogen producing enzymes, which catalyze the reaction:



According to the literature, all known enzymes that have a capacity of hydrogen evolution contain complex metal clusters as the active sites. Nitrogenase, Fe-hydrogenase and NiFe-hydrogenase enzymes are presently known enzymes that are carrying out this reaction (Hallenbeck and Benemann 2002). Nitrogenase enzyme is used in photofermentation processes and Fe-hydrogenase enzyme is used in biophotolysis processes (Manish and Banerjee 2008). Biohydrogen production technologies are categorized as light dependent and light independent methods. Furthermore, biohydrogen production methods can be classified as heterotrophic, photoheterotrophic and photoautotrophic based on the different types of microorganisms used. Photofermentation (photoheterotrophic) and biophotolysis

(photoautotrophic) are light dependent whereas dark fermentation (heterotrophic) is light independent.

Biophotolysis is simply a hydrogen production mechanism in which water is separated into hydrogen and oxygen molecules by light energy. CO₂ is the carbon source found in cyanobacteria and microalgae (Ghirardi et al. 2000). Photofermentation is a biohydrogen production process in which organic compounds are decomposed into small molecules by photosynthetic bacteria in the presence of light (Azwar, Hussain, and Abdul-Wahab 2014). In photofermentation, the organic waste can be used as biomass by the photosynthetic bacteria. In this way, organic waste is reduced and it can be treated as a renewable energy source in photofermentation. The biological hydrogen production processes are described below.

2.2.1. Biophotolysis

Biophotolysis is described as splitting water into molecular hydrogen and oxygen with light energy by green algae and blue-green algae (cyanobacteria). The hydrogenase enzyme is inhibited by even small amount of oxygen leading a decrease in hydrogen production during biophotolysis reaction (Benemann et al. 2006). Most of the microalgae, especially green algae, produce hydrogen after hydrogenase enzyme is synthesized and activated where small amount of hydrogen is produced under anaerobic conditions in the dark. After this process, the adapted algae are exposed into light under anaerobic conditions, which often results a dramatic increase in hydrogen production rates. However, hydrogen evolution stops when normal photosynthesis is reestablished.

2.2.1.1. Direct Biophotolysis

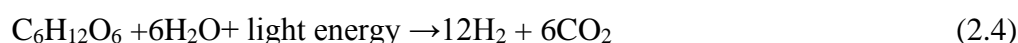
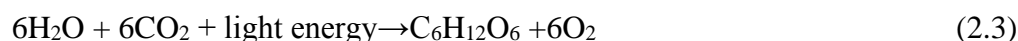
In direct biophotolysis, water is split and converted directly to hydrogen with solar energy as shown in Equation (2.1).



The main problem in direct biophotolysis is the extreme oxygen sensitivity of Fe-hydrogenase enzyme activity (Hallenbeck and Benemann 2002). The hydrogenase and nitrogenase enzymes are likely to be inactivated even at low partial pressures of oxygen. The hydrogen production rates were reported around 0.07 mmol/h.L in literature for direct biophotolysis (Kosourov et al. 2002; Melis et al. 2000).

2.2.1.2. Indirect Biophotolysis

Cyanobacteria have the ability to use CO₂ as a carbon source with solar energy (Equation 2.3). Then, cellular substances produced from CO₂ are used for H₂ production (Equation 2.4). The overall hydrogen production in cyanobacteria can be summarized by the following reactions:

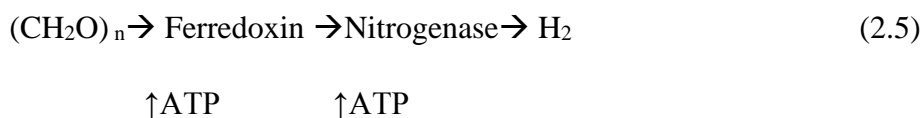


The main disadvantage of this method is that separation of hydrogen and oxygen is required which evolve in the overall reactions as shown in Equations 2.3-2.4 (Manish and Banerjee 2008). Furthermore, metabolic engineering is required to increase the hydrogen production efficiency since the photochemical efficiencies are low (Brentner, Jordan, and Zimmerman 2010). In indirect biophotolysis *Anabaena* strains have been frequently used in literature since they have relatively higher hydrogen production rates (Levin, Pitt, and Love 2004). The hydrogen production rates were reported around 0.355 mmol/h.L for indirect biophotolysis of *Anabaena variabilis* (Sveshnikov et al. 1997).

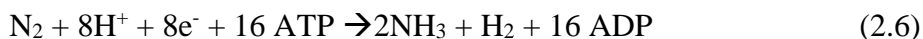
2.2.2. Photofermentation

Photosynthetic bacteria produce hydrogen gas using carbon sources (organic acids and sugars) and solar energy under anaerobic conditions. (Levin, Pitt, and Love 2004). The carbon sources are used as electron donors and transported to the nitrogenase enzyme by ferredoxin enzyme using ATP energy. The nitrogenase enzyme is able to reduce proton into the hydrogen using extra ATP energy with the

absence of nitrogen (Akkerman et al. 2002). The overall result of the biochemical pathways for photofermentative hydrogen production is shown as (Das, Nejat, and Glu 2001):



The enzyme nitrogenase is responsible from the hydrogen production for photofermentation. The nitrogen fixation reaction by nitrogenase enzyme to produce hydrogen is shown below (Androga et al. 2012).



Besides nitrogenase, hydrogenase is also a significant enzyme, which is responsible from oxidation and reduction of hydrogen. The types of hydrogenase enzyme are FeFe-hydrogenase, NiFe-hydrogenase and Fe-hydrogenase. While hydrogen is produced by FeFe-hydrogenase enzyme activities, it is consumed by NiFe-hydrogenase. (Androga et al., 2012). The photofermentative hydrogen production mechanism by PNS bacteria is shown in Figure 2.4. The generated electrons by oxidation of organic acids are transferred to Cyt c (cytochrome c) and then transferred to ferredoxin (Fd) by several electron transport proteins. Meanwhile, protons are transferred through the membranes forming a proton gradient. The proton gradient triggers the enzyme of ATP synthase and then ATP is produced. Finally, the electrons are moved to the nitrogenase by ferredoxin and thus molecular hydrogen is produced (Androga et al. 2012).

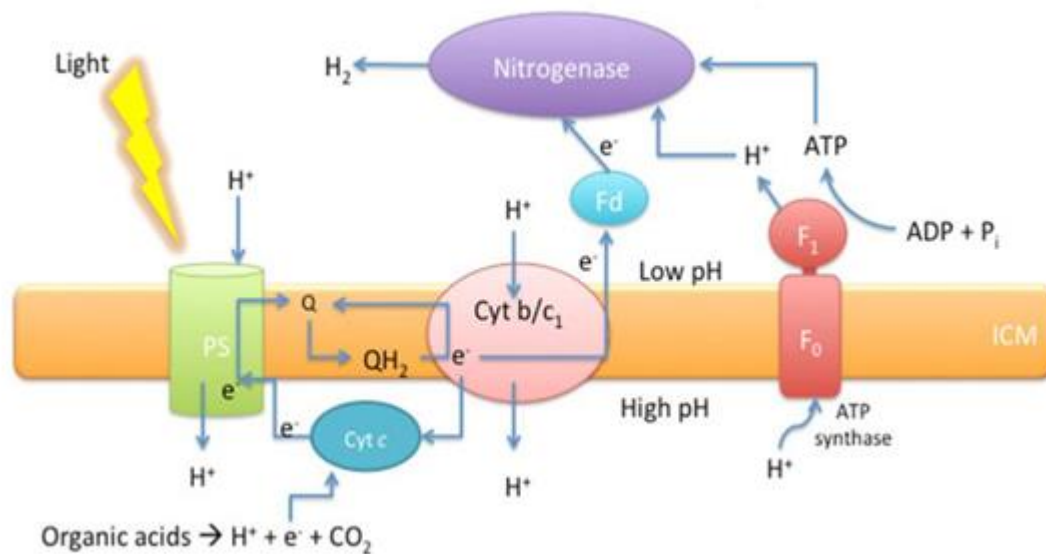
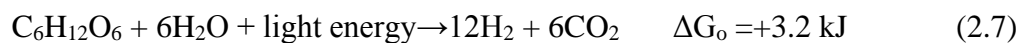


Figure 0.4. Photofermentative hydrogen production mechanism by PNS bacteria (Androga et al. 2012).

The hydrogen production pathway is affected mainly by three factors; the type of carbon source, availability of oxygen and presence of light. PNS bacteria can utilize various carbon sources such as short chain organic acids, sugars, alcohols and amino acids. The overall reaction of hydrogen production from glucose is shown below:



Carbon monoxide (CO) can also be used for hydrogen production by photosynthetic bacteria with a microbial shift reaction as shown below (Uffen 1976);



Productivity is defined as the amount of hydrogen produced (moles) per volume of the reactor (L) and duration (hour). The term of hydrogen productivity (rate of hydrogen production) allows comparing experimental results with the other studies found in literature. Another term to compare the results of biohydrogen production processes is the substrate conversion efficiency (yield). The yield is defined as the actual moles of hydrogen produced per the theoretical moles of hydrogen produced,

which is calculated by assuming all the consumed substrate (carbon source) is used for hydrogen production.

In literature, hydrogen production rates have been reported around 0.15 mol/m³.h for photofermentation (Manish and Banerjee 2008). Phototrophic bacteria are indicated in literature as one of the most promising microbial systems for biohydrogen production (Fascetti and D'addario 1998; Fascetti and Todini 1995). However, one of the main disadvantages of photofermentation is the presence of hydrogen uptake enzyme, which enables the reuse of some of the produced hydrogen by the bacteria (Das and Veziroglu 2008). In order to overcome this drawback, *R. capsulatus* bacterium was genetically modified by deleting hydrogen uptake enzyme and the mutant species was named as *R. capsulatus* YO₃ (*hup*⁻) by Ozturk et al. (2006) and hydrogen production efficiencies were found to be increased by deleting this enzyme. The other known disadvantages of photofermentation are inhibition of nitrogenase and Fe-hydrogenase enzymes by oxygen, a light source requirement and difficulties in scale-up (Das and Veziroglu 2008). On the other hand, there are many advantages of photofermentation and the major ones are listed below (Das, Nejat, and Glu 2001);

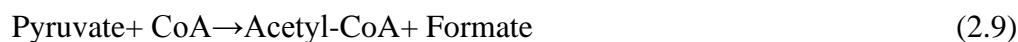
- There is a high theoretical substrate conversion yield.
- A large scale of the light energy spectrum can be utilized by the bacteria
- The oxygen evolving is less, which reduces the possibility of oxygen inactivation of the biological systems.
- Since consumed organic substrates can be obtained from wastes, there is a potential of waste treatment.

2.2.3. Dark fermentation

Another method of biohydrogen production is dark fermentation, where carbohydrate used as a substrate by anaerobic bacteria in the dark. The most of the hydrogen production depends on anaerobic pyruvate metabolism that is produced

during catabolism of substrates. The pyruvate degradation is catalyzed by one of the enzymatic reactions shown below (Hallenbeck and Benemann 2002);

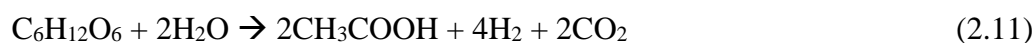
1. Pyruvate: formate lyase (PFL)



2. Pyruvate: ferredoxin oxidoreductase (PFOR)



Theoretically maximum four moles hydrogen per one mole glucose is produced in strict anaerobic bacteria (Equation 2.11), whereas maximum two moles hydrogen per one mole glucose can be obtained in facultative anaerobes (such as *Escherichia coli*).



The major advantage of dark fermentation method is that hydrogen can be produced by fermentative bacteria constantly during day and night by using organic substrates. In addition, fermentative bacteria can have a good cell growth rate (Das, Nejat, and Glu 2001). However, the major disadvantage of dark fermentation is low hydrogen yield are obtained with low hydrogen purity. Furthermore, the produced biogas from dark fermentation needed to be purified to obtain the hydrogen gas (Brentner et al. 2010). Although theoretically 12 moles of hydrogen gas can be produced from glucose, typically about one third of the theoretical maximum yields are obtained. As a result of these low yields, side products are produced in large amounts, which causes a problem of waste disposal (Hallebeck et al. 2014).

The advantages and disadvantages of biological hydrogen production by biophotolysis, photofermentation and dark fermentation processes are shown in Table 2.3.

Table 0.3. *The advantages and disadvantages of biophotolysis, photofermentation and dark fermentation processes (Rahman et al. 2016).*

Process	Advantages	Disadvantages
Biophotolysis ($2\text{H}_2\text{O} + \text{light} \rightarrow 2\text{H}_2 + \text{O}_2$)	Hydrogen is directly produced from water and sunlight. No nutrients needed for substrate. The only substrate is plenty of water.	Sunlight as a light energy source is limited by the day-night cycle. Other light sources cause additional costs. Relatively low light efficiencies are observed which causes low hydrogen yields and production rates.
Photofermentation ($\text{CH}_3\text{COOH} + 2\text{H}_2\text{O} + \text{light} \rightarrow 4\text{H}_2 + 2\text{CO}_2$)	A large scale of the light energy spectrum can be utilized by the bacteria. The substrate is an organic compound that can be converted completely to H_2 and CO_2 . Hydrogen can also be produced from renewable feedstock such as wastewater and side-products. High yields from substrate.	Sunlight as a light energy source is limited by the day-night cycle. Other light sources cause additional costs. Low production rates.
Dark fermentation ($\text{C}_6\text{H}_{12}\text{O}_6 + 2\text{H}_2\text{O} \rightarrow 2\text{CH}_3\text{COOH} + 2\text{CO}_2 + 4\text{H}_2$)	Highest hydrogen production rates. Hydrogen can be produced all day since light source is not needed. Various carbon sources can be used such as wastes.	Due to the low percentage of H_2 evolved, there is an additional cost resulting from the separation unit to separate the CO_2 and H_2 product mixture.

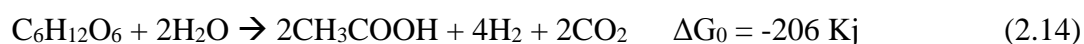
2.2.4. Sequential dark and photofermentation

Sequential dark and photofermentation systems consist of the dark fermentative bacterial cultures in combination with photofermentative cultures with carbohydrate rich substrates. This method consists of separate and sequential steps of dark fermentation and photofermentation processes rather than a single process as in the case of combined dark and photofermentation. The metabolic bacterial activities significantly change under dark fermentative and photofermentative conditions. The hydrogen production efficiency depends mainly on the enzyme types involved in the hydrogen production (Patel and Kalia 2013). The major enzymes that are involved in hydrogen production are hydrogenase and nitrogenase for dark fermentative process (Das and Veziroglu 2008). During the process of hydrogen production from substrates, some intermediate products are also produced such as volatile fatty acids (VFAs) and alcohols. In dark fermentative process, efficiency is governed by VFAs. For example, acetic acid production is expected to generate 4 moles of hydrogen while butyric acid production theoretically leads to 2 moles of hydrogen production per mole of substrate as shown below (Patel and Kalia 2013);



The reactions of sequential dark and photofermentation with glucose substrate are shown in Equations 2.14, 2.15, 2.16 where the only VFA product is acetic acid (Manish and Banerjee 2008).

Dark fermentation;



Photofermentation;



Sequential (or combined) dark and photofermentation reaction (overall reaction);



As seen from Equation 2.16, theoretically 12 moles of hydrogen can be produced from glucose substrate when the only VFA is acetic acid. However, the yields obtained in the real experiments are much lower than the theoretical value because a mixture of VFAs are produced and substrate is also used for maintenance, growth and PHB formation (Argun and Kargi 2010; Argun, Kargi, and Kapdan 2008). In sequential dark and photofermentation process, overall hydrogen production yield aimed to be at least 8 moles H₂/mole glucose for an economically feasible process (Chen et al. 2010).

It was previously reported the highest hydrogen production yield as 7.2 moles H₂/mole glucose by sequential dark and photofermentation method in fed-batch mode (Yokoi et al. 2002). Previously, hydrogen production using sugar beet molasses was conducted by *C. saccharolyticus* and *R. capsulatus hup⁻* bacterial strains in sequential dark and photofermentation process (Özgür, Mars, et al. 2010). While the maximum hydrogen yield was 4.75 mole H₂/mole glucose by *R. capsulatus hup⁻* bacteria, the overall hydrogen yield of sequential dark and photofermentation was reported as 6.85 mole H₂/mole glucose (Özgür, Mars, et al. 2010). In the study of Özgür, Uyar, et al. 2010, hydrogen production was carried out using sugar beet molasses by bacterial strains used for both dark fermentation (*Caldicellulosiruptor saccharolyticus*) and photofermentation (*R. capsulatus*, *R. capsulatus hup⁻* and *Rhodopseudomonas palustris*) in sequential dark and photofermentation process. It was found that while overall maximum hydrogen yield in dark fermentation was 4.2 mole H₂/mole sucrose, it was increased to 13.7 mole H₂/mole sucrose with sequential dark and photofermentation (Özgür, Mars, et al. 2010). According to the study of Argun et al. 2011 the overall yields of sequential dark and photofermentation were higher than single stage processes (dark or photofermentation). However, hydrogen formation rates were found lower than

700mL H₂/L.h, which is significantly lower than single stage dark fermentation (Avcioğlu et al. 2011). In addition, sequential dark and photofermentation process is hard to operate because there are two different systems and different bacterial species needed to deal with. This method is also disadvantageous when the economical feasibility of the biohydrogen production was concerned because the biogas obtained from dark fermentation stage has to be purified due to low hydrogen purity (Brentner et al. 2010).

2.2.5. Combined dark and photofermentation

In this method, dark and photo fermentation is conducted simultaneously in a single reactor where the produced VFAs by dark fermentation are converted to hydrogen and carbon dioxide by photofermentation. In combined dark and photo fermentation method, theoretically 12 moles of H₂/mole glucose can be produced (Equation 2.15). The theoretical hydrogen production yield of combined dark and photofermentation (12 moles H₂/mole glucose) is higher than dark fermentation (4 moles H₂/mole glucose) and photofermentation (8 moles H₂/mole glucose) alone. As shown in Equations 2.14 and 2.15, produced acetate in the dark fermentation can be oxidized by photofermentation to produce hydrogen. Therefore, combined dark and photofermentation processes can provide a continuous hydrogen production. However hydrogen formation rates were found lower than 35 mL H₂/L.h which is significantly lower than single stage dark fermentation (Argun and Kargi 2011). Asada et al. (2006) was conducted combined fermentation experiment with *Lactobacillus delbrueckii* NBRC 13953 and *R. sphaeroides*-RV using glucose as substrate at 30 °C and pH of 6.8. The major VFAs produced were acetate and lactate and the maximum hydrogen yield was reported as 7.1 mole H₂/mole glucose. Optimum optical density (OD) ratio of *Lactobacillus delbrueckii* to *R. sphaeroides*-RV was reported as 1/5 in order to obtain the highest hydrogen formation. For this process, the same economical and operating disadvantages of sequential dark and photofermentation method are valid because of the hydrogen impurity and two nested systems.

2.3. General Characteristics of Purple non-sulphur Bacteria

In 1949 Gest, Kamen and Bregoff reported molecular hydrogen production from purple non-sulphur (PNS) bacterium for the first time (*Rhodospirillum rubrum*). PNS bacteria are able to use sulfide as an electron donor during growing. However, they do not use sulfide as high concentrations as sulfur bacteria, that's why they are called as “non-sulfur” (Basak et al. 2014).

PNS bacteria are able to utilize carbon sources such as glucose and sucrose rather than VFA for hydrogen production under anoxygenic conditions, as reviewed by Argun et al., 2011. There are various PNS bacteria used in biohydrogen production by photofermentation. The most widely used ones are *Rhodobacter sphaeroides* O.U001, *Rhodobacter sphaeroides* RV, *Rhodobacter capsulatus*, *Rhodobacter sulfidophilus*, *Rhodospirillum rubrum* and *Rhodopseudomonas palustris* (Basak and Das 2007). Hydrogenase and nitrogenase are the enzymes used in photofermentative hydrogen production by PNS bacteria (Sinha et al. 2011). It is known that the main enzyme responsible for hydrogen production under anoxygenic condition is nitrogenase.

The two important criteria used for evaluating the performance of biological hydrogen production are hydrogen production rate (productivity) and the substrate conversion efficiency (yield). Among PNS bacteria, *Rhodobacter sphaeroides* were reported as one of the most promising bacteria for photofermentative biohydrogen production (Wu et al. 2012). This photosynthetic bacterium is widely used in biohydrogen production from organic wastewater such as olive mill wastewater (E. Eroglu et al. 2010; Eroğlu et al. 2006, 2004) and dark fermentation effluent (Argun and Kargi 2010; Uyar et al. 2009). In the studies of molasses utilized as substrate; *R. sphaeroides*, *R. capsulatus* and *Rp. palustris* have been found to produce hydrogen successfully (Eroğlu et al. 2004). In a study of Öztürk et al. (2006), the hydrogen production of *R. capsulatus* was improved by deleting the hydrogen uptake enzyme and it is called as *R. capsulatus hup⁻* bacteria. In previous studies, photofermentation

of *R. capsulatus hup⁻* have been resulted in stable outdoor operations when molasses was utilized (Kayahan, Eroglu, and Koku 2017; Savasturk, Kayahan, and Koku 2018). In literature, biohydrogen production by PNS bacteria is suggested as promising for large-scale operations because various carbohydrates including waste products are able to be utilized by these bacteria (Shi and Yu 2006).

2.4. Parameters Affecting Photofermentative Hydrogen Production

The critical parameters that affect photofermentative hydrogen production can be sum up as temperature, pH, substrate type and concentration, C/N ratio, light intensity and distribution, metal ion addition and the inoculum age of PNS bacteria. In literature, optimization of these parameters is found to increase the hydrogen productivity (Das, Nejat, and Glu 2001). Hydrogen yields may further be improved with a favorable C/N ratio, uniform light distribution through PBR, maximum activity of nitrogenase and minimum activity of hydrogenase enzymes as reviewed by Basak et. al, 2014. In a previous outdoor study, temperature, light intensity and feed composition were found significantly influencing the bacterial growth and hydrogen production rate (Androga et. al, 2011). It was reported that the yield factor was correlated to daily total solar radiation up to 8000 W.h/m². In addition, the cell growth rate was found to increase with increasing temperature and light intensity. However, it was also found that at high bacterial cell concentrations, light penetration into the PBR and therefore hydrogen productivity decreased (Androga, Ozgur, et al. 2011).

2.4.1. Temperature

In order to shift the bacterial metabolism towards hydrogen production, utilizing an optimum temperature to the PBR is an important issue. Sasikala et al., 1993 reviewed that the optimum temperature for photofermentative hydrogen production was suggested between 30°C - 40°C and the maximum hydrogen productivity was observed at 27.5°C (Androga et al. 2014). Furthermore, the cell growth of the PNS bacteria is not observed below 20°C or above 45°C (Androga et al. 2014). In a

previous study, the experimental results from *R. capsulatus* DSM 1710 bacteria were analyzed to obtain the maximum rate and yield of hydrogen production with respect to temperature and light intensity with 3k general full factorial design. According to the ANOVA results, maximum rate of hydrogen production (0.566 mmol H₂/L.h) was obtained at 27.5°C and 287 W/m², while maximum hydrogen yield (0.326 mol H₂/mol substrate) was obtained at 26.8°C and 285 W/m² (Androga et al. 2014). In another study, the optimum temperature range for *Rhodobacter* sp. was reported as between 31°C and 36°C for hydrogen production (Basak and Das 2007). Previously, it was stated that for most of the integrated dark and photofermentation processes, the optimal temperature range was found between 31°C-37°C for the dark phase and 30°C for the light phase (Patel and Kalia 2013).

Another important issue is to maintain constant and uniform temperature distribution through the PBR. However, it is difficult to provide a constant temperature in the outdoor experiments because of the temperature fluctuations during the day and night cycles. In a previous study, the effect of daily fluctuating temperature on hydrogen production was investigated using acetate as substrate by *R. capsulatus* and its hydrogenase uptake enzyme deleted strain (*R. capsulatus hup⁻*) in indoor and outdoor conditions (Özgür, Uyar, et al. 2010). It was observed that daily fluctuating temperatures (between 15°C and 40°C) decreased the hydrogen production by 50% compared to the hydrogen production at a constant temperature (30°C) at indoor conditions. Furthermore, another 50% decrease was observed when 16h light and 8h dark cycles were applied, besides fluctuating temperatures (between 15°C and 40°C) (Özgür, Uyar, et al. 2010). Therefore, minimizing the temperature fluctuations is necessary for an efficient hydrogen production in outdoor conditions. Temperature controller systems can be used to maintain constant temperature at an optimum value during hydrogen production by PNS bacteria. The temperature controller system may be cooling water circulation in water jacket surrounding the bioreactor or in manifold type glass tubes inserted in bioreactor. The economic evaluation of temperature controller system is also another important factor.

2.4.2. pH

In literature, bacterial growth was observed between pH of 6-9 and maximum hydrogen production was observed at pH of 7 (Sasikala et. al, 1991). The pH drop during photofermentation is a common trend observed in bacteria utilizing simple and complex sugars as carbon sources (Boran et al. 2012a; Sagir, Alipour, et al. 2017; Kayahan, Eroglu, and Koku 2017; Savasturk, Kayahan, and Koku 2018) due to organic acid by-products of the photofermentative metabolism (Keskin et. al, 2012). The applied methods to overcome the later decrease in pH are to use buffer solutions and slightly increase the initial pH. The optimal initial pH and temperature values were reported in a range of 6.8-7.5 and 31-36°C, respectively (Basak et al. 2007).

2.4.3. Substrate Type and Concentration

In literature, various substrates have been utilized such as organic acids (e.g. acetic acid, lactic acid) and sugars (glucose, fructose and sucrose) in the studies of photofermentative hydrogen production (Barbosa et al. 2001; Kayahan, Eroglu, and Koku 2017). In a previous work (Kapdan et. al, 2008), acid-hydrolyzed wheat starch was utilized by three different *Rhodobacter* species for photofermentative hydrogen production. It was found that biohydrogen production increased up to 8.5 g/L total sugar concentration and optimum sugar concentration was 5 g/L, which resulted in the highest hydrogen production rate and yield. Industrial by-products and wastes are economically preferred, since sustainable processes can be carried out with these substrates. Recently, biohydrogen production from wastewaters is preferred due to its potential to decrease the cost of waste treatment (Van Ginkel, Oh, and Logan 2005). Various photofermentative bacteria can utilize wastewater like industrial effluents and sewage.

As reviewed by Ta Yeong Wu et. al (2012), the major problems in hydrogen production from industrial effluents are listed below;

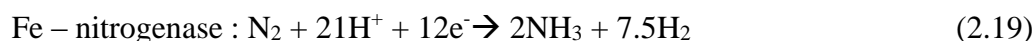
- Light transmission decreases due to the dark color of wastewater
- The hydrogen productivity may decrease because of high ammonia concentration, which inhibits nitrogenase enzyme.
- Pretreatment procedures may be required before hydrogen production because of some toxic compounds such as heavy metals, phenols and polycyclic aromatic hydrocarbons (PAH) in industrial wastewaters.

Given these circumstances, industrial by-products can be considered as more promising. Especially, by-products of sugar factories such as molasses and dark fermenter effluent (DFE) have been utilized in studies of photofermentative hydrogen production and resulted in promising hydrogen yields (Androga et. al, 2014). While molasses consists of mainly sucrose (30-60% w/w), DFE contains organic acid mixtures such as acetic and lactic acid. Utilizing molasses as substrate can be more preferable since two stage operation of DFE is more complex (dark fermentation followed by photofermentation) (Chen et al. 2008). In addition, sucrose has higher stoichiometric potential for hydrogen production since it has more H₂ per molecule compared to short-chain organic acids. In a previous study, sucrose concentration in molasses was suggested to be kept around 5 mM since higher sucrose concentrations can be resulted in rapid acidification (Boran et. al, 2012).

2.4.4. C/N Ratio

As the main catalyst of photofermentativebiohydrogen production is nitrogenase, the factors affecting the activity of this enzyme also have a significant effect on hydrogen production. There are three types of nitrogenase and their hydrogen production modes with ATP are shown below (Basak and Das 2007);





The presence of ammonium (NH_4^+) ion as nitrogen source may lead to a decrease in hydrogen production by inhibiting the nitrogenase enzyme (Kayahan, Eroglu, and Koku 2016), as shown in Equations 2.17, 2.18 and 2.19 (You-Kwan Oh et al. 2004). It is notable that nitrogen sources that are non-ammonium can also cause ammonium inhibition. It was previously reported that when lactic acid was exhausted before glutamate, ammonia was produced causing an inhibition of nitrogenase enzyme (Koku et al. 2002). The carbon to nitrogen (C/N) ratio of the substrate is a critical parameter that affects biohydrogen production because of the interaction between nitrogen sources and nitrogenase enzyme (Androga, Özgür, et al. 2011). High levels of nitrogen containing substrates (i.e. low C/N ratios) may deactivate the nitrogenase enzyme, which is responsible from hydrogen production. On the other hand, nitrogen supports the growth of bacteria and leads PNS bacteria to form hydrogen-producing populations of bacteria earlier. In summary, while nitrogen is needed for the cell growth, high nitrogen concentrations may inhibit nitrogenase leading a decrease in the hydrogen production. Due to these contrast effects, selecting the optimum C/N ratio is important. In literature, the optimum C/N ratio values varies between 13 and 35 according to the bacterial cultures, carbon sources and illumination (Androga, Özgür, et al. 2011; Sagir, Alipour, et al. 2017; Avcioglu 2010). While Kuriaki et al (1998) reported the maximum hydrogen productivity for C/N ratio of 22.8, Androga et al (2009) was stated that the maximum hydrogen productivity was obtained with C/N ratio of 25. In literature various types of carbon sources such as organic acids (e.g. acetic acid, lactic acid,) and sugars (e.g. sucrose) and nitrogen sources (e.g. glutamate, ammonium chloride, yeast extract) have been utilized by PNS bacteria (Kayahan, Eroglu, and Koku 2017; Savasturk, Kayahan, and Koku 2018; Özgür, Mars, et al. 2010; Uyar et al. 2009). Previously, different substrates with same C/N ratio were utilized by *R. sphaeroides* and although the maximum cell concentrations were nearly the same, the maximum productivities and lag times of hydrogen production were different (Uyar et al. 2009). This result showed that for the same

C/N ratio, the type of carbon source utilized by bacteria is also an important factor affecting the hydrogen productivity. In literature, various carbon and nitrogen sources were utilized by *Rhodobacter* species at different concentrations with different C/N ratios, and some of them are shown in Table 2.4 in terms of hydrogen productivity and yield.

Table 0.4. Table 2.4. Hydrogen productivities and yields for outdoor photofermentative hydrogen production of *Rhodobacter* species in large-scale PBRs for different C/N ratios (Basak et al. 2014).

PBR type and volume	Type of bacteria	C and N sources	C/N ratio	H ₂ productivity [mol H ₂ /m ³ .h]	Yield (%)	References
Tubular (90 L)	<i>R. capsulatus hup⁻</i>	20mM acetate, 2mM glutamate	25	0.40	12	(Sözen et al. 2005)
Flat plate (6.5 L)	<i>R. sphaeroides</i>	15mM acetate, 2mM glutamate	20	0.45	-	(Eroglu et al. 2008)
Tubular (80L)	<i>R. capsulatus DSM 1710</i>	40mM acetate, 2mM glutamate	45	0.74	16	(Boran et al. 2010)
Flat plate (4L)	<i>R. capsulatus hup⁻</i>	40mM acetate, 4mM glutamate	25	0.51	53	(Androga et al. 2011)

Previously, biohydrogen production was conducted by *R. sphaeroides O.U.001* with different C/N ratios (65, 35, 25 and 17) and the highest hydrogen yield was found for C/N ratio of 35 (Akköse et al. 2009), as also reported in the study of Eroglu et al. (1999) (İ. Eroglu et al. 1999). Androga et al. (2011) investigated the effect of decreasing C/N ratio by increasing the nitrogen concentration (2mM, 3mM and 4mM glutamate) with constant acetate concentration (40 mM) in fed-batch mode. According to the results, reducing the C/N ratio increased the cell growth and

hydrogen productivity, while increasing the C/N ratio caused cell growth but decreased the hydrogen productivity. The optimum C/N ratio was found as 25 (40mM acetate and 4mM glutamate) with a maximum hydrogen productivity of 0.66 mmol H₂ /L.h by *R. capsulatus* hup⁻ with a panel PBR (8 L) in indoor conditions (Androga, Özgür, et al. 2011). In another previous indoor study, different substrates at various concentrations were utilized by *R. capsulatus* with 8 L PBR to observe the effect of C/N ratio on biohydrogen production. Lactic acid, acetate and glutamate at different concentrations were utilized leading the C/N ratios of 13, 15.25, 21 and 56.25. The highest hydrogen yield and productivity was obtained for the lowest carbon to nitrogen ratio (C/N=13) as 32% and 0.12 mmoles H₂/L.h, respectively. Previously, hydrogen production with different C/N ratios (C/N=15,25, 35, 45 and 55) were studied by using acetate as a carbon source and glutamate as nitrogen source by *R. capsulatus* bacteria (Özgür, Uyar, et al. 2010). The highest hydrogen productivity was found with a C/N ratio of 35 suggesting the existence of an optimum glutamate concentration. Although hydrogen was produced successfully with all C/N ratios, the hydrogen production was started faster (decreased lag time of hydrogen production) at lower C/N ratios. Therefore, lowered C/N ratio can be applied outdoors for both to increase the hydrogen productivity and decrease lag time for the hydrogen production.

2.4.5. Light Intensity and Distribution

Light intensity and distribution are other critical parameters that affect photofermentative hydrogen production (Argun et. al, 2008). A previous long-term (75 days) outdoor study showed that the pattern of hydrogen production closely followed the daily change in the light intensity (Avcioglu 2010). As reviewed by Argun et al. (2011), the suitable ranges of wavelength, light intensity and light conversion efficiencies for photofermentation were reported as 400-1000nm, 6-10 klux and 0.2-9.3%, respectively. Infrared light (750-950 nm) has been shown to play an important role in the photofermentative hydrogen production. The illumination of

PBR can be achieved with sunlight or artificial light sources such as florescent lamps, optical fibers, neon tubes, halogen lamps etc.

According to Beer-Lambert's law (Equation 2.20), there is a linear relationship between light absorbance and culture concentration. Epsilon (ϵ) is the wavelength dependent molar absorptivity coefficient ($M^{-1}.cm^{-1}$), b is the light path length (i.e. tube radius), c is the concentration of the culture medium and A is absorbance. Experimental data are frequently reported in transmittance ($T=I/I_0$) where I_0 is the incoming light intensity and I is the light intensity after it passes through the culture.

$$A = -\log(I/I_0) = \epsilon \times b \times c \quad (2.20)$$

As shown in Equation 2.20, the light energy in the liquid media decreases exponentially depending on the concentration of culture medium and the distance from the light source. Cell concentration, hydrogen productivity and molar hydrogen yield values were respectively found as 0.68 gram dry cell/Liter culture (gdcw/Lc), 0.51 mmol H_2 /Lc.h and 53% in a previous study at high temperature and light intensity (Dominic et. al, 2011). On the other hand, cell concentration, hydrogen productivity and molar hydrogen yield values were found respectively as 0.31 g/L, 0.30 mmol H_2 /L.h and 44% at low temperature and light intensity. It is noteworthy to say that daily hydrogen yield (mol H_2 /g) was found to be related with daily total solar radiation ($W.h/m^2$). However, bacterial density increases at high light intensity and thus at some point, light transmission decreases due to cell-shading effect or biofilm formation on reactor surface, which leads to a decrease in hydrogen production (Kim et al. 1987). Therefore, it is desirable to apply the optimum light intensity, where the maximum hydrogen production can be achieved. Previously, hydrogen production was found to increase with increasing light intensity until reaching its saturation at an optimum light intensity of 270 W/m^2 (Sakurai et. al, 2013).

The factors of illuminated surface area to ground area ratio and ground area to reactor volume ratio are frequently used in selecting the reactor type. In literature, the hydrogen production rates have been found different even with the same PBRs in similar environment but with different reactor volumes, due to differences in the illuminated surface areas. Applying uniform light distribution and higher illuminated surface areas enhances hydrogen production in PBRs. In a study with triple jacketed annular PBR (1L) three concentric chambers were used with *R. sphaeroides O.U.001* bacteriato increase surface to volume ratio (Basak et. al, 2009). In that study, the light conversion efficiency was obtained as 3.7%, which is quite significant value because of the high surface to volume ratio.

Another important factor in photofermentative hydrogen production in outdoor experiments is the tube radius. According to Beer-Lambert's law (Equation 2.19), the shorter light path, which means smaller tube radius, is more favorable to ensure higher light conversion efficiency. On the other hand, large tube radius should be preferred in order to achieve economically efficient hydrogen production. Therefore, applying optimum tube radius is needed to achieve an effective the hydrogen production. The tube radius should also be limited depending on the received light intensity and substrate concentration due to shading effect. In a previous study of our laboratory, the light transmission for varying depths and different substrate (molasses) concentrations was analyzed with photon count and accordingly the tube radius was suggested as between 1.5-2 cm (Kayahan et. al, 2017).

2.4.6. Metal Ion Addition

In literature, there are researches on the effect of metal ions addition (such as iron and molybdenum) on the nitrogenase activity and photofermentative hydrogen production by PNS bacteria (Laurinavichene et al. 2013). In a previous study, nitrogenase enzyme activity decreased in the absence of iron and molybdenum metal ions (Kars et al. 2006). Iron and molybdenum are necessary to increase the activity of nitrogenase because they are essential cofactors of the FeMo-nitrogenase enzyme

(Koku et al. 2002). Furthermore, various electron carriers (e.g. ferredoxin) require iron as necessary cofactor in the photosynthetic electron transfer chain. Hence, adding Mo and Fe salts properly into the growth media was found to enhance hydrogen yield for various *Rhodobacter* species (Zhu et al. 2007).

In a previous experiment, adding 0.1 mM Fe and 0.16 μ M Mo salts to olive mill wastewater (OMW) in photofermentative hydrogen production by *R. sphaeroides* was found to increase the hydrogen productivity and biomass concentration (Eroglu, Gunduz et al. 2011). The hydrogen production was found to be increased by 1.5 times for Mo-added and 3 times for the Fe-added cultures (Eroglu, Gunduz et al. 2011).

2.4.7. Inoculum age of PNS bacteria in hydrogen production media

A typical bacterial growth curve includes; lag phase, logarithmic (exponential) growth phase, deceleration phase, stationary phase and death (decline) phase. The lag phase defined as the adaptation period of the cell to the new environment, which occurs after inoculation. Depending on the nutrient composition bacteria synthesizes new enzymes and represses syntheses some of the other enzymes after inoculation into the new medium (Shuler and Kargi 2013). Although mass of the bacterial cell may increase a little, no increase in cell number density occurs during the lag phase (Shuler and Kargi 2013; Bailey and Ollis 1986).

The most suitable phase for photofermentative hydrogen production is exponential growth phase, which have been defined as the optimal phase where maximum hydrogen production can be achieved (C. H. Sasikala, Ramana, and Rao 1995; Harun Koku et al. 2003). In outdoor experiments of a previous study, the inoculation ratio of the grown bacteria into the hydrogen production media at start-up affected the duration of the batch phase (Sinha et. al, 2011). Higher inoculation ratio at the start-up resulted in higher cell concentration and more rapidly growth of the bacteria because of the quorum sensing effect, which is the gene regulation according to the changes in bacterial cell density with released chemical signals called as

autoinducers (Miller and Bassler 2001). In a previous outdoor study, 10% v/v inoculation ratio was applied in all inoculums when the OD=1.0 (at 660 nm) corresponding to cell concentration of 0.4656 g/L with sucrose contained in molasses utilized by *Rhodobacter capsulatus hup⁻*. The inoculations were made at exponential growth phase at around 0.5 g/L (Ozturk et. al, 2005), which was stated as optimal for the hydrogen production (Koku et. al, 2003).

2.5. Photobioreactors for Hydrogen Production

Photosynthetic microorganisms produce hydrogen by utilizing a light source in closed systems that are called as photobioreactors (PBRs) since adequate illumination and anaerobic conditions are needed. The PBRs are closed systems allowing to collect the hydrogen gas and to protect the bacterial medium from contamination. For sustainable and economically feasible hydrogen production, natural sunlight is preferred as the light source in the large-scale outdoor studies.

The PBR design is critical for pilot-scale outdoor studies and the ideal design parameters are listed as follows (Savasturk, Kayahan, and Koku 2018):

- The material of the reactor should be inert, transparent, and durable under outdoor conditions.
- The material of the reactor should have low hydrogen gas and air permeability
- The light distribution through the reactor should be efficient with high illuminated surface to ground area ratio
- The mixing and cooling should be effective to keep the temperature of the culture medium at the desired values.

Mainly, the photobioreactor types are divided in two groups depending on the cell condition; suspended-cell reactors and immobilized-cell reactors (Zhang et. al, 2010). Immobilized-cell reactors may lead to an increase in the bacterial concentration, stability of operation and hydrogen production rate with less retention time (Basak et al. 2014). Suspended-cell photobioreactors are more commonly used

for photofermentative hydrogen production because it is easy to operate and mass transfer (Gordon 2002). Panel (flat-plate) and tubular PBRs are two commonly preferred suspended-cell reactor types in photofermentative hydrogen production (Androga et al., 2012). In literature, some of the tubular PBRs used in photofermentative hydrogen production were designed as vertical tubular (Eroglu et al, 1999) while others as horizontal tubular (Boran et. al, 2012). The maximum illuminated surface area to ground area ratio can be achieved by designing the reactor as compact (Gebicki et al. 2010). For this purpose, a compact tubular reactor was previously designed by Kayahan et. al, (2016) which is called as “stacked U-tube photobioreactor”.

2.5.1. Immobilized-cell Photobioreactors

The other type of PBR consists of agar-bacteria frame maintained in a panel, which is called as immobilized-cell reactors. The immobilized-cell cultures occupy less space and can be used repeatedly for hydrogen production. The bacterial cell culture can be used in exponential phase of the growth curve over a very long time.

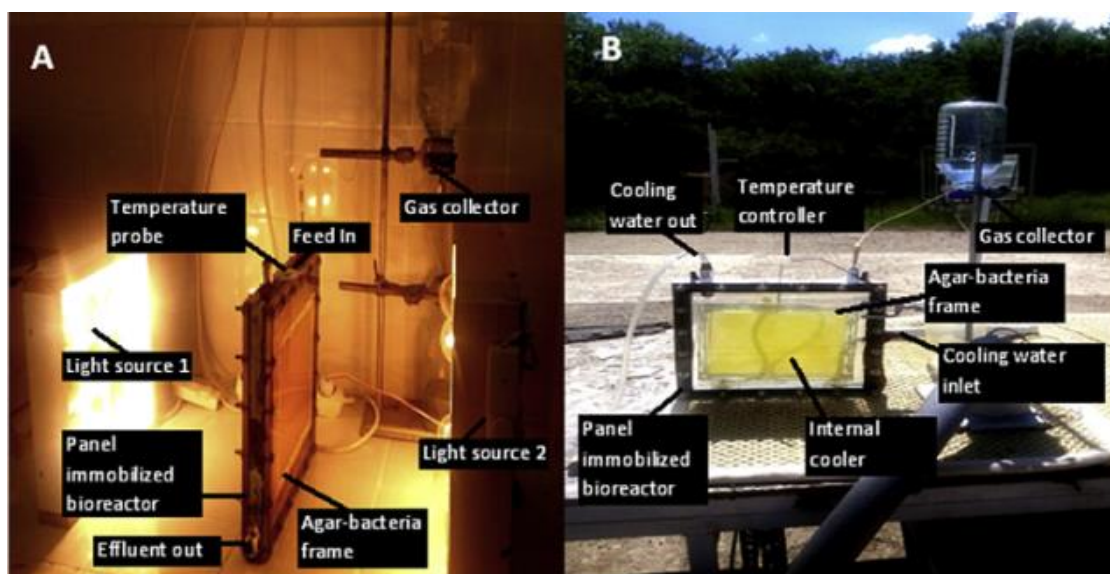


Figure 0.5. A immobilized-cell photobioreactor in A) indoor and B) outdoor conditions (Sagir et al. 2017).

In a previous study, long-term hydrogen production was obtained (64 days) in a 1.4 liters PBR by *R. capsulatus hup⁻* bacteria immobilized with 4% (w/v) agar with sucrose (5mM) and glutamate (4mM) sources (Sagir et al. 2017). The experiments were conducted with immobilized-cell PBR in sequential batch mode in indoor and outdoor conditions, as shown in Figure 2.5. The highest productivity and yield were obtained as 19 mol H₂/mol sucrose and 0.73 mmol H₂/L.h on 5 mM sucrose for indoors; 6.1 mol H₂/mol sucrose and 0.87 mmol H₂/L.h on 10 mM sucrose for outdoors, respectively (Sagir et al. 2017). In another previous study, *Rhodopseudomonas capsulate* and *Rhodobacter sphaeroides* cultures were reported to have hydrogen productions rates in a range of 80-100 ml H₂/L.h and 40–50 ml H₂/L.h, respectively (Kumar, Ghosh, and Das 2001).

The results of the experiments found in literature may indicate that hydrogen can be produced efficiently for long-term even under changing outdoor conditions. Despite these promising results, immobilized-cell PBRs have disadvantages as in panel-type PBRs such as complex start-up procedures, mechanical restrictions, limited reactor size and mixing problems. In the previous study (Sagir et al. 2017), visible crack formation was observed on the reactor indicating structural stability loss due to long-term operation. Furthermore, light conversion and substrate diffusion is limited for the immobilized-cell PBRs.

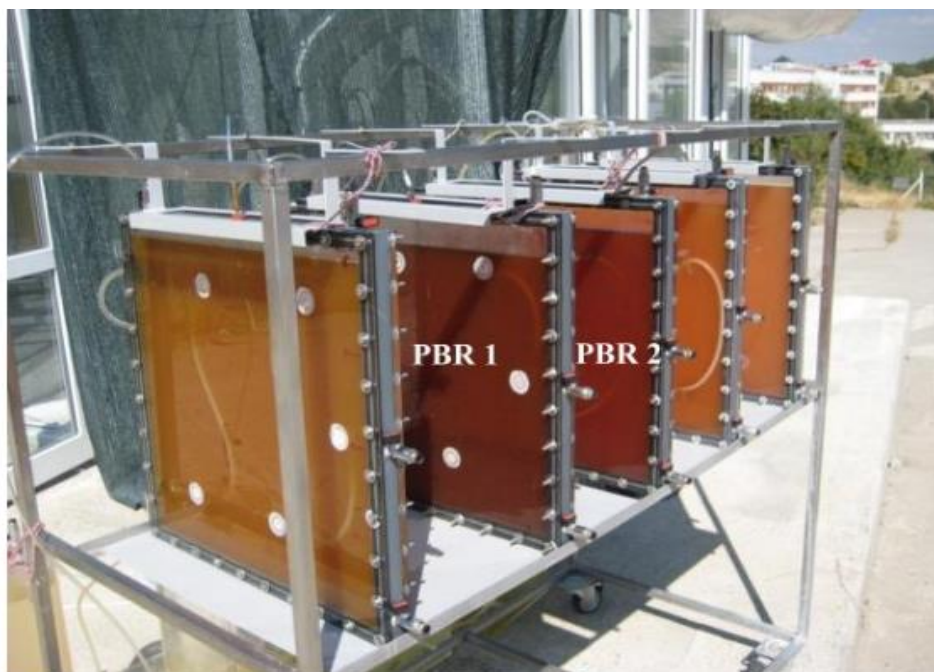
2.5.2. Suspended-cell Photobioreactors

Panel (flat-plate) and tubular PBRs are two commonly preferred suspended-cell reactor types in photofermentative hydrogen production (Androga et al. 2012).

2.5.2.1. Panel Photobioreactors

Panel photobioreactors consist of two transparent flat-plates such as glass or PMMA, which are pinned to each other with a frame (Androga et al. 2012). The space between the flat-plate panels is arranged depending on the distribution of intended light and temperature. As previously reported by Eroglu et al. (2014), the height of panels is limited depending on the hydrostatic pressure at the reactor bottom. The

illuminated surfaces of the panels are typically directed to east-west line to receive effective sunlight. A typical panel (flat-plate) PBR is shown in Figure 2.6 (Kayahan 2015).



*Figure 0.6.*Panel type photobioreactors (4L) with internal cooling system in outdoor conditions.

The illuminated reactor surface to ground area ratio for panel bioreactors is around 8:1 while it is 1:1 for tubular bioreactors (Gebicki et al., 2010). Although panel reactors are advantageous in terms of this ratio, there are some drawbacks due to its mechanical restrictions. While reactor size is limited and mixing is hard for panel reactors, scale-up is easier and mixing can easily be performed by a recirculation pump for tubular reactors. In a previous study, severe deformations were observed in a panel photobioreactor (PVC) because of the pressure (Avcioglu 2010). Thus, tubular photobioreactors are also more advantageous regarding durability under outdoor conditions.

2.5.2.2. Tubular Photobioreactors

Tubular photobioreactors consist of long transparent (glass etc.) tubes with 3-6 cm diameter and 10-100 m tube length ranges (Akkerman et al. 2002). Tubular photobioreactors can be classified mainly as vertical, helical and horizontal (Figure 2.7). In vertical PBRs (e.g. bubble columns and airlift PBRs) typically a gas is fed to the reactor for mixing. However, vertical PBRs are not very convenient for photofermentative hydrogen production because the supplied inert gas dilutes the produced hydrogen, which leads to additional separation costs. In helical PBRs, cooling is made by an exterior heat exchanger and flexible materials are preferred as reactor materials. In α -shaped helical PBRs, culture medium is raised to a tank and then flows downwards with an inclined tube. The liquid medium is collected into another air riser and then the same procedure is repeated (Dasgupta et al. 2010).

Horizontal tubular photobioreactors are preferable because high light conversion efficiencies can be achieved. Some of the horizontal PBRs have several tubes connected by manifolds that are called as nearly horizontal reactors. Although liquid recirculation is achieved by mixing with a pump, the flow distribution between the tubes was found to vary considerably (Androga et al. 2014).

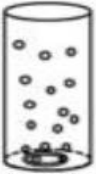
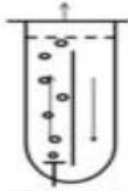
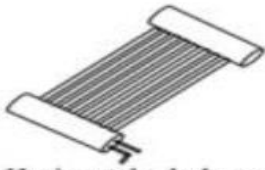
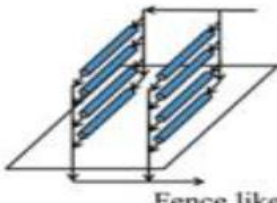

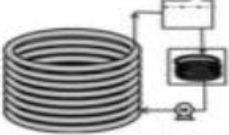
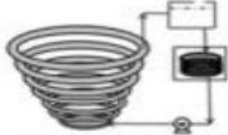
	Closed system	
Tubular photobioreactors Vertical tubular	 Bubble column	 Airlift reactor
Horizontal tubular	 Horizontal tubular reactor	 Fence like
	 α -shaped tubular	
Helical tubular	 Helical tubular (bubble train)	 Conical tubular

Figure 0.7. The types of tubular photobioreactors (Dasgupta et al. 2010).



Figure 0.8. A stacked U-tube photobioreactor with internal cooling by manifolds in outdoor conditions.

The scale-up strategies are mainly based on the packed bed reactor (PBR) or continuous stirred tank reactor (CSTR) types. A method for scale up of a liquid phase CSTR is geometric similarity of reactor geometry, which is shown below (Junker 2004);

$$D_{T2}/D_{T1} = (V_{T2}/V_{T1})^{1/3} \quad (2.21)$$

where D_{Ti} is the tank diameter and V_{Ti} is the total tank volume. The liquid volume (V_{Li}) can be used as alternative to tank volume (V_{Ti}). It assumes constant impeller geometry such as impeller diameter and number. Another method used for scale-up is similar impeller Reynold's number (N_{Re}), which can be adapted for similar tube Reynold's number as shown below;

$$N_{Re1} = N_{Re2} \quad (2.22)$$

$$\frac{\rho_1 \bar{u}_1 D_1^2}{\mu_1} = \frac{\rho_2 \bar{u}_2 D_2^2}{\mu_2} \quad (2.23)$$

where ρ is fluid density, \bar{u} is velocity of the fluid, μ is viscosity and D is the diameter.

For constant viscosity and density, the expression simplifies to;

$$\frac{\bar{u}_2}{\bar{u}_1} = \left(\frac{D_1}{D_2}\right)^2 \quad (2.24)$$

where \bar{u} is velocity of the fluid in one tube and D is diameter of the tube. An effective design should provide uniform light distribution and mixing, high illuminated surface area to ground area ratio, low hydrogen gas permeability and sufficient cooling system to maintain optimum temperature. Previously, a stacked U-tube photobioreactor which meeting these demands was designed by Kayahan et al. 2016. The design consisted of four glass U-tubes connected to each other by one inlet and one outlet vertical glass manifolds (Figure 2.8). Effective cooling was achieved by cold water flow inside the capillary tubes in the manifolds. While the main objective of an typical reactor for scale-up is to achieve high conversion efficiency or selectivity, the photobioreactor design mainly focuses on to have high illuminated surface to ground area ratio. The ratio of illuminated surface area to ground area can be increased by a compact design (Gebicki et al. 2010). With this stacked U-tube PBR, the ratio of illuminated surface area to the ground area was increased from 1:1 to 5:1 (Kayahan et al. 2016) compared to the typical horizontal tubular bioreactors (Gebicki et al. 2010). In addition, the cost of ground area also decreased because it may result in nearly 90 % of the total cost of photofermentative hydrogen production (Boran et al. 2012). With further compact scale-up studies, this cost item can be reduced and economically more feasible hydrogen production processes can be achieved.

CHAPTER 3

MATERIALS AND METHODS

3.1. The Bacterial Strain

The bacterial species used in the experiments was *Rhodobacter capsulatus* YO₃ (hup⁻) strain previously obtained from the wild-type by deletion of the uptake hydrogenase gene from *R. capsulatus* MT1131 strain (Öztürk et al. 2006) by Dr. Yavuz Öztürk (GMBE, TUBITAK MAM, Gebze).

3.2. Culture Media

Rhodobacter capsulatus hup⁻ strain was inoculated to the solid, growth, adaptation (only for pilot-scale) and hydrogen production media, respectively. All the fresh media were sterilized by an autoclave for 20 minutes at 121⁰C (Nüve - OT 90L) before inoculation of the bacteria. Vitamins, trace elements and Fe-citrate were added besides Biebl and Pfennig's medium (BPM) (Biebl and Pfennig 1981) after autoclave (Appendix A).

3.2.1. Solid Media

The bacterial colony obtained from stored bacterial medium, which was kept in storage media at -80°C, was inoculated into the solid media. Solid media were prepared by the addition of 3% w/v agar into the growth media (described in 3.2.2) and autoclaved. The prepared medium was cooled to around 40°C and poured into agar plates for solidification. The bacteria were inoculated on agar plates allowing the growth of separate colonies. The plates were kept in an incubator at 30°C in dark, until the visible colonies were obtained. The solid media allowed both observing the colonies separately and detecting the contamination.

3.2.2. Growth Media

The obtained colonies from solid media were transferred to the growth media for activation. The bacteria were activated in growth media which contained 20 mM acetate as the carbon source and 10 mM glutamate as the nitrogen source besides BPM. pH was adjusted to around 6.5 with a 5 M NaOH solution and 30 mM potassium phosphate was used as a buffer solution. After autoclaving the media, it was cooled to room temperature and vitamins, trace elements and Fe-citrate were added (Appendix A).

3.2.3. Sucrose Adaptation Media for Pilot-scale Outdoor Experiment

Before inoculation of the bacteria to the hydrogen production media, the bacteria were adapted to sucrose with adaptation media, only for the pilot-scale experiment. The media consist of the same components as the growth media with additionally 5 mM sucrose. After the OD of the inoculated bacteria reached around 1.5 at 660 nm, a second adaptation was made in the BPM containing 10 mM glutamate and 5 mM sucrose. In both adaptation media, pH was adjusted to around 6.5 with NaOH solution, and 30 mM potassium phosphate was used as a buffer solution.

3.2.4. Hydrogen Production Media for Small-scale Indoor Experiments

The hydrogen production media contained 10, 30 and 50 mM glucose or fructose besides 4 mM glutamate in the small-scale experiments. The pH was adjusted to 7.5 with 5 M NaOH solution and 30 mM potassium phosphate was used as a buffer solution.

3.2.5. Hydrogen Production Media for the Pilot-scale Outdoor Experiment

The hydrogen production media contained molasses, (from Ankara Sugar Factory, Turkey) diluted to contain 5 mM sucrose as the main carbon source. The undiluted molasses was found to contain 52% (w/w) sucrose by Düzen Norwest Laboratory in Ankara (Appendix B). Although the molasses contained Fe and Mo, the amounts of these constituents were increased by adding Fe and Mo salts to attain initial medium

concentrations of 0.1 mM Fe and 0.16 μ M Mo as suggested by previous literature (E. Eroglu et al. 2011). The glutamate was adjusted similarly, to achieve an initial glutamate concentration of 7.5 mM and an overall C/N ratio of 13. The pH was adjusted to 7.5 with 5 M NaOH solution and 30 mM potassium phosphate was used as a buffer solution.

3.2.6. Storage Media

The bacteria can be stored for long time in the storage media containing sterile glycerol (40% v/v) in addition to the growth media in cryogenic vials at -80°C. The bacteria can also be stored in growth media in +4°C refrigerator before activation, for short periods.

3.3. Experimental Set-up and Procedure

The first step, preparation of the bacteria for the hydrogen production runs for both small and large scale experiments were explained, in detail. The experimental procedures of both small-scale and large-scale experiments were explained, respectively.

3.3.1. Pretreatment Procedure

Before starting the experiments for the photofermentative hydrogen production, a number of steps were carried out to prepare the bacteria (Figure 3.1). First, the bacteria taken from the storage at -80°C were inoculated onto the solid media on agar plates to detect any contamination and select the best suitable colony. To activate the bacteria, the selected colony was inoculated into the growth media with a 10% (v/v) ratio and grown in increasing reactor culture volumes of 1.5 mL and 15 mL, respectively. Then, only for the pilot-scale experiment, inoculation into the first and second sucrose adaptation media were made after activation, respectively. Adaptation media was prepared with the same 10% (v/v) ratio until obtaining 1L of culture media. Finally, the inoculums were made into the hydrogen production media and the experiments were begun.

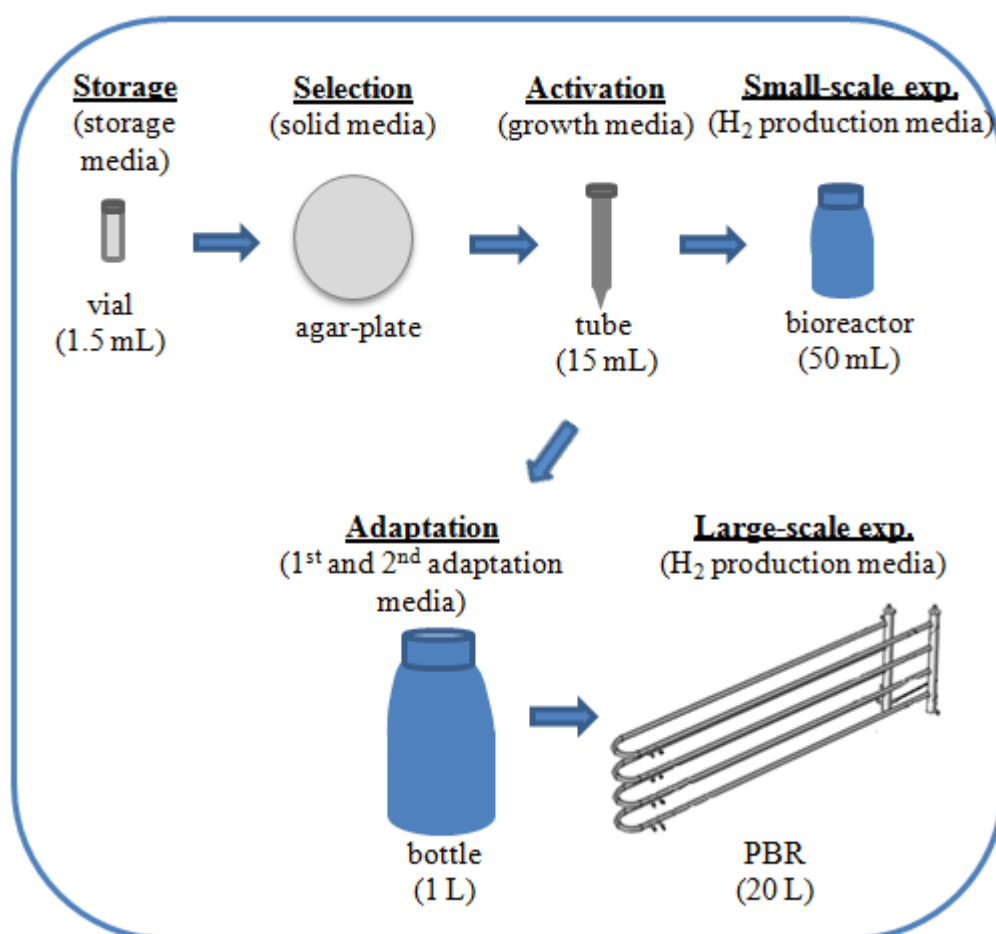


Figure 0.9. The experimental procedures of small-scale and large-scale experiments.

All adaptation and activation of inoculated cultures were held in incubators (Nüve - ES 250) at 30°C under continuous illumination with a light intensity of 2000 lux (135 W/m²). All inoculums were made when optical density (OD) of the bacteria reached around 1.5 at 660 nm with 10% (v/v) ratio which states that 10% of the media was the bacterium and the rest of it was the defined media (growth, adaptation or hydrogen production). Only inoculation into the hydrogen production media in the pilot-scale outdoor experiment was made differently such as adjusting the cell concentration to 0.23 g/L (OD=0.50) at the startup. Argon gas was sprayed for 2 minutes in each glass bottle to supply anaerobic conditions after the inoculations. Finally, total volume of 50 mL and 20 L hydrogen production media were obtained for small-scale and pilot-scale experiments, respectively.

3.3.2. Small-scale Indoor Experiments

Two small-scale indoor experiment sets were carried out between January 5th - January 14th, 2016 and February 17th – March 2nd, 2016 with *R. capsulatus hup⁻* (YO₃) using glucose and fructose as substrate, respectively. As described in pretreatment procedure (Section 3.3.1), the experiments were started after inoculation of the bacteria into the hydrogen production media. In the first small-scale experiment, the bacteria were inoculated into 10, 30 and 50 mM glucose containing hydrogen production media, respectively. In the second experiment 10, 30 and 50 mM fructose were used instead of glucose and the same procedure was applied. Photofermentative hydrogen production was observed under continuous illumination at 30°C in an incubator with 50 mL glass bottles in batch mode (Figure 3.2).



Figure 0.10. A photograph of small-scale bioreactors for glucose runs.

In the set of small-scale experiments, different concentrations of sugars (glucose or fructose) were used as carbon source and glutamate was used as a nitrogen source for *Rhodobacter capsulatus hup⁻*. 4mM glutamate and different concentrations of sugar (10mM, 30mM, and 50mM) were used to observe the effect of sugar concentration and C/N ratio on photofermentative hydrogen production. Duplicate runs were prepared for each concentration, which makes totally six runs for glucose (R1g and R2g=10Mm, R3g and R4g=30mM, R5g and R6g=50 mM glucose) and six

runs for fructose (R1f and R2f=10Mm, R3f and R4f=30mM, R5f and R6f=50 mM fructose). 25 mM KH₂PO₄ was used as a buffer solution.

The inoculation was made in solid, growth and hydrogen production media, respectively. The experiments were performed in incubators at 30 °C under continuous illumination with an intensity of around 2000 lux. Light intensity was measured with a luxmeter. Illumination was made by tungsten lamps. The evolved gas was collected in glass cylinders using the water displacement principle. The measurements and analysis of sugar concentration, organic acid concentration, pH, cell concentration (OD) and gas content were made daily. The averages of duplicates were recorded for pH and OD (Appendix D-b and D-c). The averages of duplicates were recorded for pH and OD. The other analyses were done with R1f, R2g, R3f, R4g, R5f and R6g.

Table 0.5. Carbon-to-nitrogen (C/N) ratios of the runs for the small-scale experiments.

Run	R1f and R2g	R3f and R4g	R5f and R6g
C/N ratio	20	50	80

The C/N ratios of the runs were calculated which was defined as the ratio of total carbon in glutamate and sugar (mM) to total nitrogen in glutamate (mM), as shown in Table 3.1.

3.3.3. Pilot-scale Outdoor Experiments

Photofermentative hydrogen production was carried out with the stacked U-tube reactor under outdoor conditions between August 7th and August 25th, 2016 with *R. capsulatus hup⁻* using sucrose contained molasses as substrate. A previously designed photobioreactor (Kayahan, Eroglu, and Koku 2016) was scaled up to 20 liters with some changes to improve the design, as explained in section 3.3.3.1. Before start-up of the experiment a liquid leakage test and sterilization of the reactor

was done. The experiment was started when the bacteria was inoculated into hydrogen production media after growth and adaptation periods. During the operation, molasses feeding was done to adjust the sucrose concentration of the culture media. Sampling was done twice in a day in order to analyze the culture media.

3.3.3.1. Construction: Stacked U-tube Photobioreactor

Previously designed stacked U-tube photobioreactor (PBR) (Kayahan, Eroglu, and Koku 2016) was scaled-up from 9 L to 20 L by increasing the tube radius from 1.5 cm to 2 cm. The PBR was consisting of 4 glass U-tubes vertically connected to each other with 2 manifolds. The inner tube radius is 2 cm, manifold radius is 3 cm and the length of each U-tube is 4 m. The glass tubes were fitted together with flange connections. The liquid culture was circulated with a peristaltic pump and distributed with inlet and outlet manifolds. The process flow diagram is shown in Figure 3.3 from a previous study with some changes such as reduced sampling and temperature ports (Kayahan, Eroglu, and Koku 2017).

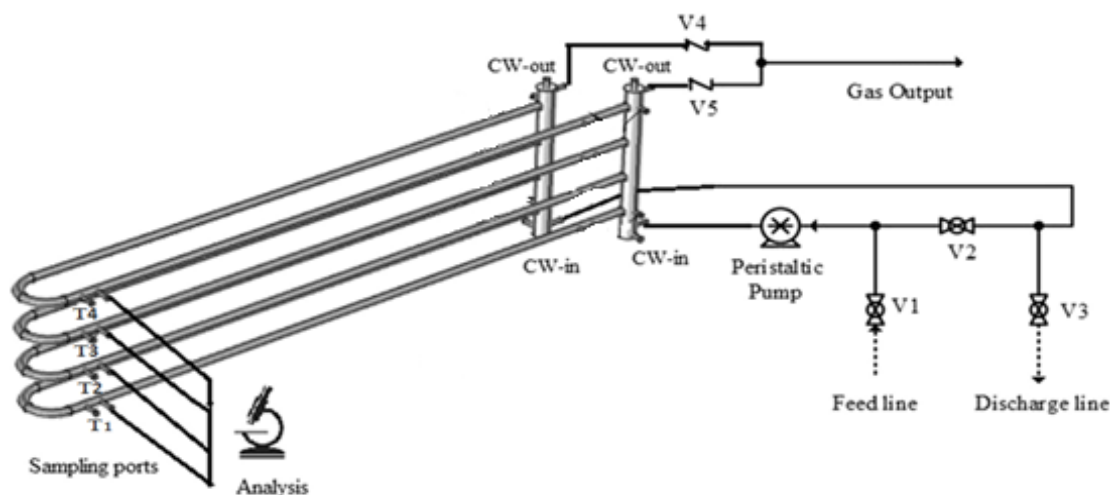


Figure 0.11. Process flow diagram of the stacked U-tube photobioreactor. T1, T2, T3 and T4 are temperature probes. V1, V2 and V3 are ball valves. V4 and V5 are check valves (1/3 psi). CW-in and CW-out are cooling water inlet and outlet in manifolds, respectively.

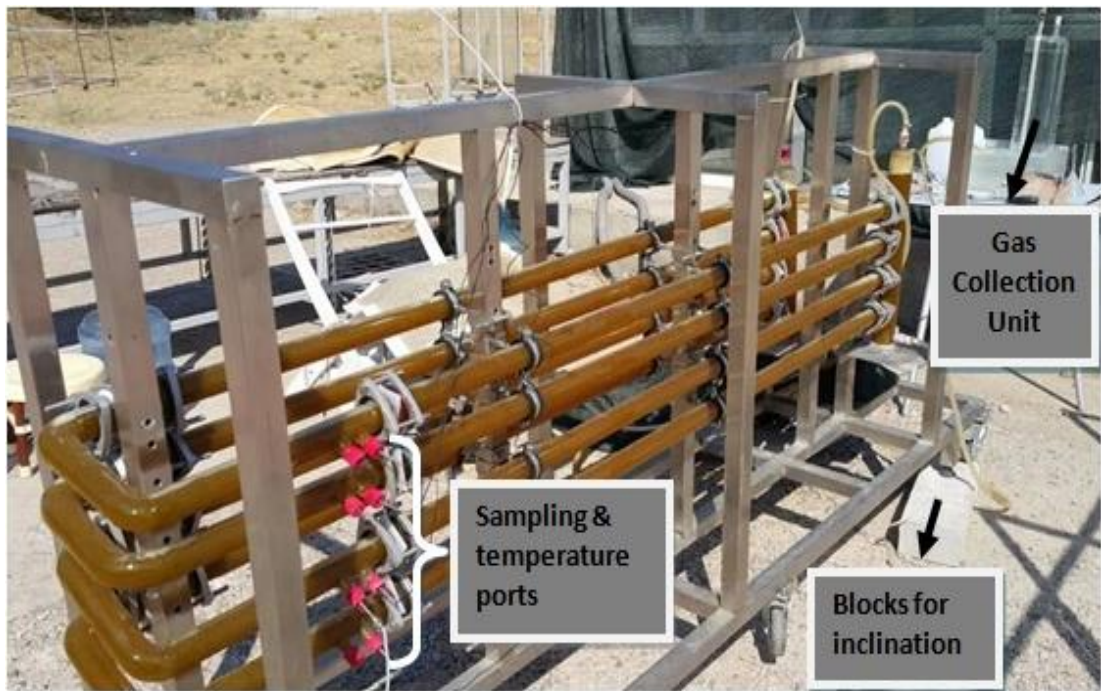
The recirculation of the liquid culture was achieved by a peristaltic pump (Cole-Parmer, Masterflex L/S). In a previous study, although the cell growth was nearly the same, peristaltic pump was suggested compared to aquarium pump since it was easier to adjust the flow rate with peristaltic pump (Kayahan 2015). It was also stated that centrifugal pump requires an additional recycle loop (to reduce the flow rate to the targeted Reynolds number range) which brings extra connections causing potentially leakage problem. Furthermore, most of the connections of centrifugal pump are metal which can affect the hydrogen production and bacterial growth (Avcioglu 2010). Therefore, peristaltic pump was preferred as a suitable pump type for the pilot-scale outdoor experiment.

The fluid was distributed to the tubes by one inlet and one outlet manifold, which were identical and made of glass. The cooling of the overheated culture medium during summer was achieved by coolant water circulation from glass cooling coils inserted into the manifolds. The temperature of the liquid culture was maintained below 40°C by circulating coolant water at a temperature around 10°C with a PID temperature controller system (PNÖSO PSS 6 D). Cooling water inlet (CW-in) and cooling water outlet (CW-out) of the inlet manifold were shown in Figure 3.4b. The liquid temperature of the bacterial culture was measured by thermocouples inserted into the temperature ports, and sampling was done from sampling ports of the U-tubes. The number of temperature and sampling ports were reduced from 12 to 4 compared to the previous design (Kayahan 2015) to prevent the potential leakage problem (Figure 3.4a).

Manifolds allowed both circulation of the fluid in four glass tubes and collection of the produced gas at the upper side of the manifold. When the gauge gas pressure inside manifolds reached 1/3 psi, the check valves (V4 and V5 Figure 3.3) opened and gas transferred to the gas collection unit with polyurethane pipes. The volume of the produced gas was measured by the water displacement method at an atmospheric pressure. In order to collect gas easily 30° angle was given to the tubes on their horizontal axes as in the study of Kayahan et al. 2017. Apart from previous design, a

slight inclination (about 10°) from the ground was given to the reactor to facilitate the collection of the produced gas using blocks. Also wheels were fitted to the stand for ease of movement. A photograph of the reactor taken during the experiment is given in Figure 3.4a. The flow rate in a single tube was set to 10.5 L/h corresponding to a Reynolds number (Re) of 92, because that value was resulted in the least pressure drop and the most uniform flow profile for the same reactor type (stacked U-tube PBR) in smaller volume (Kayahan, Eroglu, and Koku 2016).

(a)



(b)



Figure 0.12. A photograph of (a) stacked U-tube photobioreactor (b) inlet manifold performed with *R. capsulatus* hup- on molasses. CW-in and CW-out are coolant water inlet and outlet, respectively. The experiment started on August 7th, 2016.

3.3.3.2. Start-up: Leakage Test, Sterilization and Inoculation

After construction, the photobioreactor was filled with water to test the leakage from the fittings. After no leakage was observed, the reactor was sterilized by the circulation of a 3% H₂O₂ solution for 24 hours, and then washed with distilled water twice before start-up of the experiment.

Bacteria was inoculated into hydrogen production media containing molasses diluted to have 5mM sucrose after the pretreatment process, which includes colony selection, growth and adaptation periods. At the start-up, the inoculation was made by adjusting the cell concentration to 0.23 g/L corresponding to the exponential growth phase which was previously described as the optimal phase for hydrogen production (C. H. Sasikala, Ramana, and Rao 1995; Harun Koku et al. 2003).

3.3.3.3. Operation: Feeding and Sampling

Initially, the sucrose concentration in the reactor was adjusted to 5 mM by dilution of molasses. When the sucrose consumption nearly stopped, the sucrose concentration was adjusted to 5 mM by feeding diluted molasses. The sucrose feedings were done on 7th, 11th and 16th days of the experiment when the sucrose consumption nearly stopped for 3-4 days. No glutamate addition was done. During feeding, 1 L feed was given to the reactor while 1 L reactor fluid was discharged at the same time to maintain the same reactor volume. Once in the morning and once in the evening, 40 mL from the reactor was sampled for analyses of cell, sugar and organic acid concentrations besides pH analysis. The produced gas was sampled daily and analyzed. The sampling ports are shown in Figure 3.4a and all analyses were explained in detail in Section 3.4.

3.4. Analyses and Measurements

Twice in a day, 40 mL culture media was taken to analyze pH, bacterial growth, gas composition, sugar concentration and organic acid concentration. The produced gas was collected into the gas collection unit and sampled daily for the analysis of the gas component. In addition, online measurements of solar irradiation, rain and air temperature was done with a weather station (Davis Vantage Pro2, with solar radiation sensor). From four temperature ports, online measurement of the reactor temperature was also done with thermocouples.

3.4.1. Temperature

For indoor experiments, temperature was maintained around 30°C inside incubator. The temperatures of the reactor and the ambient air were monitored continuously for the outdoor experiment. The reactor temperature was monitored by Fe-constantan J-type thermocouples in 15 minute intervals with an online data logger (Ordel UDL100) connected to a computer. One temperature measurement was done from each tube from a total of four temperature ports as shown in Figure 4a. The ambient air temperature was also measured by the online weather station.

3.4.2. Light Intensity

For indoor small-scale experiments, light intensity was measured with a luxmeter (Lutron LX-105 Light Meter). The bioreactors kept in an incubator were illuminated by 100 W tungsten lamps. The light intensity on the surface of the bioreactors was adjusted around 2000 lux. In the outdoor experiment, light intensity (solar irradiation) was measured by the solar radiation sensor of the weather station. In addition, the rain data was measured with the weather station for the outdoor experiment. The online measurements of the weather station were recorded with 5 minute intervals.

3.4.3. pH

The pH was measured with a pH meter (Ezdo MP-103) during the experiments. Initial pH of the hydrogen production media was adjusted to 7.5 for both indoor and outdoor experiments. pH of the culture media was measured daily for indoors and twice in a day for the outdoor experiment (once in the morning and once in the evening). In order to increase the accuracy, the measurements were done twice in the indoor experiments and three times in the outdoor experiment for each sample and the averages were reported (Appendix D-c). The calibration of the pH meter was done daily by using standard solutions with the accuracy of at least 95%.

3.4.4. Cell Concentration

The bacterial cell concentration was measured with a UV Spectrophotometer (Shimadzu UV- 1201) at 660 nm. At this wavelength, an optical density of 1.0 corresponds to a bacterial cell concentration of 0.46 g/L for *R. capsulatus hup⁻* (Öztürk 2005). The measurements were done twice daily for the indoors and outdoor experiments (once in the morning and once in the evening). Average of the measurements for cell concentration was recorded (Appendix Db).

3.4.5. Molasses

Molasses diluted to have 5 mM sucrose in the reactor fluid was used as substrate for the outdoor experiment with the pilot-scale U-tube photobioreactor. The analysis of sugar content, total nitrogen and some elements such as sodium, potassium and calcium in molasses were done by Ankara Sugar Factory, Turkey (Appendix B). In addition, the analysis of amino acid content (i.e. glutamate), and some elements (i.e. Fe and Mo) in molasses were done by Düzen Norwest Laboratory (Ankara, Turkey) (Appendix B).

The analyzed glutamate and sucrose in molasses are the main nitrogen and carbon sources for the bacteria, respectively. Fe and Mo are also contained in molasses which are the nutrients needed for bacterial growth. After diluting the molasses to adjust the sucrose content as 5mM; extra glutamate, Fe and Mo addition was done to obtain the desired amounts in the hydrogen production media.

3.4.6. Sugar and Organic Acids

In the small-scale experiments, substrate (sugar source) was either glucose or fructose, while it was sucrose obtained by diluted molasses for the outdoor experiment. Organic acids especially lactic acid, acetic acid, and formic acid were released during the photofermentative hydrogen production.

Sugar (sucrose, glucose or fructose) and produced organic acid concentrations in the reactor medium were analyzed by High Performance Liquid Chromatography (HPLC), which was Shimadzu 20A series equipped with an Alltech IOA-1000 column of length and diameter 300 mm and 7.8 mm, respectively. Organic acids were also analyzed by HPLC (Shimadzu 20A series). Two detectors (RI and UV) connected in series were used in HPLC. The sugar concentrations were determined by the RI detector and the organic acid concentrations were determined by the UV detector. Sulfuric acid (8.5 mM) was used as a mobile phase with 0.4 mL/min flow rate and 60°C oven temperature. A UV detector (Shimadzu SPD-20A) whose

absorbance was set at 210 nm was used for the detection of organic acids. The calibration was done by using standard solutions for organic acids. The concentration of lactic acid, acetic acid and formic acid were measured according to the retention times and peak areas. The same method was used for detection of the sugar content with HPLC.

3.4.7. Gas Composition

The composition of the produced gas during the experiment was determined by a gas chromatograph (Agilent Technologies 6890N) equipped with a Supelco Carboxen 1010 column. Samples were injected to the gas chromatography with a gas-tight syringe (Hamilton, 22 GA 500 μ L) and a thermal conductivity detector was used. Argon was used as the carrier gas with a flow rate of 26 mL/min. The temperatures of the oven, injector and detector were 140, 160 and 170 °C, respectively. The produced gas was consisted of hydrogen, carbon dioxide and a neglected small amount of air which was probably due to the off-line measurement.

3.5. Data Analysis and Calculations

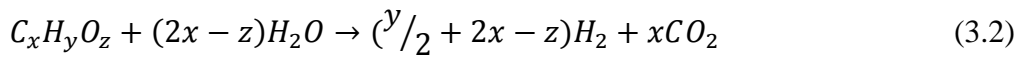
The substrate conversion efficiency (yield) and hydrogen productivity were calculated for the evaluation of the hydrogen production analysis. Furthermore, light intensity distribution inside the photobioreactor was calculated according to Beer-Lambert's law in the light of a previous study (Uyar et al. 2007).

3.5.1. Substrate Conversion Efficiency (Yield)

The substrate was glucose or fructose in the small scale experiments while sucrose obtained by diluted molasses was used as substrate in the pilot-scale experiment. The substrate conversion efficiency (yield) is defined as the actual moles of hydrogen produced over the theoretical moles of hydrogen produced that is calculated by assuming all the consumed substrate (sucrose, glucose or fructose) is used for hydrogen production (Equation 3.1).

$$\% \text{ Yield} = \frac{\text{Moles of H}_2 \text{ produced}}{\text{Theoretical limit of H}_2 \text{ production (moles)}} \times 10 \quad (3.1)$$

Theoretical moles of hydrogen were calculated from Equation 3.2 (Koku et. al, 2002). Theoretically 12 moles of hydrogen per mole of glucose or fructose can be produced since x, y and z values as 6, 12 and 6, respectively in Equation 3.2. In a same manner, theoretically 24 moles of hydrogen can be produced per mole of sucrose (C₁₂H₂₄O₁₂).



3.5.2. Hydrogen Productivity

Hydrogen productivity is defined as the amount of hydrogen produced (moles) per volume of the reactor (L) and duration (hour). Productivity, the rate of hydrogen production, allows evaluating the hydrogen production during the experiments and comparing with the other studies in literature. The formula of the productivity is shown below;

$$\text{Productivity} = \frac{\text{Moles of H}_2 \text{ produced}}{\text{Reactor volume(L)} \times \text{Time(h)}} \quad (3.3)$$

CHAPTER 4

RESULTS AND DISCUSSION

4.1. Indoor Small-Scale Photobioreactors

The small-scale indoor experiment sets were carried out with *R. capsulatus* *hup*⁻ using glucose and fructose as substrate. The first small-scale experiment was conducted with duplicate runs of 10, 30 and 50 mM glucose containing hydrogen production media (January 5th - January 14th, 2016). In the second experiment 10, 30 and 50 mM fructose were used instead of glucose and the same procedure was applied (February 17th – March 2nd, 2016).

The three substrate concentrations corresponded to three different carbon-to-nitrogen (C/N) ratios, specifically 20, 50 and 80, enabled the evaluation of the effect of C/N ratio on hydrogen production. Sucrose contained in molasses, which is the substrate of pilot-scale experiment, is used in bacterial metabolism after degradation to fructose and glucose. Therefore, the C/N effect on biohydrogen production conducted with fructose and glucose in small-scale experiments helped to decide the appropriate C/N ratio for the pilot-scale experiment. It also allowed comparison of glucose and fructose as substrates in terms of yield and hydrogen productivity. C/N ratio, sugar type and concentrations of the runs were shown in 4.1. Glutamate was adjusted to 4 mM for each run

Table 4.1. *C/N ratio, sugar type and concentrations of the runs*

Run	C/N ratio	Sugar Type	Concentration
R1f	20	Fructose	10 mM
R2g	20	Glucose	10 mM
R3f	50	Fructose	30 mM
R4g	50	Glucose	30 mM
R5f	80	Fructose	50 mM
R6g	80	Glucose	50 mM

4.1.1. Experiments with *R. capsulatus* hup⁻ on 10, 30 and 50 mM Glucose

10mM, 30mM, and 50mM glucose were used as carbon sources and 4mM glutamate was used as the nitrogen source for all bioreactors. Duplicate runs were carried out for each concentration, which makes totally six runs for glucose (R1g and R2g=10Mm, R3g and R4g=30mM, R5g and R6g=50 mM glucose). The experiments lasted for 9 days and ended when the hydrogen productions nearly stopped.

4.1.1.1. Glucose and Organic Acid Concentrations

Three bioreactors (R2g, R4g and R6g) were operated with hydrogen production media in batch mode. First, the effect of various C/N ratios at start-up on glucose consumption rates was observed in which shows the change in glucose concentration by time (Figure 4.1).

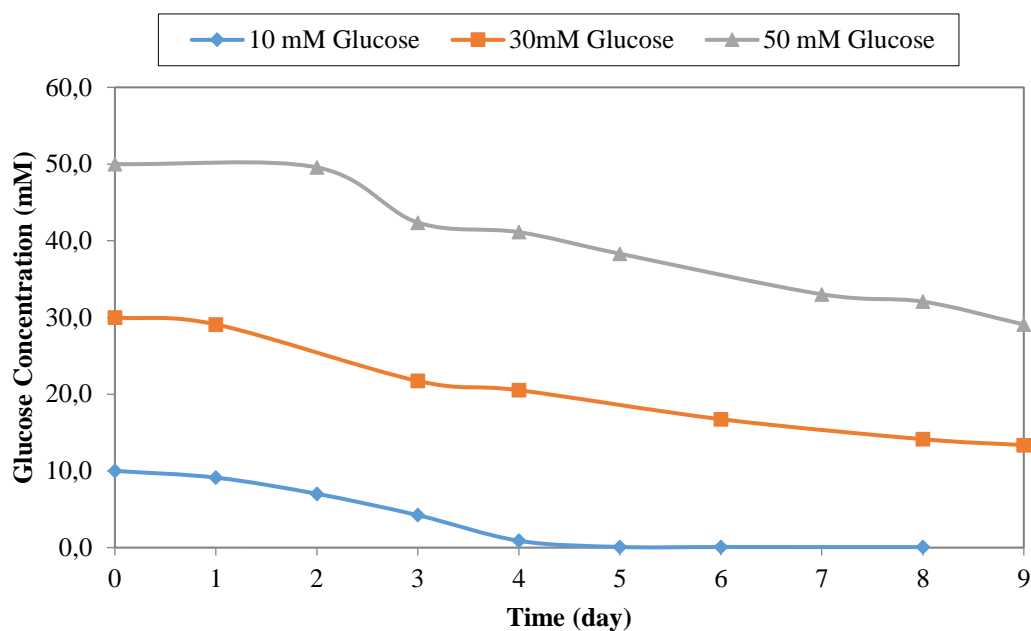


Figure 4.1. Daily change in glucose concentration for 10, 30 and 50 mM glucose feedings.

As seen from Figure 4.1 that while glucose was completely consumed in the 4th day for C/N ratio of 20 (10 mM glucose), the glucose remained unconsumed at the end of the experiment for higher C/N ratios (for 30 and 50 mM glucose).

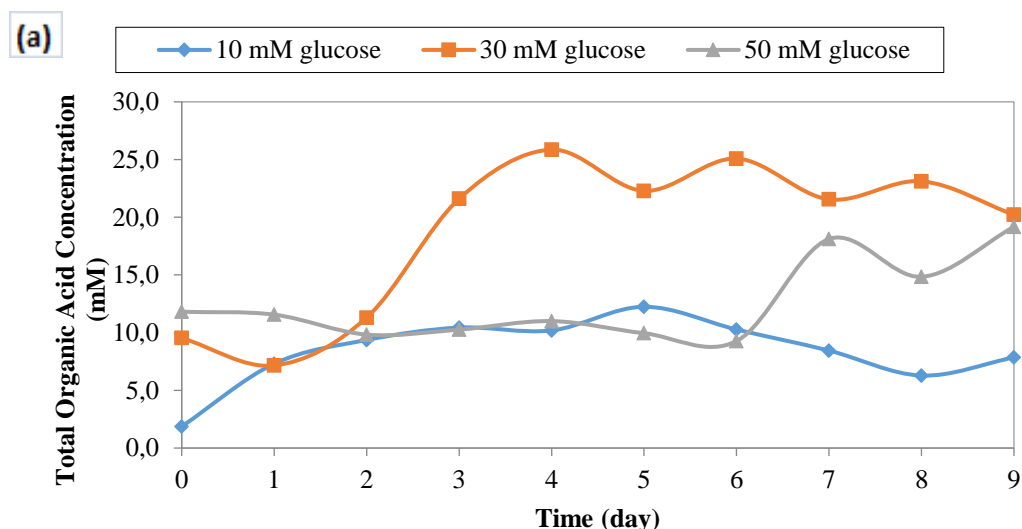
For further investigation, the term substrate conversion efficiency (% yield) is calculated for various C/N ratios. Theoretically 12 moles of hydrogen per mole of glucose can be produced. The calculated percent yields are shown in Table 4.2 for the C/N ratios of 20, 50 and 80 by using the glucose consumption data represented in Figure 4.1.

Table 4.2. Substrate conversion efficiencies (% yields) for 10mM (R2g), 30mM (R4g) and 50mM (R6g) glucose feedings at start-up.

% Yield for R2g (C/N=20)	% Yield for R4g (C/N=50)	% Yield for R6g (C/N=80)
21.0	15.1	11.4

According to Table 4.2, the substrate conversion efficiencies decreased with decreased C/N ratio. It can be suggested that a lower C/N ratio might be preferable for large-scale experiment since the highest percentage of yield (21.0%) was for the lowest C/N ratio (20).

In a previous study, bacterial growth was observed in a pH range of 6 and 9 while the maximum hydrogen production was achieved at pH=7, which is suggested as optimum pH (K. Sasikala, Ramana, and Raghuveer Rao 1991). The pH at the beginning of experiment was adjusted to 7.5 to tolerate the pH drop. The pH drop mainly caused by the produced organic acids such as formic acid, lactic acid and acetic acid during the photofermentative hydrogen production. Therefore, individual and total organic acid production for R2g, R4g and R6g were measured daily. Besides, pH change was measured every day during the experiments. The changes of total and individual organic acid concentrations and pH were shown in 4.2 and 4.3.



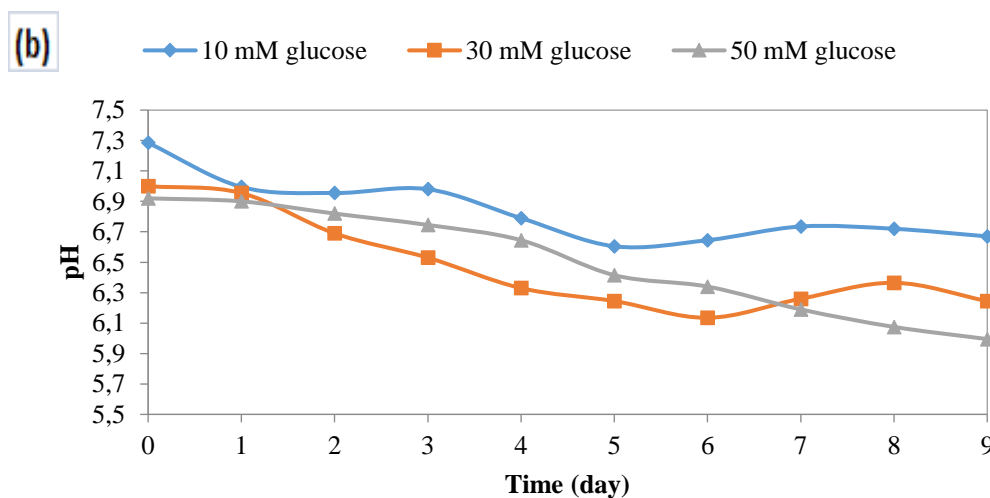


Figure 4.2.(a) Daily variations of the total organic acids (b) pH change during biogas production for 10, 30 and 30 mM glucose feedings.

It can be seen from Figure 4.2a that organic acid accumulation started on the 0th, 1st and 6th days for 10, 30 and 50 mM glucose concentrations, respectively. According to the Figure 4.2b, pH values decreased during biogas production for 10mM, 30mM and 50mM glucose feeds, as expected. The lowest pH value was observed as 6.0 for 50mM glucose while it was 6.7 for 10 mM glucose. It can be stated that as the glucose concentration and therefore the C/N ratio was increased, pH dropped more. This pH drop was an undesired situation since the optimal hydrogen production was observed around pH 7.0 as reported in previous studies (Kayahan, Eroglu, and Koku 2017; K. Sasikala, Ramana, and Raghuvver Rao 1991). This also supported the proposition that a lower C/N ratio might be preferred for the pilot-scale experiment for less pH drop.

Poly- β -hydroxybutyrate (PHB) is produced with an increase in the organic acid as carbon source (Wu et al., 2012). Since organic acids are also carbon sources for hydrogen production, PHB production pathway becomes favorable when organic acids accumulated, which decreases the hydrogen production (Doğan E.M., MSc. Thesis, 2016). Therefore, carbon balance was done to investigate whether the organic acids produced are directed towards PHB production. The carbon balance

was done for C/N of 50 (30 mM glucose and 4mM glutamate), since the most organic acid accumulation was obtained compared to other C / N ratios.

Table 4.3. The carbon balance for 30 mM glucose (C/N=50).

(1) Uptake of carbon* (Δmmol)	(2) Lactic acid (mmol ΔC)	(3) Formic acid (mmol ΔC)	(4) Acetic acid (mmol ΔC)	(5) CO _{2(aq.)} + HCO _{3(aq.)} (mmol ΔC)	(6) CO _{2(gas)} (mmol ΔC)	(7) Biomass (mmol ΔC)	(8) Total carbon of products** (mmol ΔC)
4.00	-0.28	0.35	0.56	1.43	0.50	0.52	3.08

* Carbon uptake from glucose and glutamate.

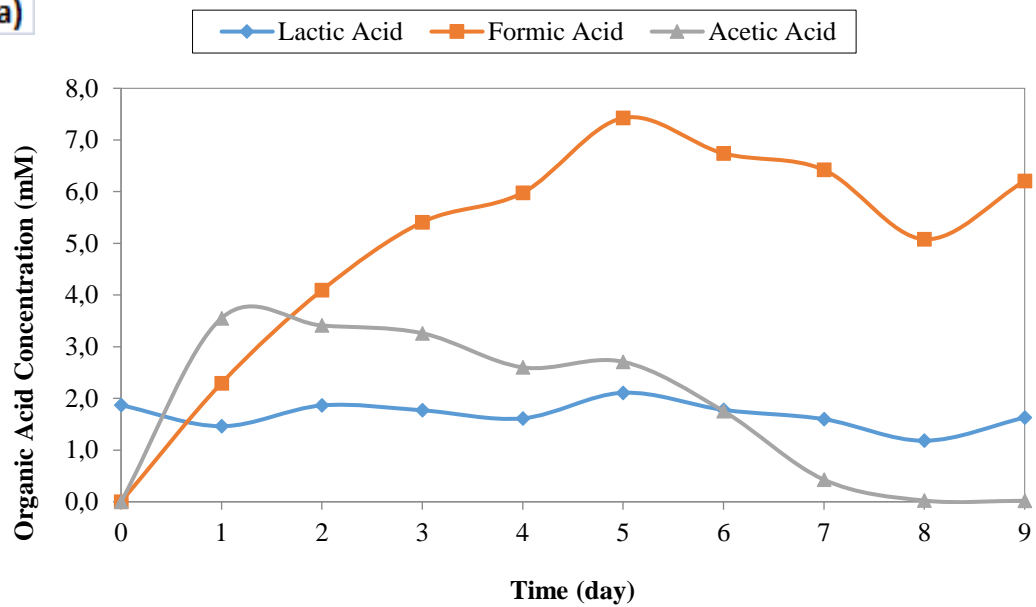
** Sum of values of columns (2) to (7)

The carbon balance for 30 mM glucose was shown in Table 4.3. It was found that 10 mM of the glucose was consumed during the entire run. Thus the total moles of carbon uptake was calculated as 4 mmoles from glucose and glutamate, assuming all glutamate in the feed was consumed by the bacteria. The total moles of carbon of the final quantifiable product distribution was calculated from difference between initial and final concentrations of organic acids (acetate, formate and lactate), carbon dioxide (in aqueuos and gas phase), bicarbonate and biomass. The liquid phase mole fraction of the carbon dioxide was calculated by using the following equation;

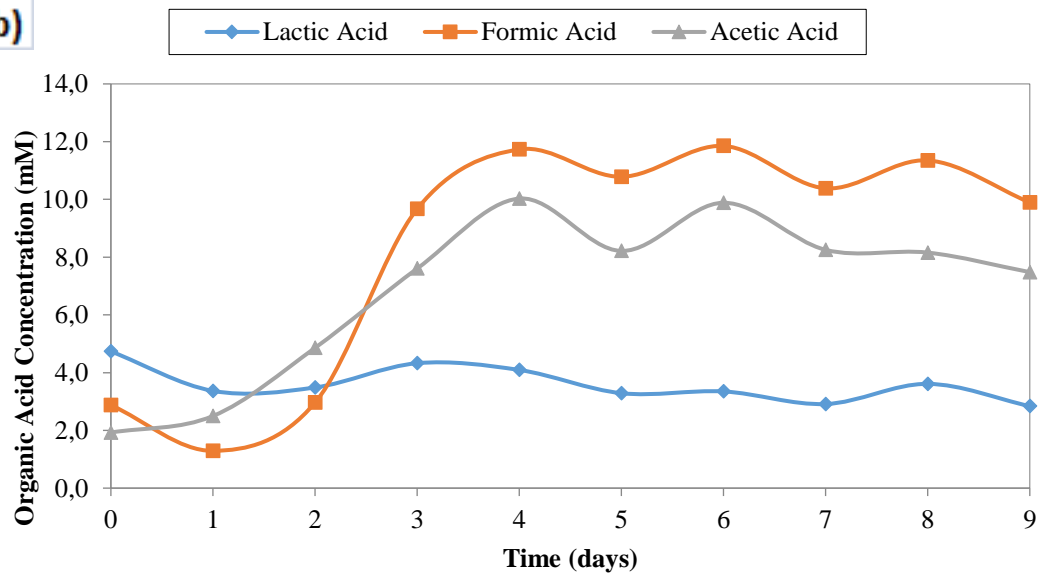
$$y.P = x.H \quad (4.1)$$

where y is mole fraction in gas phase, x is mole fraction in aqueous phase, P is total pressure and H is Henry's Law constant (1651.9 bar for CO₂). Bicarbonate was calculated according to a previous study, where mole fraction of carbon dioxide-to-bicarbonate is 0.3/0.7 for the average pH_{avg.} = 6.6 (Koku et al. 2002). According to Table 4.3, the amount of carbon due to the measurable concentrations of the final product was found to be less than the carbon uptake via glucose and glutamate, which indicates that some of the given carbon might be used for other bacterial metabolism such as PHB formation, that could not be measured. Furthermore, produced organic acids were measured individually to understand the bacterial mechanism and which acid/acids mainly responsible from pH drop to 4.3.

(a)



(b)



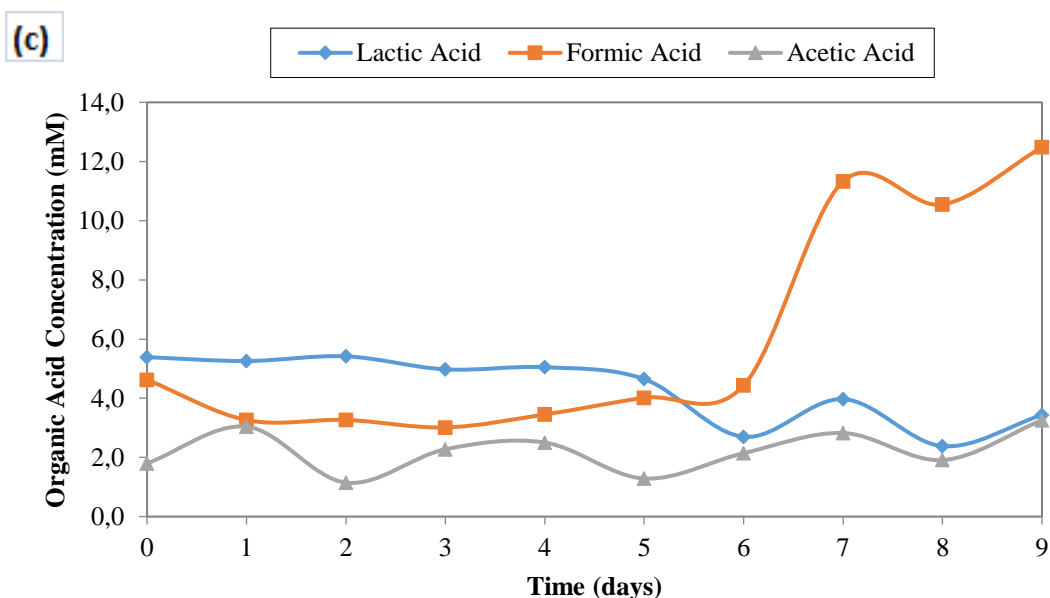


Figure 4.3. Daily change in organic acid concentrations for (a) R2g (10mM Glucose), (b) R4g (30mM Glucose) and (c) R6g (50mM Glucose).

Lactic acid and acetic acid are commonly utilized substrates by *R. capsulatus* in photofermentative hydrogen production. It was previously reported that these bacteria can also consume some of the produced acids. For instance, it was reported that *R. capsulatus* has formate dehydrogenases enzymes which catalyze the oxidation of formate to CO_2 and H^+ (Hartmann, T. and Leimkühler, S., 2013). Therefore after 4th day, decrease in acetic acid and formic acid concentration might be attributed with a start of the consumption of these acids as presented in Figure 4.3a. In Figure 4.3b similar oscillations of formic and acetic acids were noticed while lactic acid concentration was nearly stable around 4mM during this period. On the other hand in Figure 4.3c, acetic acid and lactic acid concentrations remained around 2-3 mM concentrations while formic acid concentration reached around 12 mM at the end of the experiment. It can be concluded that C/N ratios also affected the amount and percentage of the produced organic acids.

According to Figure 4.3a-b-c, most of the accumulated acid was formic acid for all glucose concentrations. Since lactate and acetate are more commonly utilized substrates compared to formate, they remained in relatively lower concentrations.

Therefore, most of the pH drop was due to the formic acid accumulation according to the all three figures. PNS bacteria metabolism was previously modeled and the least effective organic acid for hydrogen production was found as formic acid (Doğan E. M., MSc. Thesis, 2016). Therefore, it might affect hydrogen production negatively since mostly formic acid was found to be accumulated.

4.1.1.2. Growth and Hydrogen Productivity

Growth of bacteria is an important parameter because low cell concentrations lead less hydrogen production while very high concentrations reduce or stop hydrogen production by preventing sufficient light into the photobioreactor. Therefore, sustaining optimal bacterial concentrations for efficient biohydrogen production is crucial. In this study, the effect of C/N ratios (20, 50 and 80) on bacterial growth was investigated for 10mM and 30mM glucose feedings with 4mM glutamate.

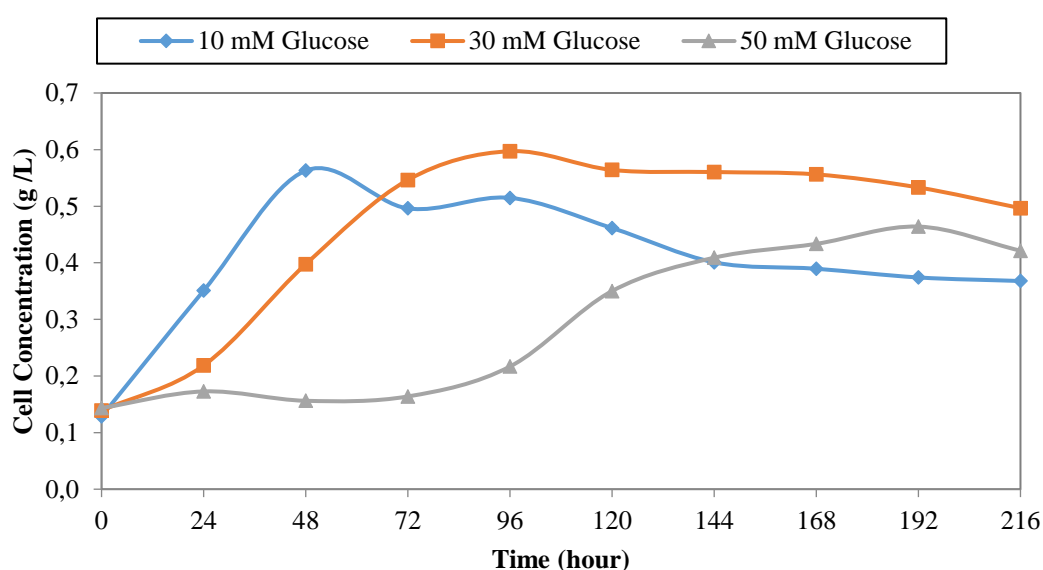


Figure 4.4. Change in cell concentration in gram dry cell weight over liter culture (g/L) with respect to time for 10, 30 and 30 mM glucose feedings.

Another important factor is lag phase which is defined as adaptation period of bacteria to the substrate. After lag phase, exponential growth phase begins where the

hydrogen production mostly occurs. Therefore, lower lag phases are preferable to fasten the adaptation of bacteria and to start hydrogen production earlier.

As seen in Figure 4.4, the adaptation period of bacteria was longer for higher glucose concentrations. While exponential growth phase was observed in the first day for 10 mM glucose, it was observed after 3 days for 50 mM glucose medium. It was concluded that lower C/N ratio might be preferred for the pilot-scale experiment also to reduce the adaptation period of the bacteria. Maximum growth was observed as around 0.55 ± 0.05 gdcw/Lc for all runs.

Finally, the total produced hydrogen during the experiment was recorded daily and shown in Figure 4.5.

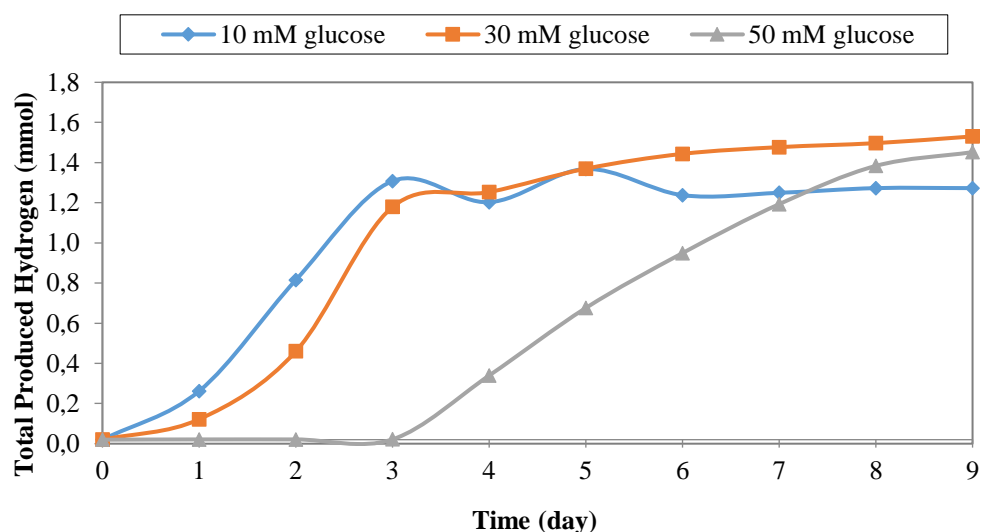


Figure 4.5. Total produced hydrogen for 10, 30 and 50 mM glucose having C/N ratio of 20, 50 and 80, respectively.

According to Figure 4.5 hydrogen productions started later for higher glucose concentrations (C/N ratios) due longer adaptation periods. Hydrogen production started on 0th, 1st and 3th days for C/N ratios of 20, 50 and 80, respectively (Figure 4.4). It can be concluded that the lag phase for hydrogen production decreased with decreased C/N ratio. In order to reduce the lag phase for hydrogen production, lower C/N ratio could be preferred for the pilot-scale outdoor experiment. These longer lag

periods for hydrogen production can be due to the late adaptation of the bacteria for higher C/N ratios as seen in Figure 4.4.

It results that adaptation of the bacteria to the sugar before the experiment can decrease the lag period. Therefore, sucrose adaptation was done for the pilot-scale experiment aiming to start hydrogen production earlier.

Most of the hydrogen was produced during the growth phases for all C/N ratios, as previously reported that the growth phase was the optimal stage for hydrogen production (C. H. Sasikala, Ramana, and Rao 1995; Harun Koku et al. 2003). The highest value of maximum hydrogen productivities was 0.45, 0.60 and 0.28 (mol H₂/(m³.h) for 10, 30 and 50 mM glucose, respectively. The maximum hydrogen percentage in produced biogas was determined as 85% for 10 mM glucose.

4.1.2. Experiments with *R. capsulatus* hup- on 10, 30 and 50 mM Fructose

The same experiment was done by using fructose instead of glucose to observe the effect of substrate (glucose or fructose) on hydrogen production. The substrate of pilot-scale experiment was sucrose (contained in molasses) which consists of glucose and fructose. Therefore, it was also observed how glucose and fructose are used differently in pilot-scale biohydrogen production after degradation of sucrose.

10mM, 30mM, and 50mM fructose with 4mM glutamate were used to observe the effect of fructose concentration and C/N ratio on photofermentative hydrogen production. Duplicate runs were prepared for each concentration, which makes totally six runs for fructose (R1f and R2f=10Mm, R3f and R4f=30mM, R5f and R6f=50 mM fructose). The results of fructose and organic acid concentrations, cell growth and hydrogen productivity are given and discussed for R1f, R3f and R5f. The experiments were lasted for 12 days and were ended when the hydrogen productions nearly stopped.

4.1.2.1. Fructose and Organic Acid Concentrations

Three bioreactors were operated with 10, 30 and 50 mM fructose containing hydrogen production and same glutamate concentration (4 mM). The experiments were conducted in batch mode. The change in substrate (fructose) concentration during the experiment is shown in Figure 4.6.

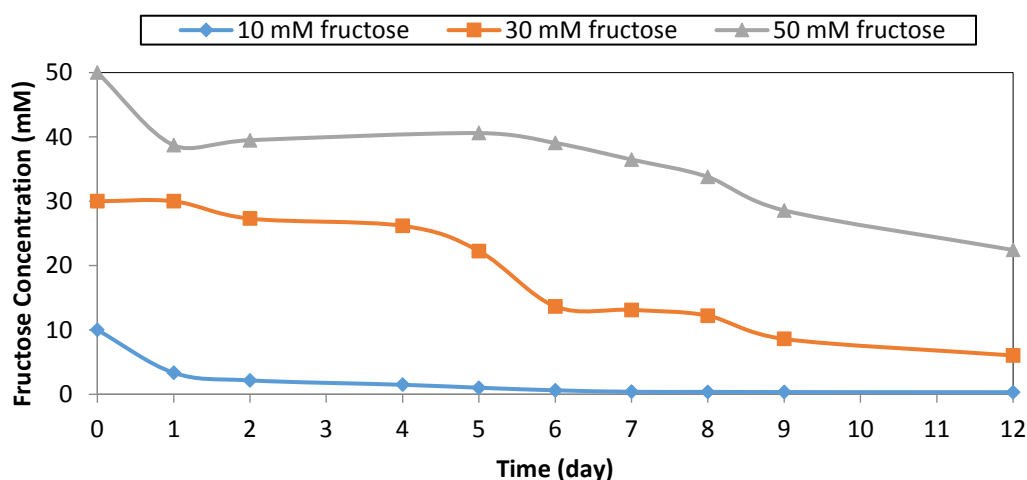


Figure 4.6. Daily change in fructose concentration for 10, 30 and 30 mM fructose feedings.

C/N ratios of the 10, 30 and 50 mM glucose and fructose were the same (20, 50 and 80, respectively). As in the glucose feedings, it was also observed that C/N ratio at start-up affected the substrate (fructose) conversion Figure 4.6. In order to further investigate the effect of initial fructose concentration of hydrogen production, substrate conversion efficiencies (yields) were calculated and indicated in Figure 4.3.

Table 4.4. Substrate conversion efficiencies (yields) for 10mM (R1f), 30mM (R3f) and 50mM (R5f) fructose feedings at start-up.

% Yield for R1f (C/N=20)	% Yield for R3f (C/N=50)	% Yield for R5f (C/N=80)
13.8	7.0	3.7

Similar to glucose feedings, the substrate conversion efficiency (yield) value increased with decreased C/N ratio Figure 4.3. It was suggested that low C/N ratio might be preferable for large-scale experiment since the highest percentage of yield (13.8%) was for the lowest C/N ratio (20). The change of produced individual and total organic acids and pH drop were shown in Figure 4.7 and Figure 4.8.

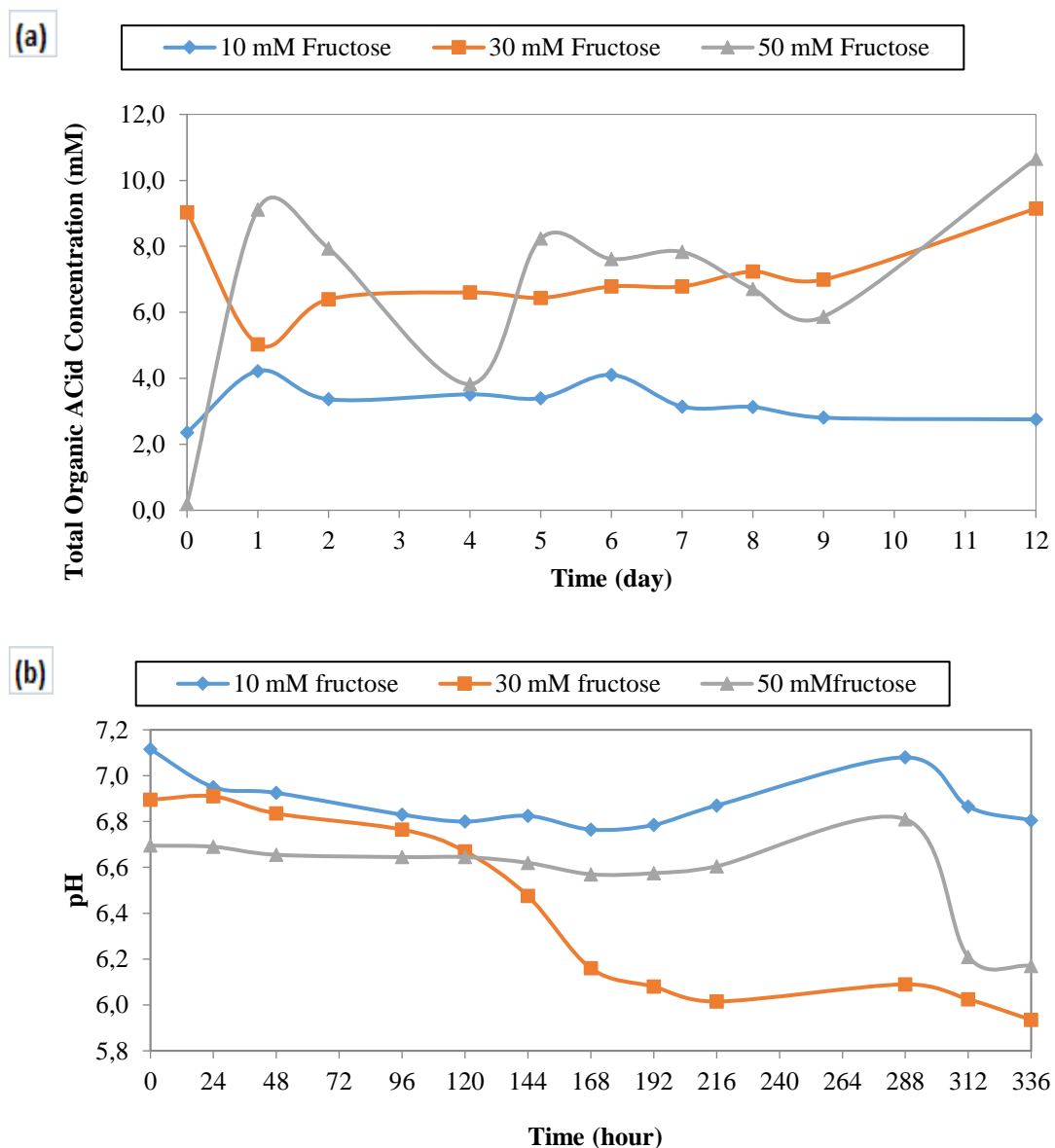
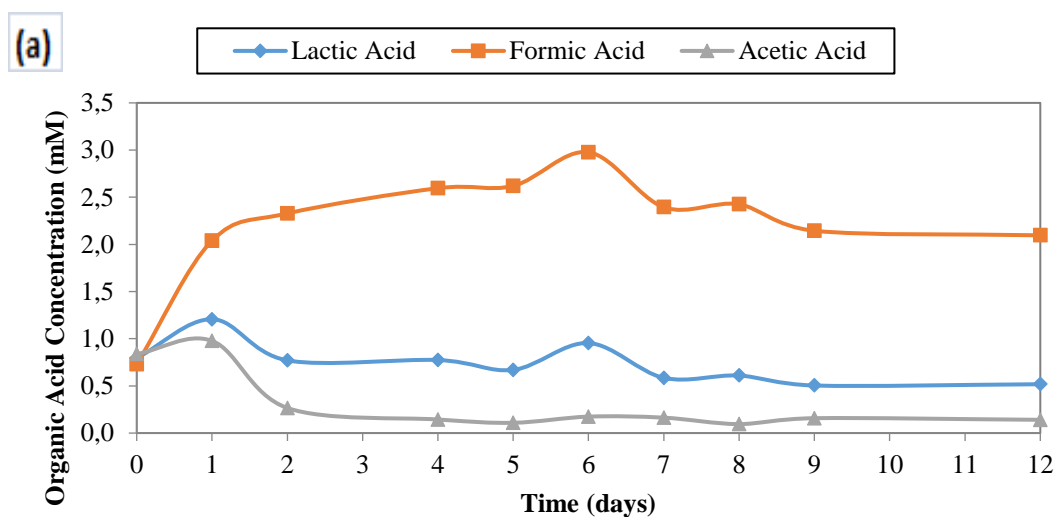


Figure 4.7. Daily variations of the total organic acids (b) pH change during biogas production for 10, 30 and 30 mM fructose feedings.

As seen in Figure 4.7a, while the total amount of organic acid in the liquid medium for 30 and 50 mM fructose was around 9-10 mM, it was around 3 mM for 10 mM fructose (C/N=20). As a result of this low organic acid production, the least pH drop was observed (6.8) for C/N=20, while the pH of the others decreased to around 6.0 ± 1 as shown in Figure 4.7b. It was concluded that the least pH drop was observed for the lowest C/N ratio. It was reported in a previous study that the maximum hydrogen production was obtained at pH=7 (K. Sasikala, Ramana, and Raghuvveer Rao 1991). Therefore, hydrogen productivity can be increased by lowering the C/N value since the closest value to optimal pH (pH=7) was obtained for the lowest C/N ratio.



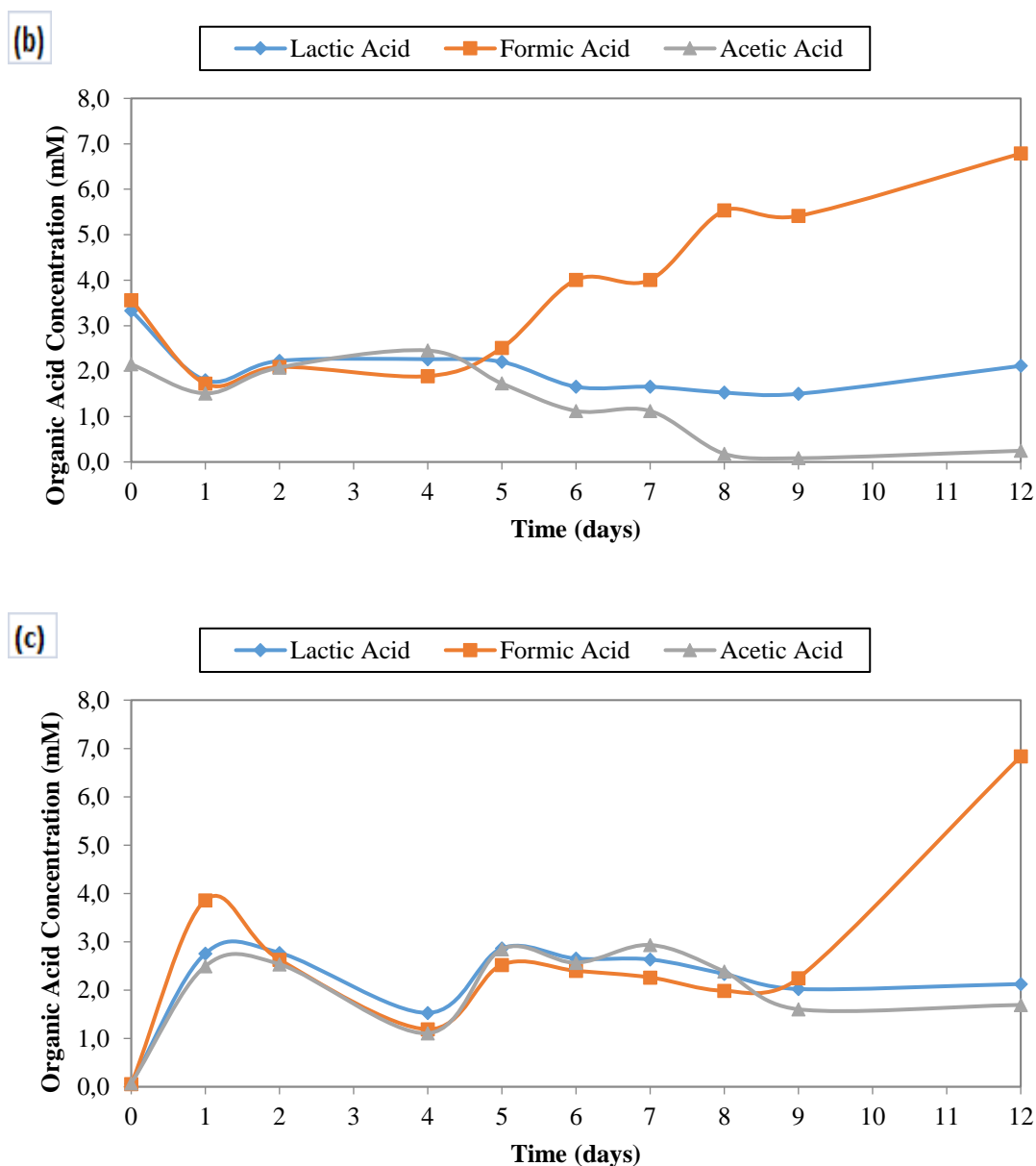


Figure 4.8. Daily change in organic acid concentrations for (a) R1f (10mM Fructose) (b) R3f (30mM Fructose) and (c) R5f (50mM Fructose).

Produced organic acids (lactic acid, formic acid and acetic acid) were also measured individually as in the glucose experiments. According to Figure 4.8, the most accumulated acid was determined as formic acid for all C/N ratios as in the glucose feeding. Since lactate and acetate are commonly utilized substrates by *R. capsulatus*

they had relatively lower concentrations compared to formic acid as in the case of glucose feeding. According to the all three graphs of Figure 4.8, it can be concluded that most of the pH drop was due to the formic acid production. Previously, the least effective organic acid for hydrogen production was reported as formic acid. Therefore, hydrogen production might be affected negatively since mostly formic acid was found to be accumulated, as in the glucose substrate (Doğan E. M., MSc. Thesis, 2016).

4.1.2.2. Growth and Hydrogen Productivity

Sustaining optimal bacterial concentrations for efficient biohydrogen production is crucial. Therefore, the effect of C/N ratios (20, 50 and 80) on bacterial growth was investigated for 10mM and 30mM fructose feedings with 4mM glutamate.

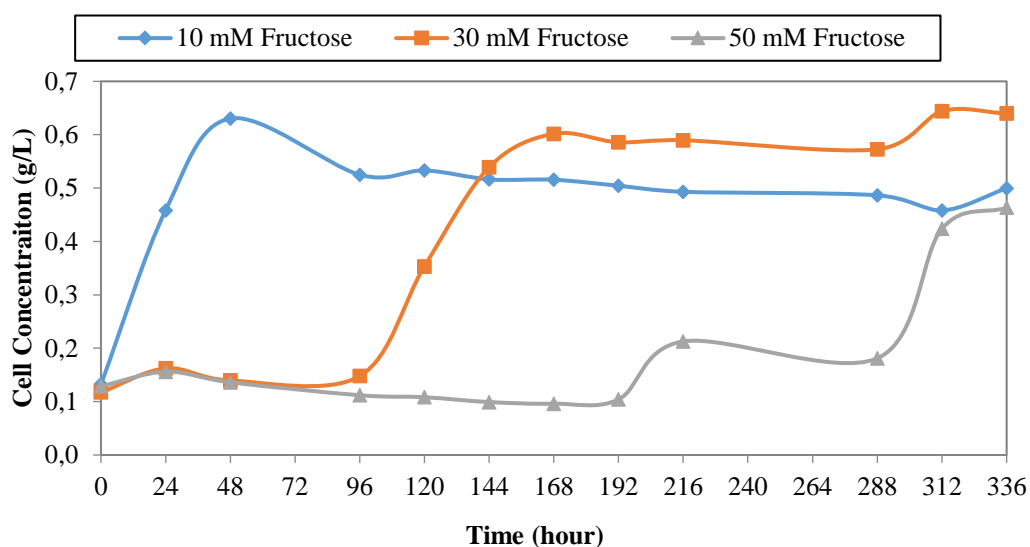


Figure 4.9. Change in cell concentration in gram dry cell weight over liter culture (g/L) with respect to time for 10, 30 and 30 mM fructose feedings

As seen in Figure 4.9, the exponential growth phases were observed on the 1st, 4th and 8th days for 10, 30 and 50mM fructose feedings. It can be concluded that the adaptation of bacteria to the fructose was longer for higher concentrations as in the case of glucose. Therefore, lower concentrated sugars (or lower C/N ratio) could be applied in outdoor experiment to reduce the adaptation period of the bacteria.

According to all glucose and fructose experiments, adaptation of the bacteria to the sugar source before starting the experiment seemed to be needed to reduce the lag phase for growth of the bacteria. It can be seen that the adaptation period for fructose (Figure 4.9) was much longer than glucose (Figure 4.4) for all three C/N ratios. The bacteria adapted to sugar easier and substrate conversion was started earlier for glucose than fructose since the decomposition pathway of glucose (Entner-Doudoroff pathway) was probably more preferable than that of fructose (Embden-Meyerhoff pathway) shown in the Figure 4.10.

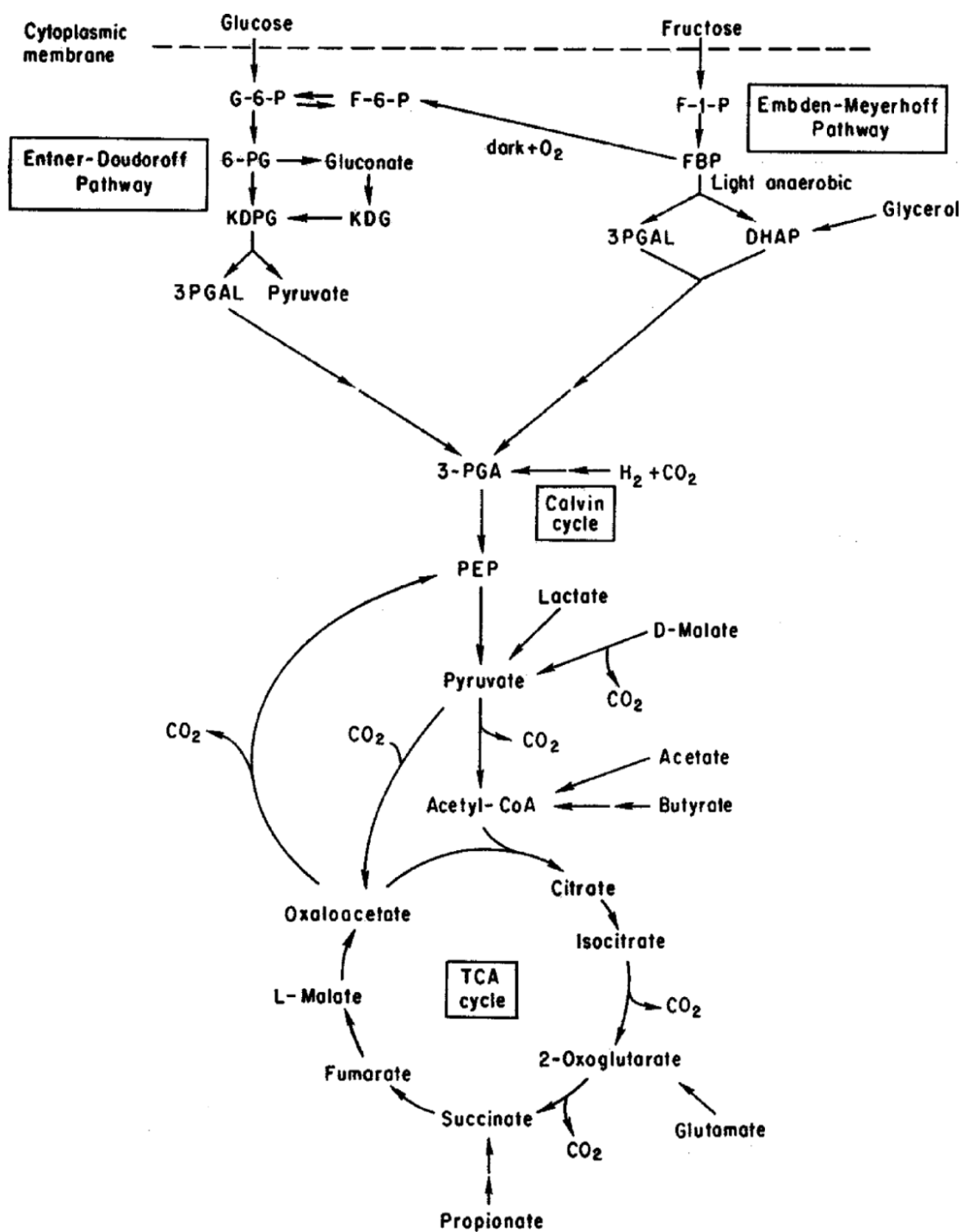


Figure 4.10. A simplified overall scheme of the carbon metabolism in PNS bacteria. (Koku et al. 2002).

At last, the total produced hydrogen during the experiment was recorded daily and shown in Figure 4.11.

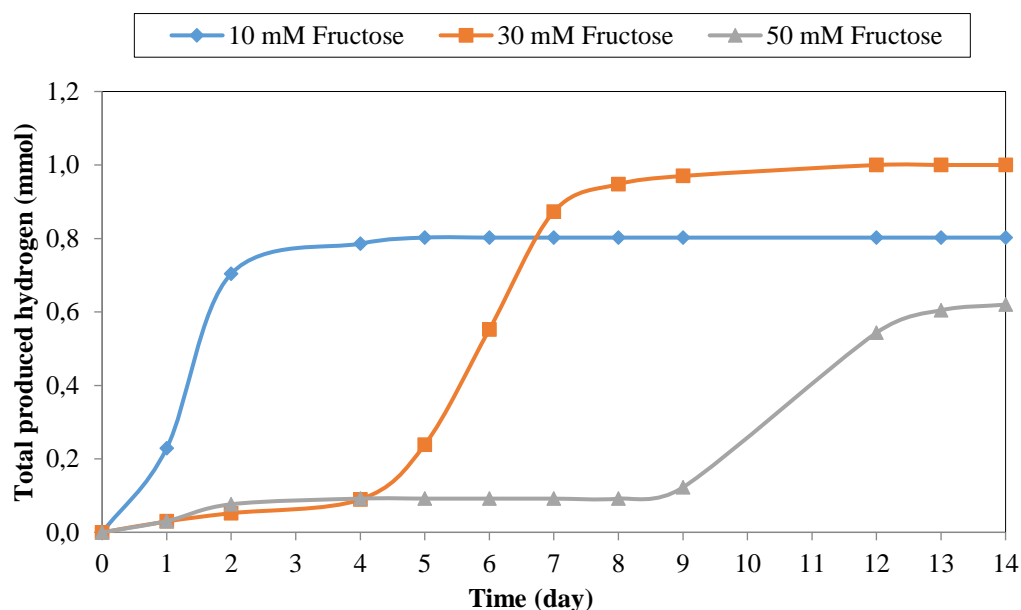


Figure 4.11. Total produced hydrogen for 10, 30 and 50 mM fructose feedings.

As shown in Figure 4.11 the lag phase of hydrogen production was longer for higher concentrations of fructose (higher C/N ratios) as in glucose. Since it was important to reduce the lag phase for hydrogen production to be feasible, a lower C/N ratio can be preferred for the pilot-scale experiment. Furthermore, adaptation of the bacteria to the sugar source before starting the experiment expected to eliminate both the adaptation period and lag period for hydrogen production. The hydrogen productions were started on the 1st, 4th and 8th days for 10, 30 and 50mM fructose feedings following a same trend with the adaptation periods for the bacteria (Figure 4.9). It can be concluded that both lag phase for hydrogen production and adaptation period of the bacteria decreased with decreased C/N ratio for glucose and fructose substrates on *R. capsulatus hup⁻* in indoor photofermentative hydrogen production.

For all C/N ratios, most of the hydrogen was again produced during their the growth phase which was the optimal stage for hydrogen production as previously reported

(C. H. Sasikala, Ramana, and Rao 1995; Harun Koku et al. 2003). The highest value of maximum hydrogen productivities was 0.40, 0.26 and 0.36 (mol H₂/(m³.h) for 10, 30 and 50 mM fructose, respectively. Comparing with glucose, less total amount (moles) of hydrogen and lower hydrogen percentage (80%) in produced gas was determined for fructose.

4.1.3. Comparison of Productivities with Other Small-scale Studies

Comparing the results of two small-scale experiments, it was found that more hydrogen gas was produced by glucose and the adaptation process was shorter for glucose compared to fructose. The productivity term is commonly used to compare the results of the experiments with literature. Comparison of the productivities of the experiments with other studies is shown in Table 4.5. According to the study of Sagir, E. et al. (2017) which was conducted with *R. capsulatus hup⁻*, the highest productivity was also obtained for the lowest C/N ratio.

Table 4.5. Comparison of productivities with other small-scale studies (in glass bottles) with *R. capsulatus hup⁻* in batch mode.

Volume (L)	Substrate	C/N	Productivity (mol H ₂ /(m ³ .h)	Reference
0.055	Acetate, lactate	46	0.44	Özgür, E. <i>et al.</i> (2010)
0.050	Glucose	20	0.60	Current Study
0.050	Fructose	20	0.40	Current Study
0.055	Beet Molasses	35	0.55	Sagir, E. et al. (2017)
		50	0.13	
		65	0.10	

4.2. Outdoor Pilot-Scale Stacked U-Tube Photobioreactor

Photofermentative hydrogen production was carried out with the stacked U-tube reactor under outdoor conditions between August 7th and August 25th, 2016 with *R. capsulatus hup⁻* using “sucrose contained in molasses” as substrate. The previously designed photobioreactor (Kayahan, Eroglu, and Koku 2016) was scaled up from 9 liters to 20 liters with some improvements to the design by increasing the diameter from 3cm to 4cm. The following sections describe the selection of parameters and the results of the operation, in detail.

4.2.1. C/N Ratio Selection

The C/N ratio is a fundamental parameter for photofermentative hydrogen production. Up to now, most of the *outdoor* studies of photofermentative hydrogen production with *molasses* substrate were conducted with C/N ratios of between 25 and 35 (Kayahan, Eroglu, and Koku 2017; Avcioglu et al. 2011; Özgür, Mars, et al. 2010; Sagir, Ozgur, et al. 2017; Sağır 2012). In this pilot-scale study C/N ratio was selected as 13 which is a relatively lower ratio compared to the other outdoor studies in literature. Lowering the C/N ratio was preferred in the pilot-scale experiment according to the results of the small-scale experiments in the current study. According to the results of the small-scale experiments, it was found that a lower C/N ratio resulted in the least pH drop being closer to the optimal value (pH=7) for the hydrogen production. A lower C/N also reduced the lag phase for hydrogen production, reduced the adaptation period for the growth of the bacteria and resulted in higher yield of hydrogen from the substrate.

In a previous study, the C/N ratio was set to 35 conducted with the same bacteria and reactor type as in the current outdoor study (Kayahan, Eroglu, and Koku 2017). Since the results of the small-scale experiments supported that lower C/N ratios can be tried for the large-scale experiment, C/N ratio was reduced from 35 to 13 in the current study. Using molasses, a by-product of sugar factory, as carbon source

instead of using glucose or fructose is more feasible for sustainable and renewable energy production. The molasses was diluted to lower concentrations because of the thickness of molasses, which might prevent the transmission of the sunlight through the reactor. Consequently, 5 mM sucrose containing molasses was selected since it was suggested in a previous study for effective hydrogen production (Kayahan, Eroglu, and Koku 2016). The C/N value of the current study was based on a previous study investigating the effect of various C/N ratios, in which the highest yield was achieved with a C/N ratio of 13 in indoor conditions (Avcioglu 2010). The C/N ratio was adjusted to 13 with 5 mM sucrose and 7.5 mM glutamate feeding at start-up of the experiment. It is the lowest C/N ratio applied in pilot-scale photofermentative hydrogen production experiment, to the best of our knowledge.

4.2.2. Diameter Selection

Diameter selection is very critical for design of a photobioreactor. Tubes having large diameters prevent the transmission of light into the center of the tubes. On the other hand, tubes having small diameters result in high ground area to volume ratio which is not economical.

In a previous study, the effect of light intensity on hydrogen production was investigated and lower hydrogen productivity was observed with decreased light penetration into a reactor with 3 cm tube radius (Boran et al. 2012a). In another study, no hydrogen gas was produced with culture depths of 1.5 cm or greater and with a light intensity of 360 W/m² on the surface (Nakada et al. 1995). Molasses diluted to utilize sucrose as a substrate for hydrogen production is intensified fluid which might prevent light penetration. Therefore, in a previous study, photon count measurements were done for molasses to observe the dependence of light intensity to tube radius. The range of 1-2 cm tube radius was stated as suitable tube radius and 1.5 cm was chosen according to the results. However, the photon count experiment was done with thin compartments and without any mixing (Kayahan, Eroglu, and Koku 2017). In this study, tube radius was increased from 1.5 to 2 cm with scale-up

since the light transmission can be increased by the effect of mixing. As a scale-up strategy, the similar Reynold's number method was applied by setting the flow rate in a single tube to 10.5 L/h corresponding to Reynold's number of 92, which was previously resulted in the least pressure drop and the most uniform flow profile for the same reactor type (stacked U-tube PBR) in smaller volume [34]. The pressure drop of the current bioreactor due to the hydraulic resistance from the pipes and the fittings was calculated and for Reynolds number of 92. The total friction loss was calculated from the following equation (Geankoplis 2003).

$$\sum F = \left(4f \frac{\Delta L}{D} + K_f \right) \frac{v^2}{2} \quad (4.2)$$

where L is the tube length, D is tube diameter, v is the average velocity in the tube, K_f is the loss factor for the fitting and f is friction factor for laminar flow as shown below (Geankoplis 2003).

$$f = \frac{16}{N_{Re}} \quad (4.3)$$

The calculation was done by considering two elbows for each of the four tubes of the reactor (neglecting manifolds and pump connection lines). The calculated friction value was inserted in the overall macroscopic energy equation as shown below;

$$\sum F = \frac{\Delta P}{\rho}$$

The values of the parameters for this calculation are listed in Table 4.6 below.

Table 4.6. *Parameters of the pressure drop calculation*

Parameters	Reynolds number (Re)	Linear velocity (m/s)	Friction factor (f)	Fitting loss (K_f)	Length of U-tube (m)	Diameter of tube (m)	Number of tubes	Number of U-bends
Values	92	0.0023	0.167	7	4	0.04	4	8

Based on these equations and parameter values, the total pressure drop was estimated as 0.85 Pa.

While the main objective of an typical reactor for scale-up is to achieve high conversion efficiency or selectivity, the photobioreactor design mainly focuses on to have high illuminated surface to ground area ratio. The maximum illuminated surface area to ground area ratio can be achieved by designing the reactor as compact [35]. In the current study, previously designed compact tubular reactor (Stacked U-tube photobioreactor) was scaled-up from 9L to 20 L by increasing tube radius from 1.5 cm to 2 cm [34]. The comparison of illuminated surface to ground area ratio and ground area to reactor volume ratio with different tubular reactors is shown in Table 4.7.

Table 4.7. Comparison of ground area to volume and illuminated surface to ground area and ratios for outdoor experiments with *Rhodobacter capsulatus* YO3 (hup-) strain with different tubular reactors.

Reactor type	Reactor volume (L)	Illuminated surface area per ground area	Ground area per volume (m^{-1})	Reference
Stacked U-tube (2 cm radius)	20	6.7	16.5	This study
Stacked U-tube (1.5 cm radius)	9	5.4	34.6	(Kayahan et al. 2017)
Horizontal tubular	90	1.1	26.0	(Boran et al. 2012)

According to a previous techno-economic study, up to 92% of the capital cost of photofermentation consists of the large land area occupied by photobioreactors (Urbaniec and Grabarczyk 2014). High illuminated surface area to ground area ratio and low ground area to volume ratio is preferred for an economically feasible biohydrogen production. Therefore, these ratios are significantly improved in the current study, as shown in Table 4.7.

4.2.3. Solar Irradiation and Temperatures

The experiment was operated with U-tube photobioreactor between August 7th and August 25th. The solar irradiance change during 17 days and temperature variations of reactor medium and ambient air are indicated in Figure 4.12. The temperature measurement was done from a temperature port inserted into the second tube counted from the ground.

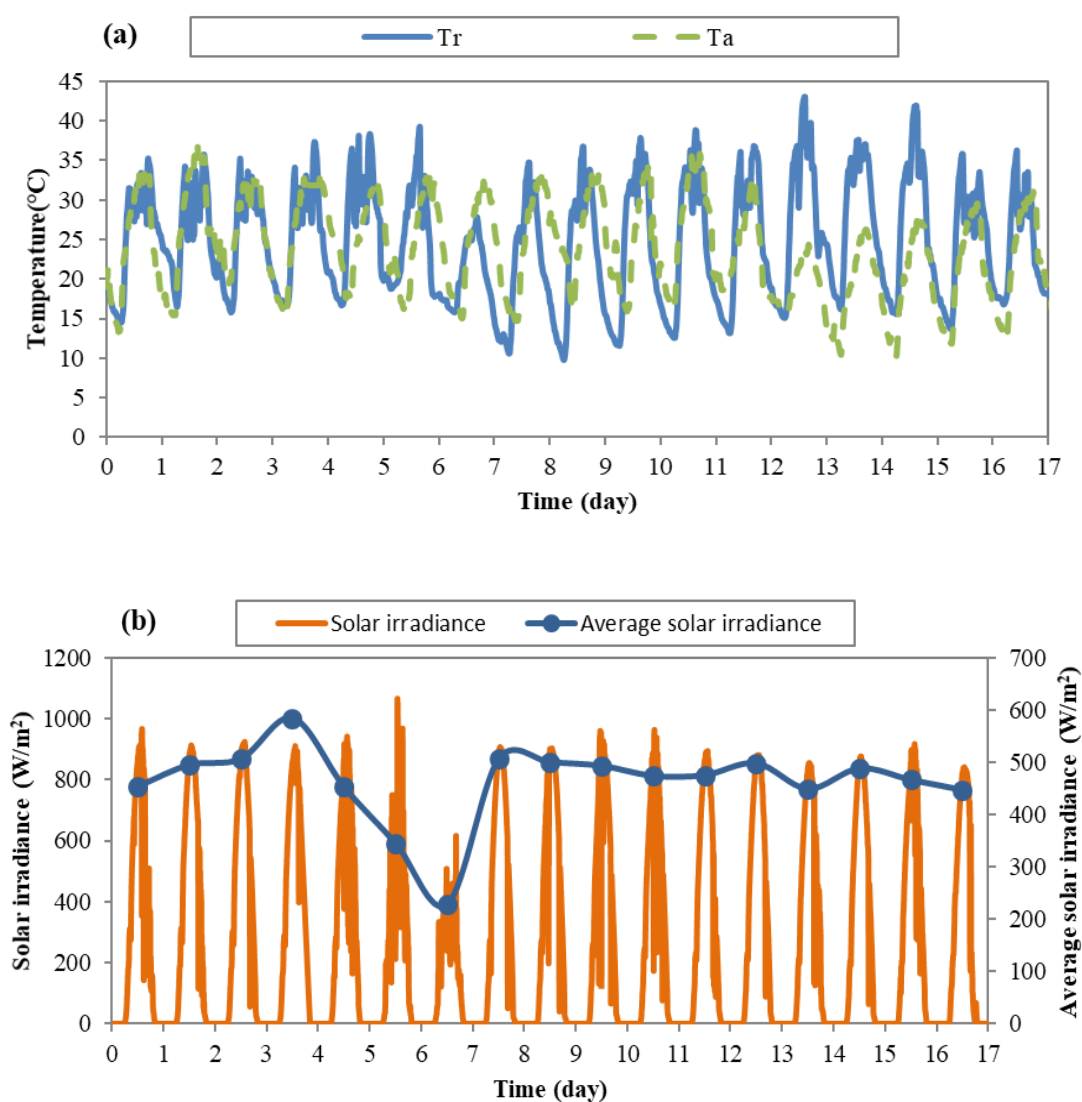


Figure 4.12.(a) The temperature change of the reactor liquid and ambient air (b) the change in daily and average solar irradiance. T_a and T_r is the ambient temperature and temperature of the reactor (second tube counted from the ground), respectively.

The temperature of the reactor fluid changed according to the ambient temperature, which is correlated with solar radiation during day/night cycles. The temperature control system was only based on cooling the reactor during daytime. Therefore, temperature values recorded as low as 12°C during night due to the absence of heating system. On the other hand, the temperature of the reactor was maintained in a range of 30 - 40°C during daytime, so it can be concluded that efficient cooling was achieved.

The solar radiation values varied according to the ambient weather during the experiment. The average solar radiation mostly varied between 400-500 W/m² during day time. However, during the 4th-6th days intermittent rain and cloudy periods were observed and daily average radiation values decreased as low as 200 W/m². It is observed that daily light intensity and temperature fluctuations during the day-night cycles appeared to be harmful for bacterial growth (Özgür, Uyar, et al. 2010). Therefore, the temperature fluctuations may have led a decrease in hydrogen productivity after the second day, as discussed in Section 4.2.7.

4.2.4. Light Distribution in the Photobioreactor

For a further investigation of the light distribution inside the photobioreactor, light intensity variance was calculated according to Beer-Lambert's law. In addition, the tube thickness was segmented hypothetically into optimal, feasible and dark regions based on a previous study, which explains the effect of light intensity on hydrogen production. It was already stated that the light penetration into the culture obeys the Beer-Lambert's law for photofermentative bacteria (Nakada et al. 1995). According to Beer-Lambert's law (Equation 4.5), there is a linear relationship between absorbance and culture concentration. Epsilon (ϵ) is the wavelength dependent molar absorptivity coefficient (M⁻¹.cm⁻¹), b is the light path length (i.e. tube radius), c is the concentration of the culture medium and A is absorbance.

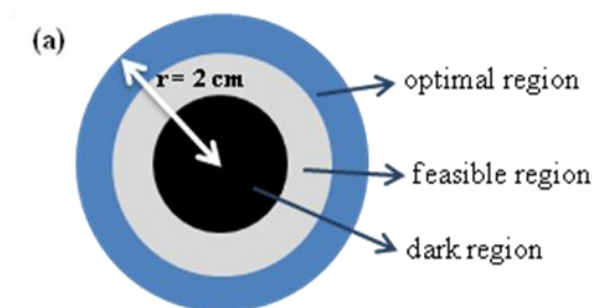
$$A = \epsilon \times b \times c \quad (4.5)$$

Experimental data are frequently reported in transmittance ($T=I/I_0$) where I_0 is the incoming light intensity and I is the light intensity after it passes through the culture as shown in Equation 4.6.

$$A = -\log(I/I_0) \quad (4.6)$$

According to the Equation (4.5) and (4.6), the light energy in the culture media decreases exponentially depending on the concentration of the culture medium and the distance of the light source.

It was previously reported that the hydrogen production increased with increased light intensity and reached saturation around the light intensity of 270 W/m^2 (Uyar et al. 2007). Therefore, at least 270 W/m^2 light intensity at the darkest region of the PBR may be suggested to obtain high hydrogen production rates. In the current study, the thickness from surface of the tube exposed to light intensity higher than 270 W/m^2 was calculated by Beer-Lambert's law. The calculated tube thickness is defined as *optimal region* where presumably hydrogen production rate is high, in the light of the previous study (Uyar et al. 2007). It was also previously showed that hydrogen production nearly stopped for a light penetration of 3% of 360 W/m^2 which corresponds to a light intensity of 10.8 W/m^2 (Nakada et al. 1995). Therefore, the tube thickness from the tube surface exposed to light intensity of between 10.8 W/m^2 and 270 W/m^2 was calculated by Beer-Lambert's law and defined as the *feasible region* where hydrogen production is possible. Deeper region of the tube corresponding the light intensity of lower than 10.8 W/m^2 was assumed as unfeasible for hydrogen production and defined as the *dark region*.



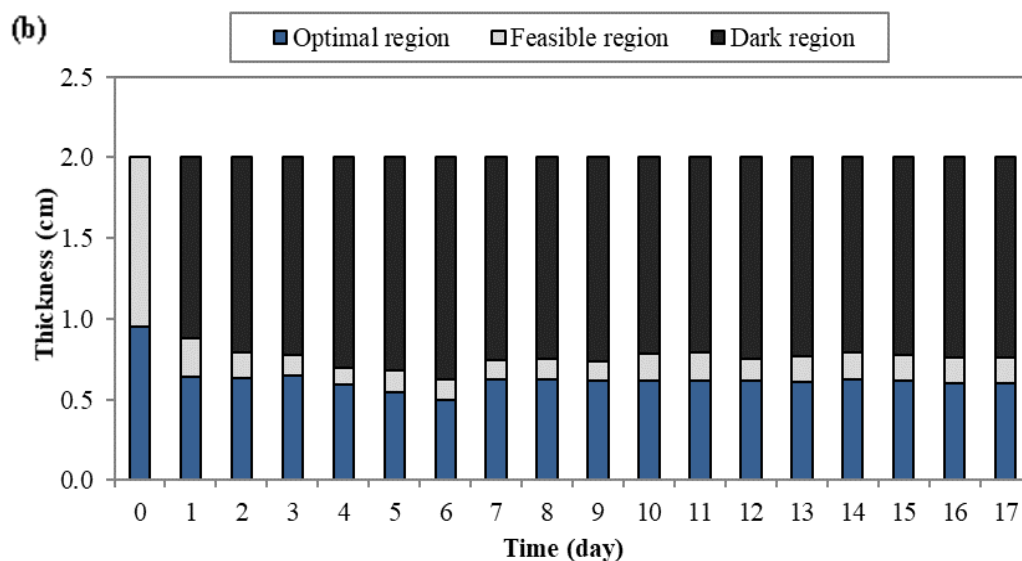


Figure 4.13.(a) Schematic representation of the regions in the tubes.(b) The thickness of optimal, feasible and dark region (cm) in the tube during the experiment. Tube radius is 2 cm.

The calculated thicknesses for hypothetical regions are shown in Figure 4.13 and calculations are based on the average daily radiation at the surface of the reactor. The optimal region is in the range of 0-0.6 cm thickness where the high hydrogen productivity is occurred. In conclusion, 0.6 cm from tube surface corresponded to the optimal region and hydrogen production was found to be possible for 0.8 cm thickness from tube surface (sum of the optimal and feasible regions). Although it might seem that hydrogen is produced only 0.8 cm of the 2 cm tube, real thickness where hydrogen production is possible must be higher due to the mixing effect because previous work was for a stagnant system (Nakada et al. 1995). This would explain that the rate of hydrogen production in the present study was increased when the tube diameter was increased from 1.5 cm to 2.0 cm compared to previous study (Kayahan, Eroglu, and Koku 2017). In the light of the current study, dilution of the culture volume can be suggested to maintain light penetration in an optimum range.

4.2.5. Sucrose Concentration and Feeding Strategy

The experiment was started by adjusting sucrose to 5 mM concentration at the start-up. During the experiment, sucrose was utilized by the bacteria as substrate for hydrogen production. Therefore, sucrose concentration was adjusted to 5 mM with sucrose feeding during the experiment. The daily sucrose consumption per liter culture volume is shown in Figure 4.14.

During the experiment, it was observed that the sucrose consumption was nearly stopped for a few days. For example, on the third day, the sucrose concentration dropped to around 3.2 mM and nearly no sucrose was consumed for 3 days. The addition of sucrose was done when the sucrose consumption was almost stopped for a few days. It is noteworthy that the sucrose consumption resumed immediately after sucrose feedings, suggesting that below a certain concentration (or C/N ratio) the sucrose consumption rate decreased to very low values. Therefore, the feeding strategy was to adjust sucrose concentration to 5 mM (C/N ratio of 13) by feeding diluted molasses to the reactor when the sucrose consumption was nearly stopped for around 3-4 days (arrows in Figure 4.14).

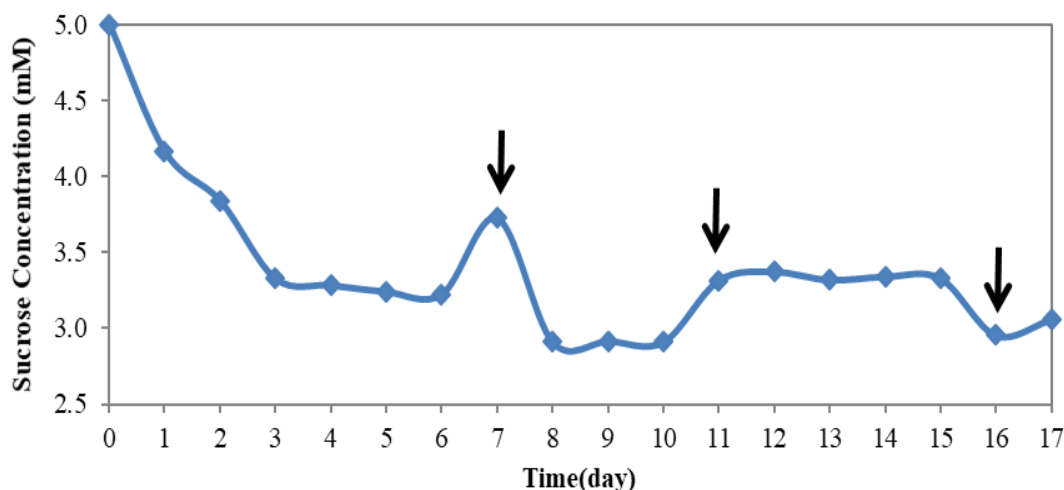


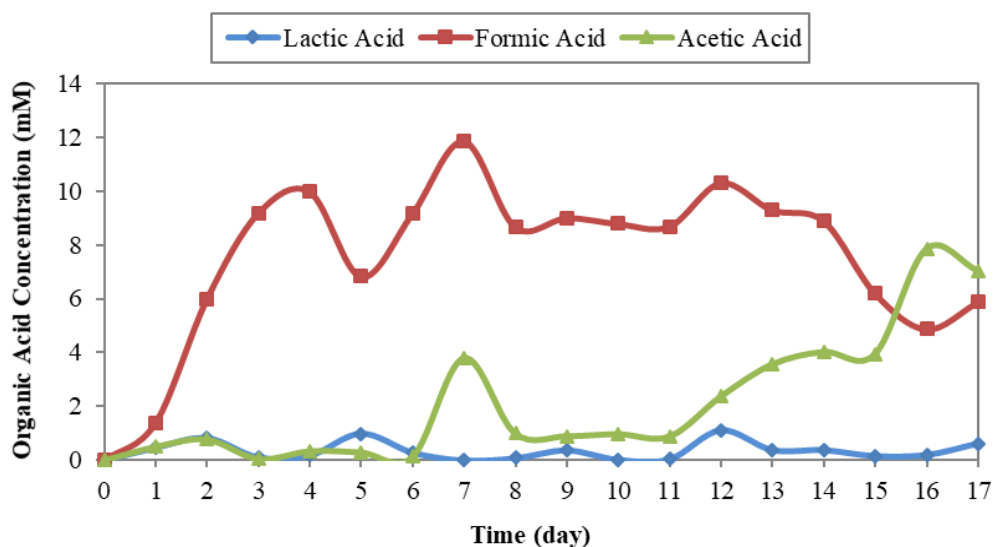
Figure 4.14. Sucrose concentration change during the experiment. Sucrose contained molasses were fed on the 7th, 11th and 16th days as shown by the arrows. On the feeding days, the sucrose concentration values measured approximately 3-4 hours after feeding.

4.2.6. Organic Acid Concentrations and pH

Mainly produced acids were lactic, formic and acetic acid by the bacteria during the experiment as shown in Figure 4.15a. Lactate and acetate concentrations are relatively lower than formic acid, most likely they are consumed by the bacteria since lactate and acetate are commonly utilized substrates by *R. capsulatus*. In a previous study, acetic acid concentration increased while formic acid concentration decreased after continuous feeding started (Kayahan, Eroglu, and Koku 2017). It is interesting that the same trend was observed in the current study where after 7th day (first day of sucrose feeding) formic acid concentration decreased while acetic acid concentration increased. While acetic acid is commonly used by *R. capsulatus* for photofermentative hydrogen production formic acid consumption is hardly reported in literature. Therefore, the reason of decrease in formic acid concentration while acetic acid concentration was increasing, might be due to a metabolic shift to another mode instead of hydrogen production. PNS bacteria metabolism was modeled in a previous study and the most effective organic acid was found as acetic acid, while the least effective one was formic acid for hydrogen production (Doğan 2016). As shown in Figure 4.25-a, mostly formic acid was found to be accumulated in the media, which also supports a shift in the bacterial metabolism rather than hydrogen production. Poly- β -hydroxybutyrate (PHB) is produced with an increase in the organic acid as carbon source (Wu et al. 2012). Since organic acids are also carbon sources for hydrogen production, PHB production pathway becomes favorable when organic acids accumulated, which decreases the hydrogen production (Doğan 2016). Therefore, the metabolic shift can be due to the accumulated organic acids at the end of 6th day (Figure 4.15) could result in a PHB formation rather than hydrogen production. It should also be considered that, while intracellularly produced organic acids promote PHB formation against hydrogen production, extracellular organic acids in the medium increases the hydrogen production (Doğan 2016). Further investigation is needed to better understand the sucrose metabolism and metabolic fluctuations.

As shown in the (Figure 4.15b), the pH decreased rapidly for the first 2 days and remained almost constant until the 11th day with a pH of around 6.5. The molasses fed on the 7th day increased the organic acid production but it did not affect the pH significantly. On the other hand, pH decreased significantly after molasses feedings on 11th and 16th days. As discussed in Section 4.2.7, the highest hydrogen productivity was observed on the 1st day of the experiment when the pH was 7. This result complies with previous studies in which the optimum pH value is suggested as 7 for hydrogen production (Sasikala et al. 1991). Therefore, it can be said that pH drop below 7 effects the hydrogen production negatively. Previously, pH decrease in the medium was found to affect hydrogen production negatively (Sagir *et al.* 2012). The lowest pH values were 5.0 (Kayahan, Eroglu, and Koku 2016) and 5.9 (Kayahan, Eroglu, and Koku 2017) in similar pilot-scale experiments done with *Rhodobacter capsulatus*, whereas it was 6.4 in the current study.

(a).



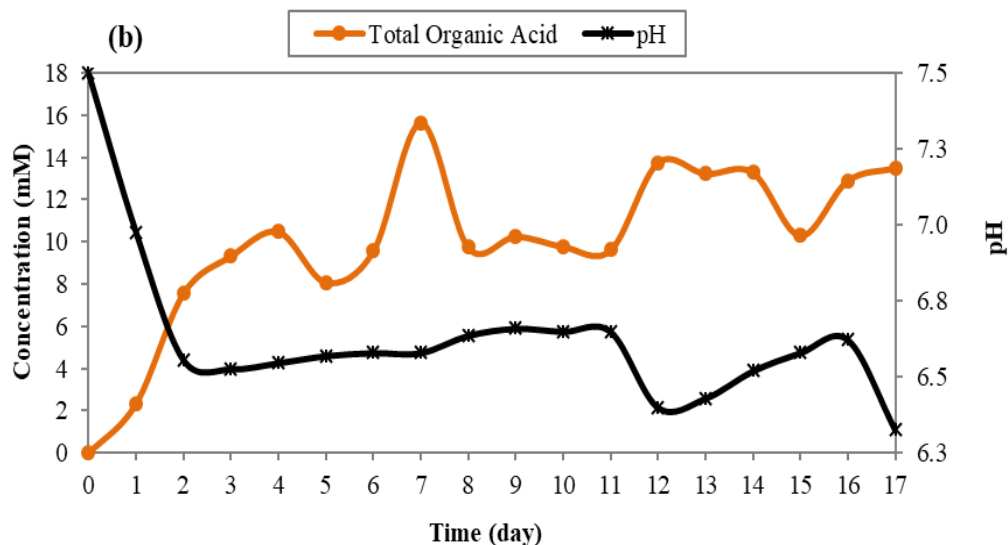


Figure 4.15. Daily variation in (a) individual organic acid concentration and (b) total organic acid concentration and pH during the experiment.

Besides organic acids, poly- β -hydroxybutyrate (PHB) can be also produced by bacteria to remove extra electron carriers of the carbon flow. The PHB synthesizing increases in a nitrogen-lack environment with excess carbon and energy resources (Doğan E. M., MSc. Thesis, 2016). The parameters of the media, such as substrate type and pH, can affect the PHB production rate. (Chen *et al.*, 2011). PHB production pathway competes with hydrogen production pathway for electrons, since both are favorable pathways for unbalanced cell growth (Vincenzini *et al.*, 1997). In a previous study where PNS metabolism was modeled, PHB production is suggested as zero for a maximum hydrogen production, since the organic acids are also carbon sources for hydrogen production. Therefore, PHB production pathway becomes favorable when organic acids accumulated, which decreases the hydrogen production (Doğan E. M., MSc. Thesis, 2016).

4.2.7. Growth and Hydrogen Productivity

A previous experiment was carried out with the same parameters such as the bacteria type (*R. capsulatus hup⁻*), carbon source (sucrose contained in molasses) and reactor type (stacked U-tube PBR) except the C/N ratio (35) for a 9 L reactor (Kayahan, Eroglu, and Koku 2017). Therefore, the results of the current study are directly comparable to those obtained by the previous study in terms of C/N ratio effect on bacterial growth and thereby hydrogen production. The purpose of choosing a lower C/N ratio in the current study was to support bacterial growth and reduce the lag period for hydrogen production. It was shown in Figure 4.16 that the rate of bacterial growth and final bacterial concentration was significantly increased with increased C/N ratio leading a higher relative hydrogen content at startup compared to the similar previous study (Kayahan, Eroglu, and Koku 2017).

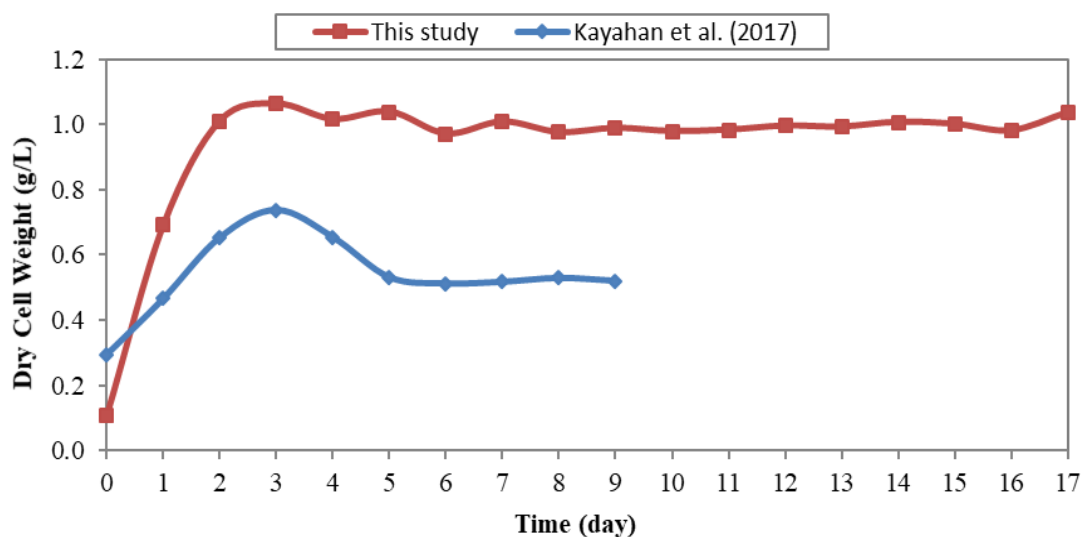


Figure 4.16. Daily variation in cell concentration of this study and a previous study having higher C/N value (35) and a lower reactor volume (9L) (Kayahan et al. 2017).

As shown in Figure 4.16 the exponential cell growth lasted for 2 days and the bacterial concentration stabilized around 1 g/L in the stationary phase. The bacterial cell concentration stabilized around 1 g/L in the 2nd day of the current study while it

was stabilized around 0.5g/L on the 5th day of the previous work (Kayahan, Eroglu, and Koku 2017).

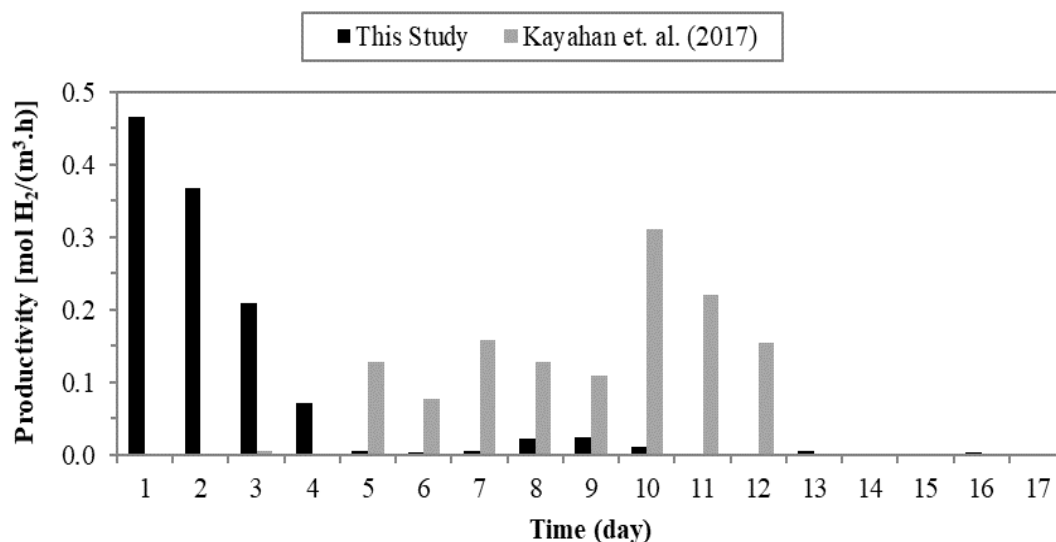


Figure 4.17. Comparison of the hydrogen productivity of the current study with a previous study (Kayahan et al. 2017) with the smaller volume (9L) and higher C/N ratio (35).

Hydrogen productivities obtained in the current study and the previous study with higher C/N ratio (35) and lower reactor volume (9L) are shown in Figure 4.17. As shown in Figure 4.17, the hydrogen gas was begun to be produced from the first day of the experiment while it started around 3th day in the previous work, which states that lag phase for hydrogen production is decreased. In the current study hydrogen gas produced mostly in the growth phase as in the previous studies indicating the growth phase as an optimal stage for hydrogen production (C. H. Sasikala, Ramana, and Rao 1995; Harun Koku et al. 2003). In most cases, productivity decreases with scale up of a reactor due to the difficulty of maintaining uniform mixing, temperature and light distribution and for the larger volume. Nevertheless, hydrogen production started earlier and significantly higher productivities were achieved in the current work with a larger reactor volume compared to the earlier study with the 9 L reactor volume. The highest hydrogen productivity was found as 0.47 mol H₂/(m³.h)

while it was 0.31 mol H₂/(m³.h) in the previous smaller scale work (Kayahan, Eroglu, and Koku 2017).

In the current study, the reason of higher maximum hydrogen productivity obtained compared to the previous small scale study might be correlated with;

- Higher pH values during the experiment which were closer to the optimal (pH=7),
- Lower C/N ratio at startup leading earlier growth of the hydrogen producing populations since nitrogen promotes growth,
- Reduced the probability of hydrogen gas leakage from fittings due to the improvements done to the reactor design such as;
 - Reducing number of glass fittings
 - Tilting the reactor which reduced the retention time of the hydrogen gas
 - Adding flange connections which are more reliable than plastic cuffs used in the previous design (Kayahan, Eroglu, and Koku 2017).

In a previous *indoor* study, the maximum hydrogen productivity was found as 0.41 mol H₂/(m³.h) with same bacteria (*R. capsulatus hup⁻*) and carbon source (5mM sucrose) under constant temperature and continuous illumination. Although, lower productivities are expected for outdoor studies compared to indoors due to the fluctuating temperature and light during day and night cycles, a higher maximum productivity was achieved in the current *outdoor* study (Sagir, Ozgur, et al. 2017).

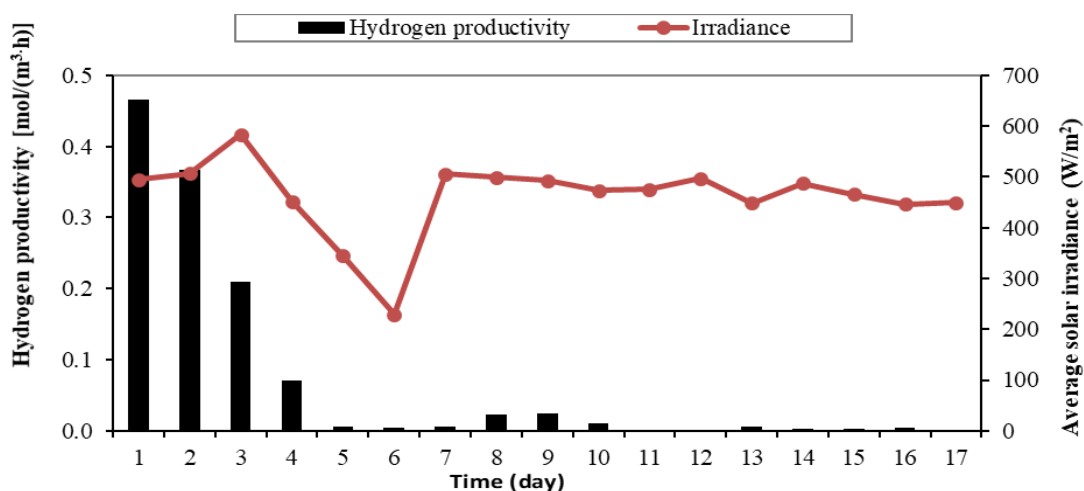


Figure 4.18. Daily variation in the hydrogen productivity and average solar irradiance.

Hydrogen productivity was highest in the first day and decreased over time. Hence, the average hydrogen productivity remained lower compared to the previous experiment (Kayahan et al. 2017). The reasons for this decline in productivity are likely to be the reduction in light transmittance through the reactor due to increased cell concentration Figure 4.16 and decreased solar radiation caused by clouds and rain between the 3rd and 6th days (Figure 4.18). Although the increase in solar radiation and the sucrose feeding on the 7th day increased partially the productivity, it was observed that the most of the hydrogen was produced in the first 3 days. Most of the hydrogen was produced during the exponential growth phase of the bacteria (first 3 days). Poly- β -hydroxybutyrate (PHB) is produced with an increase in the organic acid as carbon source (Wu et al. 2012). Therefore, a metabolic shift may have occurred on the 7th day because the accumulated organic acids (Figure 4.15) may have resulted in a PHB formation rather than hydrogen production, as discussed in Section 4.2.6. It was observed that high bacterial concentration (around 1 g/L) and inadequate solar radiation probably prevented sufficient light transmission into the reactor and led to a decrease in hydrogen productivity. Therefore, glutamate feeding was not done except at the start-up to prevent further increase in bacterial cell concentration since nitrogen promotes growth. Different feeding strategies can be

applied such as diluting the liquid reactor medium to increase light transmission and keep the bacterial cell concentration in the optimal range.

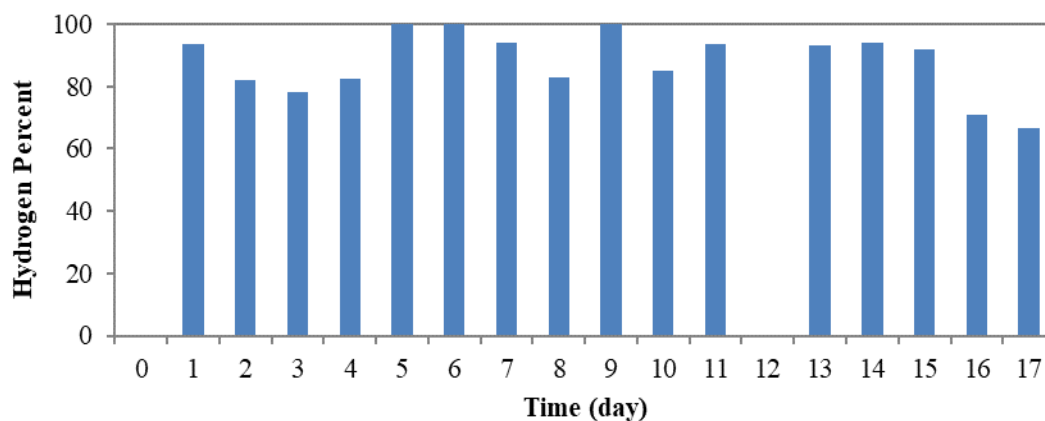


Figure 4.19. Percent hydrogen in the produced gas during the experiment. The rest of the produced gas is carbon dioxide.

The composition of the produced biogas was continuously monitored and its daily variation is shown in Figure 4.19. The average hydrogen percent in the produced biogas was calculated as 82.8% while it was 32.6 % in the previous outdoor study of Kayahan et al. 2017 which states that high hydrogen purity was obtained. This can be illustrated with difference in pH values during the experiment; the minimum pH was 6.5 in the current study while it was 5.9 in that previous study (Kayahan, Eroglu, and Koku 2017).

Besides its effects on productivity, the pH of the liquid culture also affects the biogas composition. In the pH range of 7.0-8.5 the most of the produced carbon dioxide dissociates to bicarbonate and traps as bicarbonate in the liquid medium decreasing the CO₂ percentage in the evolved gas. On the other hand, in the pH range of 4.0-6.0 the CO₂ is the dominant species rather than bicarbonate (Kayahan, Eroglu, and Koku 2017). Therefore, the CO₂ level in the produced gas increases at low pH values, leading to a decrease in the hydrogen percentage and purity.

4.2.8. Comparison of Productivities with Other Outdoor Studies

Since the previous experiment with smaller volume (9L) was conducted with nearly the same parameters of the current study except higher C/N ratio, the comparison of the most important results are shown in Table 4.8. It can be seen that maximum hydrogen productivity is higher and hydrogen gas started to be produced earlier in the current study. The average and maximum hydrogen percentage values were 82.8 and 94.1 in the current study while they were 32.6 and 84.7 for the previous study, respectively. The reason of this higher purity obtained in the current study presumably because of the higher pH values during the experiment. In addition, the lag time to start of hydrogen production is significantly lower as indicated in Table 4.8. The comparison of the some of the studies found in literature in terms of hydrogen productivity for different C/N ratios is shown in Table 4.9.

Table 4.8. *Summary of results and comparison with the 9L volume study.*

	Current study	(Kayahan et al. 2017)
Volume of the reactor (L)	20	9
Amount of hydrogen produced (L)	15.9	4.56
Maximum hydrogen productivity mol/(m ³ .h)]	0.47	0.31
Average hydrogen productivity (mol/(m ³ .h))	0.07	0.11
Average hydrogen percentage of produced gas	82.8	32.6
Maximum hydrogen percentage of produced gas	94.1	84.7
Minimum pH	6.5	5.8
Maximum bacterial concentration (g/L)	1.09	0.58
Lag time to start of hydrogen production (hr)	18	96

Table 4.9. Comparison of the outdoor studies conducted with *R. capsulatus* hup- bacteria.

Reactor Type	Mode	Reactor Volume (L)	Substrate	C/N	Productivity [mol H ₂ / (m ³ .h)]	Reference
Tubular	Fed-batch	20	Molasses	13	0.47	This Study
Tubular	Fed-batch	9	Molasses	35	0.31	(Kayahan, Eroglu, and Koku 2017)
Panel	Seq-batch	1.4	Sucrose	35	0.87	(Sagir, Alipour, et al. 2017)
Tubular	Fed-batch	90	Acetate	25	0.40	(Boran et al. 2012a)
Glass Bottles	Batch	0.55	Acetate, Lactate	46	0.44	(Özgür, Uyar, et al. 2010)
Panel	Fed-batch	4	DFE of sugarbeet thick juice	17	1.12	(Özkan 2011)

CHAPTER 5

CONCLUSION

In the indoor studies, the effect of carbon to nitrogen (C/N) ratios (20, 50 and 80) on photofermentative hydrogen production was investigated with 10, 20 and 30mM glucose and fructose feedings. The small-scale experiments helped to decide the appropriate C/N ratio for the pilot-scale outdoor experiment. In literature, fructose has not been studied as much as glucose and sucrose as sugar source in photofermentative hydrogen production. Therefore, small-scale experiments also allowed the comparison of glucose and fructose as substrates in terms of yield and hydrogen productivity.

According to the results of small-scale experiments, lower C/N ratio was found to be preferable for the pilot-scale outdoor experiment to reduce the lag phase for hydrogen production and the adaptation period of the bacteria. Most of the hydrogen was found to be produced during the growth phases for all C/N ratios, which was previously reported as the optimal phase for hydrogen production (C. H. Sasikala, Ramana, and Rao 1995; Harun Koku et al. 2003). The maximum hydrogen productivity was obtained as 0.60 mol H₂/m³.h for 30 mM glucose and the maximum hydrogen percentage in produced biogas was determined as 85% for 10 mM glucose. However, when the C/N ratio was increased, pH dropped more which was an undesired situation since the optimal hydrogen production was around pH=7 (Sasikala et. al, 1991). This result also supported that a lower C/N ratio can be tried for the pilot-scale experiment to reduce pH drop. Furthermore, produced organic acids were measured individually and most of the pH drop was found due to the formic acid accumulation. According to all glucose and fructose experiments, adaptation of the bacteria to the sugar source before starting the experiment was found essential to reduce the lag phase for growth of the bacteria and hydrogen

production. In addition, the adaptation period for fructose was much longer than glucose for all C/N ratios in the small-scale experiments.

In the pilot-scale outdoor experiment, using molasses (a by-product of sugar factory) as carbon source is more suitable for sustainable and renewable energy production compared to glucose or fructose as in small-scale experiments. A previously designed photobioreactor was scaled up from 9 liters to 20 liters by increasing the tube radius from 1.5 cm to 2 cm and higher maximum hydrogen productivity and purity was obtained. In addition, C/N ratio was lowered from 35 to 13 since small-scale experiments of the current study showed that lower C/N ratio resulted in the least pH drop and reduced the lag phase for hydrogen production. The reduced C/N ratio accelerated the rate of cell growth and resulted in a lower lag-time (4 days earlier) for hydrogen production and higher daily hydrogen productivities in the exponential growth phase. However, it also resulted in a high cell concentration and therefore hydrogen production stopped with the combined effects of cloudy and rainy weather conditions and low pH values.

For a further investigation of the light distribution inside the photobioreactor, light intensity variance through the tube radius was calculated according to Beer-Lambert's law. Although hydrogen was seemed to be produced in nearly half of the tube radius, the real thickness where hydrogen production is possible should be higher due to the effect of mixing, because the calculations done by using "Beer-Lambert's Law" was for a stagnant system. This would explain that the rate of hydrogen production in the present study was increased with increased tube diameter from 1.5 cm to 2.0 cm compared to the previous study of Kayahan et al. 2017.

Concentration of culture media is a significant parameter since low cell concentrations can lead less hydrogen production while very high concentrations reduce or stop hydrogen production by preventing sufficient light into the photobioreactor. Therefore, sustaining optimal cell concentrations for efficient biohydrogen production is crucial. According to the results of the outdoor study,

dilution of the liquid culture may be suggested to maintain light penetration at an optimum range, since the bacterial cell concentration reached at high values (1 g/L). Applying effective feeding strategy and pH control system may provide to maintain optimum C/N ratio and pH during the experiment and further increase the hydrogen productivity. In the present study, the highest hydrogen productivity was increased from 0.31 mol H₂/(m³.h) to 0.47mol H₂/(m³.h) compared with the previous smaller scale work (9L) with same bacteria, substrate and reactor type (Kayahan, Eroglu, and Koku 2017). The reasons of this higher maximum productivity may be related to lower pH drop, lower hydrogen leakage probability due to improvements made in reactor design (e.g. reduced number of fittings) and lower C/N ratio, which promotes growth and reduces lag-time for hydrogen production. To the best of our knowledge, this the lowest C/N ratio applied in pilot-scale photofermentative hydrogen production.

REFERENCES

- Abo-Hashesh, Mona, Nicolas Desaunay, and Patrick C. Hallenbeck. 2013. "High Yield Single Stage Conversion of Glucose to Hydrogen by Photofermentation with Continuous Cultures of *Rhodobacter Capsulatus* JP91." *Bioresource Technology*. doi:10.1016/j.biortech.2012.10.091.
- Akkerman, Ida, Marcel Janssen, Jorge Rocha, and René H. Wijffels. 2002. "Photobiological Hydrogen Production: Photochemical Efficiency and Bioreactor Design." *International Journal of Hydrogen Energy* 27 (11–12): 1195–1208. doi:10.1016/S0360-3199(02)00071-X.
- Akköse, Sevilay, Ufuk Gündüz, Meral Yücel, and Inci Eroglu. 2009. "Effects of Ammonium Ion, Acetate and Aerobic Conditions on Hydrogen Production and Expression Levels of Nitrogenase Genes in *Rhodobacter Sphaeroides* O.U.001." *International Journal of Hydrogen Energy* 34 (21): 8818–27. doi:10.1016/j.ijhydene.2009.08.040.
- Androga, Dominic Deo, Ebru Ozgur, Ufuk Gunduz, Meral Yucel, and Inci Eroglu. 2011. "Factors Affecting the Longterm Stability of Biomass and Hydrogen Productivity in Outdoor Photofermentation." *International Journal of Hydrogen Energy* 36 (17). Elsevier Ltd: 11369–78. doi:10.1016/j.ijhydene.2010.12.054.
- Androga, Dominic Deo, Ebru Özgür, Inci Eroglu, Ufuk Gündüz, and Meral Yücel. 2011. "Significance of Carbon to Nitrogen Ratio on the Long-Term Stability of Continuous Photofermentative Hydrogen Production." *International Journal of Hydrogen Energy* 36 (24): 15583–94. doi:10.1016/j.ijhydene.2011.09.043.
- Androga, Dominic Deo, Pelin Sevinç, Harun Koku, Meral Yücel, Ufuk Gündüz, and Inci Eroglu. 2014. "Optimization of Temperature and Light Intensity for Improved Photofermentative Hydrogen Production Using *Rhodobacter Capsulatus* DSM 1710." *International Journal of Hydrogen Energy* 39 (6):

2472–80. doi:10.1016/j.ijhydene.2013.11.114.

Argun, Hidayet, and Fikret Kargi. 2010. “Photo-Fermentative Hydrogen Gas Production from Dark Fermentation Effluent of Ground Wheat Solution: Effects of Light Source and Light Intensity.” *International Journal of Hydrogen Energy* 35 (4). Elsevier Ltd: 1595–1603. doi:10.1016/j.ijhydene.2009.12.040.

Argun, Hidayet, Fikret Kargi. 2011. “Bio-Hydrogen Production by Different Operational Modes of Dark and Photo-Fermentation: An Overview.” *International Journal of Hydrogen Energy* 36 (13). Elsevier Ltd: 7443–59. doi:10.1016/j.ijhydene.2011.03.116.

Argun, Hidayet, Fikret Kargi, and Ilgi K. Kapdan. 2008. “Light Fermentation of Dark Fermentation Effluent for Bio-Hydrogen Production by Different Rhodobacter Species at Different Initial Volatile Fatty Acid (VFA) Concentrations.” *International Journal of Hydrogen Energy*. doi:10.1016/j.ijhydene.2008.09.059.

Avcioglu, Sevler Gökçe, Ebru Özgür, Inci Eroglu, Meral Yücel, and Ufuk Gündüz. 2011. “Biohydrogen Production in an Outdoor Panel Photobioreactor on Dark Fermentation Effluent of Molasses.” *International Journal of Hydrogen Energy* 36 (17). Elsevier Ltd: 11360–68. doi:10.1016/j.ijhydene.2010.12.046.

Avcioglu, Sevler Gokce. 2010. “Scale up of Panel Photobioreactors for Hydrogen Production by PNS Bacteria.” *M.Sc. Thesis. Chemical Engineering Department, Middle East Technical University*, no. September.

Azwar, M. Y., M. A. Hussain, and A. K. Abdul-Wahab. 2014. “Development of Biohydrogen Production by Photobiological, Fermentation and Electrochemical Processes: A Review.” *Renewable and Sustainable Energy Reviews* 31. Elsevier: 158–73. doi:10.1016/j.rser.2013.11.022.

Bailey, James E., and David F. Ollis. 1986. *Biochemical Engineering Fundamentals*.

Barbosa, Maria J., Jorge M S Rocha, Johannes Tramper, and Rene H. Wijffels. 2001.

- “Acetate as a Carbon Source for Hydrogen Production by Photosynthetic Bacteria.” *Journal of Biotechnology* 85 (1). Elsevier Sci B.V.: 25–33.
- Basak, Nitai, and Debabrata Das. 2007. “The Prospect of Purple Non-Sulfur (PNS) Photosynthetic Bacteria for Hydrogen Production: The Present State of the Art.” *World Journal of Microbiology and Biotechnology*. doi:10.1007/s11274-006-9190-9.
- Basak, Nitai, Asim Kumar Jana, Debabrata Das, and Dipankar Saikia. 2014. “Photofermentative Molecular Biohydrogen Production by Purple-Non-Sulfur (PNS) Bacteria in Various Modes: The Present Progress and Future Perspective.” *International Journal of Hydrogen Energy* 39 (13). Elsevier Ltd: 6853–71. doi:10.1016/j.ijhydene.2014.02.093.
- Benemann, J. R., J. A. Berenson, N. O. Kaplan, and M. D. Kamen. 2006. “Hydrogen Evolution by a Chloroplast-Ferredoxin-Hydrogenase System.” *Proceedings of the National Academy of Sciences* 70 (8): 2317–20. doi:10.1073/pnas.70.8.2317.
- Biebl, Hanno, and Norbert Pfennig. 1981. “Isolation of Members of the Family Rhodospirillaceae.” In *The Prokaryotes*, edited by Mortimer P. Starr, Heinz Stolp, Hans G. Trüper, Albert Balows, and Hans G. Schlegel, 267–73. Springer-Verlag.
- Boran, Efe, Ebru Özgür, Job Van Der Burg, Meral Yücel, Ufuk Gündüz, and Inci Eroglu. 2010. “Biological Hydrogen Production by Rhodobacter Capsulatus in Solar Tubular Photo Bioreactor.” *Journal of Cleaner Production* 18 (SUPPL. 1). Elsevier Ltd: S29–35. doi:10.1016/j.jclepro.2010.03.018.
- Boran, Efe, Ebru Özgür, Meral Yücel, Ufuk Gündüz, and Inci Eroglu. 2012a. “Biohydrogen Production by Rhodobacter Capsulatus Hup - Mutant in Pilot Solar Tubular Photobioreactor.” *International Journal of Hydrogen Energy* 37 (21): 16437–45. doi:10.1016/j.ijhydene.2012.02.171.

- Boran, Efe, Ebru Özgür, Meral Yücel, Ufuk Gündüz, İnci Eroğlu. 2012b. "Biohydrogen Production by *Rhodobacter Capsulatus* in Solar Tubular Photobioreactor on Thick Juice Dark Fermenter Effluent." *Journal of Cleaner Production* 31. Elsevier Ltd: 150–57. doi:10.1016/j.jclepro.2012.03.020.
- Brentner, Laura B., Peccia And Jordan, and Julie B. Zimmerman. 2010. "Challenges in Developing Biohydrogen as a Sustainable Energy Source: Implications for a Research Agenda." *Environmental Science and Technology* 44 (7): 2243–54. doi:10.1021/es9030613.
- Chen, Chun Yen, Mu Hoe Yang, Kuei Ling Yeh, Chien Hung Liu, and Jo Shu Chang. 2008. "Biohydrogen Production Using Sequential Two-Stage Dark and Photo Fermentation Processes." *International Journal of Hydrogen Energy*. doi:10.1016/j.ijhydene.2008.06.055.
- Chen, Chun Yen, Kuei Ling Yeh, Yung Chung Lo, Hui Min Wang, and Jo Shu Chang. 2010. "Engineering Strategies for the Enhanced Photo-H₂ Production Using Effluents of Dark Fermentation Processes as Substrate." *International Journal of Hydrogen Energy* 35 (24). Elsevier Ltd: 13356–64. doi:10.1016/j.ijhydene.2009.11.070.
- Corbo, Pasquale, Fortunato Migliardini, and Ottorino Veneri. 2011. *Hydrogen Fuel Cells for Road Vehicles. Green Energy and Technology*. Vol. 11. doi:10.1007/978-0-85729-136-3.
- Das, Debabrata, T Nejat, and Veziroğlu. 2001. "Hydrogen Production by Biological Processes: A Survey of Literature." *International Journal of Hydrogen Energy*. Vol. 26. www.elsevier.com/locate/ijhydene.
- Das, Debabrata, and T. Nejat Veziroğlu. 2008. "Advances in Biological Hydrogen Production Processes." *International Journal of Hydrogen Energy* 33 (21). Elsevier Ltd: 6046–57. doi:10.1016/j.ijhydene.2008.07.098.
- Dincer, Ibrahim, and Canan Acar. 2014. "Review and Evaluation of Hydrogen

- Production Methods for Better Sustainability.” *International Journal of Hydrogen Energy*. doi:10.1016/j.ijhydene.2014.12.035.
- Doğan, Ezgi Melis. 2016. “Understanding Carbon Metabolism In Hydrogen Production By PNS Bacteria.” *IOSR Journal of Economics and Finance* 3 (1): 56. doi:https://doi.org/10.3929/ethz-b-000238666.
- EIA. 2017. “International Energy Outlook 2017 Overview.” *U.S. Energy Information Administration* IEO2017 (2017): 143. doi:www.eia.gov/forecasts/ieo/pdf/0484(2016).pdf.
- Eroğlu, Ela, İnci Eroğlu, Ufuk Gündüz, Lemi Türker, and Meral Yücel. 2006. “Biological Hydrogen Production from Olive Mill Wastewater with Two-Stage Processes.” *International Journal of Hydrogen Energy*. doi:10.1016/j.ijhydene.2006.06.020.
- Eroglu, Ela, Ufuk Gunduz, Meral Yucel, and İnci Eroglu. 2010. “Photosynthetic Bacterial Growth and Productivity under Continuous Illumination or Diurnal Cycles with Olive Mill Wastewater as Feedstock.” *International Journal of Hydrogen Energy* 35 (11). Elsevier Ltd: 5293–5300. doi:10.1016/j.ijhydene.2010.03.063.
- Eroğlu, Ela, Ufuk Gündüz, Meral Yücel, İnci Eroğlu. 2011. “Effect of Iron and Molybdenum Addition on Photofermentative Hydrogen Production from Olive Mill Wastewater.” *International Journal of Hydrogen Energy*. doi:10.1016/j.ijhydene.2011.02.062.
- Eroğlu, Ela, Ufuk Gündüz, Meral Yücel, Lemi Türker, and İnci Eroğlu. 2004. “Photobiological Hydrogen Production by Using Olive Mill Wastewater as a Sole Substrate Source.” *International Journal of Hydrogen Energy* 29 (2): 163–71. doi:10.1016/S0360-3199(03)00110-1.
- Eroglu, İnci, Kadir Aslan, Ufuk Gündüz, Meral Yücel, and Lemi Türker. 1999. “Substrate Consumption Rates for Hydrogen Production by Rhodobacter

- Sphaeroides in a Column Photobioreactor.” *Progress in Industrial Microbiology* 35 (C): 103–13. doi:10.1016/S0079-6352(99)80104-0.
- Fascetti, E., and E. D’addario. 1998. “Photosynthetic Hydrogen Evolution with Volatile Organic Acids Derived from the Fermentation of Source Selected Municipal Solid Wastes.” *Journal of Hydrogen* 23 (9): 753–760. <http://www.sciencedirect.com/science/article/pii/S0360319997001237>.
- Fascetti, E., and O. Todini. 1995. “Rhodobacter Sphaeroides RV Cultivation and Hydrogen Production in a One- and Two-Stage Chemostat.” *Applied Microbiology and Biotechnology* 44 (3–4): 300–305. doi:10.1007/BF00169920.
- Geankoplis, Christie J. 2003. *Transport Processes and Unit Operations*.
- Gebicki, Jakub, Michael Modigell, Matthias Schumacher, Job Van Der Burg, and Eugen Roebroek. 2010. “Comparison of Two Reactor Concepts for Anoxygenic H₂ Production by Rhodobacter Capsulatus.” *Journal of Cleaner Production* 18 (SUPPL. 1). Elsevier Ltd: S36–42. doi:10.1016/j.jclepro.2010.05.023.
- Gest, Howard, D Kamen, and Herta Maas Bregoffs. 1949. “Studies on the Metabolism of Photosynthetic Bacteria V. Photoproduction of Hydrogen and Nitrogen Fixation by Rhodospirillum Rubrum.”
- Ghirardi, Maria L, Liping Zhang, James W Lee, Timothy Flynn, Michael Seibert, and Elias Greenbaum. 2000. “Microalgae : A Green Source of Renewable H₂” 18 (December): 506–11.
- Ginkel, Steven W. Van, Sang-Eun Oh, and Bruce E Logan. 2005. “Biohydrogen Gas Production from Food Processing and Domestic Wastewaters.” *Int J Hydrogen Energy* 30 ((15)): 1535–42.
- Gordon, Jeffrey M. 2002. “Tailoring Optical Systems to Optimized Photobioreactors.” *International Journal of Hydrogen Energy* 27 (11–12): 1175–84. doi:10.1016/S0360-3199(02)00113-1.

- Hallenbeck, Patrick C., and John R. Benemann. 2002. "Biological Hydrogen Production; Fundamentals and Limiting Processes." In *International Journal of Hydrogen Energy*. doi:10.1016/S0360-3199(02)00131-3.
- Hallenbeck, Patrick C., and Yuan Liu. 2016. "Recent Advances in Hydrogen Production by Photosynthetic Bacteria." *International Journal of Hydrogen Energy* 41 (7). Elsevier Ltd: 4446–54. doi:10.1016/j.ijhydene.2015.11.090.
- Holladay, J. D., J. Hu, D. L. King, and Y. Wang. 2009. "An Overview of Hydrogen Production Technologies." *Catalysis Today* 139 (4): 244–60. doi:10.1016/j.cattod.2008.08.039.
- International Energy Agency. 2017. "Key World Energy Statistics."
- Johnston, Brenda, Michael C. Mayo, and Anshuman Khare. 2005. "Hydrogen: The Energy Source for the 21st Century." *Technovation*. doi:10.1016/j.technovation.2003.11.005.
- Jones, Benjamin L, and Kenneth J Monty. 1979. "Glutamine as a Feedback Inhibitor of the Rhodopseudomonas Sphaeroides Nitrogenase System." *JOURNAL OF BACTERIOLOGY*. Vol. 139.
- Junker, Beth Helene. 2004. "Scale-up Methodologies for Escherichia Coli and Yeast Fermentation Processes." *Journal of Bioscience and Bioengineering* 97 (6): 347–64. doi:10.1016/S1389-1723(04)70218-2.
- Kars, Gökhan, Ufuk Gündüz, Meral Yücel, Lemi Türker, and Inci Eroglu. 2006. "Hydrogen Production and Transcriptional Analysis of nifD, nifK and hupS Genes in Rhodobacter Sphaeroides O.U.001 Grown in Media with Different Concentrations of Molybdenum and Iron." *International Journal of Hydrogen Energy*. doi:10.1016/j.ijhydene.2006.06.021.
- Kayahan, Emine. 2015. "Design and Analysis of Tubular Photobioreactors for Biohydrogen Production." *M.Sc. Thesis. Chemical Engineering Department, Middle East Technical University*, no. September.

- Kayahan, Emine, Inci Eroglu, and Harun Koku. 2016. "Design of an Outdoor Stacked - Tubular Reactor for Biological Hydrogen Production." *International Journal of Hydrogen Energy* 41 (42). Elsevier Ltd: 19357–66. doi:10.1016/j.ijhydene.2016.04.086.
- Kayahan, E., I. Eroglu, H. Koku. 2017. "A Compact Tubular Photobioreactor for Outdoor Hydrogen Production from Molasses." *International Journal of Hydrogen Energy* 42 (4). Elsevier Ltd: 2575–82. doi:10.1016/j.ijhydene.2016.08.014.
- Keskin, Tugba, and Patrick C. Hallenbeck. 2012. "Hydrogen Production from Sugar Industry Wastes Using Single-Stage Photofermentation." *Bioresource Technology* 112. Elsevier Ltd: 131–36. doi:10.1016/j.biortech.2012.02.077.
- Kim, J.S., K Ito, K Izaki, and Takabatake H. 1987. "Production of Molecular Hydrogen by a Semi-Continues Outdoor Culture of Rhodopseudomonas Sphaeroides." *Agric Biol Chem* 7 (51(4)): 1173–4.
- Koku, H., I. Eroglu, U. Gunduz, M. Yucel, and L. Turker. 2002. "Aspects of the Metabolism of Hydrogen Production by Rhodobacter Sphaeroides." *Int J Hydrogen Energy* 27: 1315–29. doi:10.1016/S0360-3199(02)00127-1.
- Koku, Harun, İnci Eroğlu, Ufuk Gündüz, Meral Yücel, and Lemi Türker. 2003. "Kinetics of Biological Hydrogen Production by the Photosynthetic Bacterium Rhodobacter Sphaeroides O.U. 001." *International Journal of Hydrogen Energy* 28: 381–88.
- Kosourov, Sergey, Anatoly Tsygankov, Michael Seibert, and Maria L. Ghirardi. 2002. "Sustained Hydrogen Photoproduction by Chlamydomonas Reinhardtii: Effects of Culture Parameters." *Biotechnology and Bioengineering* 78 (7): 731–40. doi:10.1002/bit.10254.
- Krujatz, Felix, Paul Härtel, Karsten Helbig, Nora Haufe, Simone Thierfelder, Thomas Bley, and Jost Weber. 2015. "Hydrogen Production by Rhodobacter

- Sphaeroides DSM 158 under Intense Irradiation.” *Bioresource Technology* 175. Elsevier Ltd: 82–90. doi:10.1016/j.biortech.2014.10.061.
- Kumar, Narendra, Agnidipta Ghosh, and Debabrata Das. 2001. “Redirection of Biochemical Pathways for the Enhancement of H₂ Production by Enterobacter Cloacae,” 537–41.
- Laurinavichene, Tatyana V., Kestutis S. Laurinavichius, Boris F. Belokopytov, Daniela K. Laurinavichyute, and Anatoly A. Tsygankov. 2013. “Influence of Sulfate-Reducing Bacteria, Sulfide and Molybdate on Hydrogen Photoproduction by Purple Nonsulfur Bacteria.” *International Journal of Hydrogen Energy* 38 (14). Elsevier Ltd: 5545–54. doi:10.1016/j.ijhydene.2013.02.097.
- Levin, David B., Lawrence Pitt, and Murray Love. 2004. “Biohydrogen Production: Prospects and Limitations to Practical Application.” *International Journal of Hydrogen Energy* 29 (2): 173–85. doi:10.1016/S0360-3199(03)00094-6.
- Manish, S., and Rangan Banerjee. 2008. “Comparison of Biohydrogen Production Processes.” *International Journal of Hydrogen Energy* 33 (1): 279–86. doi:10.1016/j.ijhydene.2007.07.026.
- Marban, Gregorio, and Teresa Valdes-Sois. 2007. “Towards the Hydrogen Economy?” *International Journal of Hydrogen Energy* 32 (12): 1625–37. doi:10.1016/j.ijhydene.2006.12.017.
- Melis, Anastasios, Liping Zhang, Marc Forestier, Maria L. Ghirardi, and Michael Seibert. 2000. “Sustained Photobiological Hydrogen Gas Production upon Reversible Inactivation of Oxygen Evolution in the Green Alga *Chlamydomonas Reinhardtii*.” *Plant Physiology* 122 (1): 127–36. doi:10.1104/pp.122.1.127.
- Miller, Melissa B, and Bonnie L Bassler. 2001. “Quorum Sensing in Bacteria.”
- Momirlan, M, and T.N Veziroglu. 2002. “Current Status of Hydrogen Energy.”

Renewable and Sustainable Energy Reviews 6 (1–2): 141–79.
doi:10.1016/S1364-0321(02)00004-7.

Nakada, Eiju, Yasuo Asada, Takaaki Arai, and Jun Miyake. 1995. “Light Penetration into Cell Suspensions of Photosynthetic and Relation to Hydrogen Production.” *Journal of Fermentation and Bioengineering* 80 (1): 53–57.

Özgür, Ebru, Nilfer Afsar, Truus De Vrije, Meral Yucel, Ufuk Gündüz, Pieter A M Claassen, and Inci Eroglu. 2010. “Potential Use of Thermophilic Dark Fermentation Effluents in Photofermentative Hydrogen Production by *Rhodobacter Capsulatus*.” *Journal of Cleaner Production* 18 (SUPPL. 1). Elsevier Ltd: S23–28. doi:10.1016/j.jclepro.2010.02.020.

Özgür, Ebru, Astrid E. Mars, Begüm Peksel, Annemarie Louwerse, Meral Yücel, Ufuk Gündüz, Pieter A M Claassen, and Inci Eroğlu. 2010. “Biohydrogen Production from Beet Molasses by Sequential Dark and Photofermentation.” *International Journal of Hydrogen Energy* 35 (2): 511–17. doi:10.1016/j.ijhydene.2009.10.094.

Özgür, Ebru, Basar Uyar, Yavuz Öztürk, Meral Yücel, Ufuk Gündüz, and Inci Eroğlu. 2010. “Biohydrogen Production by *Rhodobacter Capsulatus* on Acetate at Fluctuating Temperatures.” *Resources, Conservation and Recycling* 54 (5): 310–14. doi:10.1016/j.resconrec.2009.06.002.

Özkan, Endam. 2011. “Photofermentative Hydrogen Production Using Dark Fermentation Effluent of Sugar Beet Thick Juice by *Rhodobacter Capsulatus*.” *M.Sc. Thesis. Biotechnology Department, Middle East Technical University*, no. September.

Öztürk, Yavuz. 2005. “Characterization of the Genetically Modified Cytochrome Systems and Their Application to Biohydrogen Production in *Rhodobacter Capsulatus*.” *Ph.D. Thesis. Biotechnology Department, Middle East Technical University*, no.

December. <http://etd.lib.metu.edu.tr/upload/3/12606961/index.pdf>.

Öztürk, Yavuz, Meral Yücel, Fevzi Daldal, Sevnur Mandacı, Ufuk Gündüz, Lemi Türker, and Inci Eroğlu. 2006. "Hydrogen Production by Using *Rhodobacter Capsulatus* Mutants with Genetically Modified Electron Transfer Chains." *International Journal of Hydrogen Energy*. doi:10.1016/j.ijhydene.2006.06.042.

Patel, Sanjay K.S., and Vipin C. Kalia. 2013. "Integrative Biological Hydrogen Production: An Overview." *Indian Journal of Microbiology*. doi:10.1007/s12088-012-0287-6.

Rahman, S. N.A., M. S. Masdar, M. I. Rosli, E. H. Majlan, T. Husaini, S. K. Kamarudin, and W. R.W. Daud. 2016. "Overview Biohydrogen Technologies and Application in Fuel Cell Technology." *Renewable and Sustainable Energy Reviews* 66. Elsevier: 137–62. doi:10.1016/j.rser.2016.07.047.

Sagir, Emrah, Siamak Alipour, Kamal Elkahlout, Harun Koku, Ufuk Gunduz, Inci Eroglu, and Meral Yucel. 2017. "Scale-up Studies for Stable, Long-Term Indoor and Outdoor Production of Hydrogen by Immobilized *Rhodobacter Capsulatus*." *International Journal of Hydrogen Energy* 42 (36): 22743–55. doi:10.1016/j.ijhydene.2017.07.240.

Sagir, Emrah, Ebru Ozgur, Ufuk Gunduz, Inci Eroglu, and Meral Yucel. 2017. "Single-Stage Photofermentative Biohydrogen Production from Sugar Beet Molasses by Different Purple Non-Sulfur Bacteria." *Bioprocess and Biosystems Engineering*. Springer Berlin Heidelberg, 1–13. doi:10.1007/s00449-017-1815-x.

Sağır, Emrah. 2012. "Photobiological Hydrogen Production from Sugar Beet Molasses." *M.Sc. Thesis. Biochemistry Department, Middle East Technical University*, no. February. doi:10.1016/j.nbt.2012.08.109.

Sakurai, Hidehiro, Hajime Masukawa, Masaharu Kitashima, and Kazuhito Inoue. 2013. "Photobiological Hydrogen Production: Bioenergetics and Challenges for

- Its Practical Application.” *Journal of Photochemistry and Photobiology C: Photochemistry Reviews* 17. Elsevier B.V.: 1–25. doi:10.1016/j.jphotochemrev.2013.05.001.
- Sasikala, C H, C H V Ramana, and P Raghuveer Rao. 1995. “Regulation of Simultaneous Hydrogen Photoproduction during Growth by pH and Glutamate in *Rhodobacter Sphaeroides* O.U. 001.” *International Journal of Hydrogen Energy* 20 (2): 123–26.
- Sasikala, K., Ch V. Ramana, and P. Raghuveer Rao. 1991. “Environmental Regulation for Optimal Biomass Yield and Photoproduction of Hydrogen by *Rhodobacter Sphaeroides* O.U. 001.” *International Journal of Hydrogen Energy* 16 (9): 597–601. doi:10.1016/0360-3199(91)90082-T.
- Savasturk, D., E. Kayahan, and H. Koku. 2018. “Photofermentative Hydrogen Production from Molasses: Scale-up and Outdoor Operation at Low Carbon-to-Nitrogen Ratio.” *International Journal of Hydrogen Energy* 43 (26). doi:10.1016/j.ijhydene.2018.01.014.
- Shi, Xian Yang, and Han Qing Yu. 2006. “Continuous Production of Hydrogen from Mixed Volatile Fatty Acids with *Rhodospseudomonas Capsulata*.” *International Journal of Hydrogen Energy* 31 (12): 1641–47. doi:10.1016/j.ijhydene.2005.12.008.
- Shuler, Michael L., and Fikret Kargi. 2013. *Bioprocess Engineering*.
- Sinha, Pallavi, and Anjana Pandey. 2011. “An Evaluatie Report and Challenges for Fermentative Biohydrogen Production.” *International Journal of Hydrogen Energy* 36 (13). Elsevier Ltd: 7460–78. doi:10.1016/j.ijhydene.2011.03.077.
- Sözen, A, E Arcalioglu, M. Ozalp, and E. G. Kani. 2005. “Solar Energy Potential in Turkey.” *Applied Energy* 80: 367 – 381.
- Sveshnikov, D. A., N. V. Sveshnikova, K. K. Rao, and D. O. Hall. 1997. “Hydrogen Metabolism of Mutant Forms of *Anabaena Variabilis* in Continuous Cultures

- and under Nutritional Stress.” *FEMS Microbiology Letters* 147 (2): 297–301. doi:10.1016/S0378-1097(97)00005-0.
- Uffen, Robert L. 1976. “Anaerobic Growth of a Rhodopseudomonas Species in the Dark with Carbon Monoxide as Sole Carbon and Energy Substrate (Hydrogen Production/carbon Dioxide Production/facultative Methylophony)” 73 (9): 3298–3302. <https://www.pnas.org/content/pnas/73/9/3298.full.pdf>.
- Urbaniec, Krzysztof, and Robert Grabarczyk. 2014. “Hydrogen Production from Sugar Beet Molasses - A Techno-Economic Study.” *Journal of Cleaner Production* 65. Elsevier Ltd: 324–29. doi:10.1016/j.jclepro.2013.08.027.
- Uyar, Basar, Inci Eroglu, Meral Yücel, and Ufuk Gündüz. 2009. “Photofermentative Hydrogen Production from Volatile Fatty Acids Present in Dark Fermentation Effluents.” *International Journal of Hydrogen Energy* 34 (10): 4517–23. doi:10.1016/j.ijhydene.2008.07.057.
- Uyar, Basar, Inci Eroglu, Meral Yücel, Ufuk Gündüz, and Lemi Türker. 2007. “Effect of Light Intensity, Wavelength and Illumination Protocol on Hydrogen Production in Photobioreactors.” *International Journal of Hydrogen Energy* 32 (18): 4670–77. doi:10.1016/j.ijhydene.2007.07.002.
- Veziroğlu, T. Nejat, and Sümer Şahin. 2008. “21st Century’s Energy: Hydrogen Energy System.” *Energy Conversion and Management* 49 (7): 1820–31. doi:10.1016/j.enconman.2007.08.015.
- Vignais, Paulette M., Annette Colbeau, John C. Willison, and Yves Jouanneau. 1985. “Hydrogenase, Nitrogenase, and Hydrogen Metabolism in the Photosynthetic Bacteria.” *Advances in Microbial Physiology* 26 (January). Academic Press: 155–234. doi:10.1016/S0065-2911(08)60397-5.
- Wu, Ta Yeong, Jacqueline Xiao Wen Hay, Liu Bi Kong, Joon Ching Juan, and Jamaliah Md Jahim. 2012. “Recent Advances in Reuse of Waste Material as Substrate to Produce Biohydrogen by Purple Non-Sulfur (PNS) Bacteria.”

Renewable and Sustainable Energy Reviews 16 (5). Elsevier Ltd: 3117–22.
doi:10.1016/j.rser.2012.02.002.

Yokoi, H., R. Maki, J. Hirose, and S. Hayashi. 2002. “Microbial Production of Hydrogen from Starch-Manufacturing Wastes.” *Biomass and Bioenergy* 22 (5): 389–95. doi:10.1016/S0961-9534(02)00014-4.

Zhang, Chuan, Xun Zhu, Qiang Liao, Yongzhong Wang, Jun Li, Yudong Ding, and Hong Wang. 2010. “Performance of a Groove-Type Photobioreactor for Hydrogen Production by Immobilized Photosynthetic Bacteria.” *International Journal of Hydrogen Energy* 35 (11). Elsevier Ltd: 5284–92. doi:10.1016/j.ijhydene.2010.03.085.

Zhu, Heguang, Herbert H.P. Fang, Tong Zhang, and Lee A. Beaudette. 2007. “Effect of Ferrous Ion on Photo Heterotrophic Hydrogen Production by *Rhodobacter Sphaeroides*.” *International Journal of Hydrogen Energy* 32 (17): 4112–18. doi:10.1016/j.ijhydene.2007.06.010.

APPENDICES

A. Composition of the Growth Media

Table 0.1. *Growth Media Component*

Component	Amount
KH ₂ PO ₄	3 g/l
MgSO ₄ .7H ₂ O	0.5 g/l
CaCl ₂ .2H ₂ O	0.05 g/l
Vitamin Solution [1]	0.1 ml/l
Fe-Citrate Solution [2]	0.5 ml/l
Trace Element Solution [3]	0.1 ml/l
Na – Glutamate (10 mM)	1.85 g/l
Acetic acid (20 mM)	1.15 ml/l

Table 0.2. *Vitamin Solution Component*

Component	Amount
Thiamin Chloride	0.05 g
Hydrochloride Niacin (Nicotinic Acid)	0.05 g
D(+)-Biotin	1.5 mg

Table 0.3. *Trace Element Solution*

Component	Amount
HCl (25% v/v)	1 ml/l
ZnCl ₂	70 mg/l
MnCl ₂ .4H ₂ O	100 mg/l
H ₃ BO ₃	60 mg/l
CoCl ₂ .6H ₂ O	200 mg/l
CuCl ₂ .2H ₂ O	20 mg/l
NiCl ₂ .6H ₂ O	20 mg/l
NaMoO ₄ .2H ₂ O	40 mg/l

Table 0.4. *Iron Citrate Solution (50X)*

Component	Amount
Fe- Citrate	5 g

(1)(2)(3) Vitamins, trace elements and Fe-citrate were stored at 4°C in dark conditions and added to the media after autoclave (Table 0.1). pH was adjusted to around 6.5 with a 5 M NaOH solution and 30 mM potassium phosphate was used as a buffer solution before autoclaving the media. The components of the vitamin, trace elements and Fe-citrate solutions were shown in Table 0.2, Table 0.3 and Table 0.4, respectively.

B. Molasses Analyses

The molasses analysis (Table 0.5) was done by Ankara Sugar Factory[76]. The analysis of amino acid content and some elements of the molasses (Table 0.6 and Table 0.7) were conducted by Düzen Norwest Laboratory, Ankara[76].

Table 0.5. *Molasses analysis produced in Ankara Sugar Factory in 2013.*

Parameter	Method	Result
Refractometric dry matter	ICUMSA Method GC 4-13	82.36
Polar sugar (%)	British Sugar Method (CCS Handbook, 213, 2956)	51.52
pH	ICUMSA method GS 1/2/3/4/7(8-23)	62.55
Invert sugar ⁽¹⁾ (%)	Berlin Institute Method (ICUMSA Sugar Analysis, 55, 1979)	8.62
Invert sugar ⁽¹⁾ (g/100 Pol)		0.229
Sucrose (w/w %)	ICUMSA method GS 4/3-7) x 0.95	51.85
Total nitrogen (%)	British sugar method (CCS Handbook, 213, 2956)	1.7
Total nitrogen (g/100Bx)		2.06
Density (g/cm ³)	Density without air	1.272
Na (mg/kg)	Inductively coupled plasma- optical emission spectrometry method	6810
K (mg/kg)		34100
Ca (mg/kg)		2750
Mg (mg/kg)		7
Fe (mg/kg)		15
Mn (mg/kg)		16
Zn (mg/kg)		9

(1) Invert sugar: The mixture of glucose and fructose.

Table 0.6. *The content of amino acid in molasses*

Amino acids	Units	Results
Aspartic Acid	g/100g	0.358
Glutamic Acid	g/100g	2.541
Asparagine	g/100g	< 0.10 ⁽²⁾
Serine	g/100g	0.229
Histidine	g/100g	< 0.25 ⁽²⁾
Glycine	g/100g	0.192
Threonine	g/100g	0.066
Citrulline	g/100g	< 0.07 ⁽²⁾
Arginine	g/100g	0.08
Alanine	g/100g	0.252
Tyrosine	g/100g	0.191
Cystine	g/100g	< 0.30 ⁽²⁾
Valine	g/100g	0.139
Methionine	g/100g	< 0.12 ⁽²⁾
Tryptophan	g/100g	< 0.28 ⁽²⁾
Isoleucine	g/100g	0.202
Omithine	g/100g	< 0.29 ⁽²⁾
Lysine	g/100g	0.172
Hydrocproline	g/100g	< 0.27 ⁽²⁾
Sarcosine	g/100g	< 0.09 ⁽²⁾
Phenylalaine	g/100g	< 0.23 ⁽²⁾
Prolin	g/100g	0.234
Total Aminoacid	g/100g	4,7

(2) MDL: Method detection limit

Table 0.7. *Analysis of the some elements in molasses.*

Elements	Units	Results
Iron (Fe)	mg/kg	14.1
Molybdenum (Mo)	mg/kg	0.22
Sulphur (S)	g/kg	1.03
Potassium (K)	g/kg	35.6

C. HPLC Calibration Curve of Sucrose

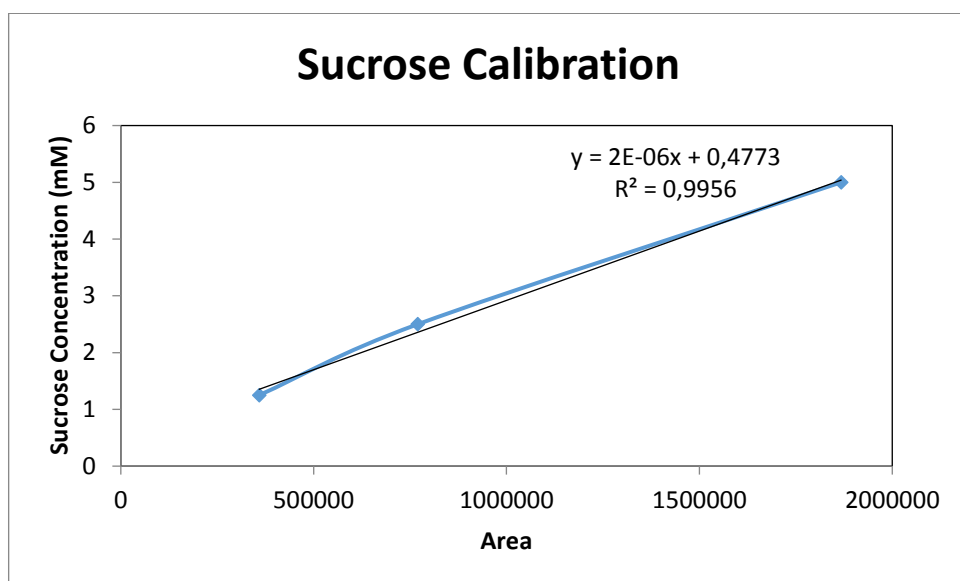


Figure 0.1. Calibration Curve for Sucrose

D. Sample HPLC and GC Chromatogram

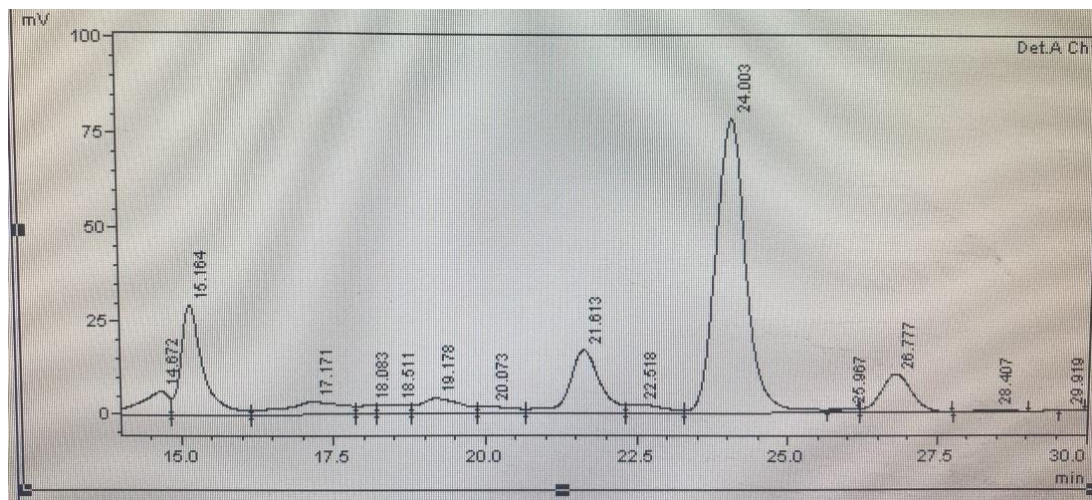


Figure 0.2. HPLC Chromatogram for organic acids. Retention times for lactic acid, acetic acid and formic acid are 21.6, 24.0 and 26.7 min, respectively (August 10th, 2016).

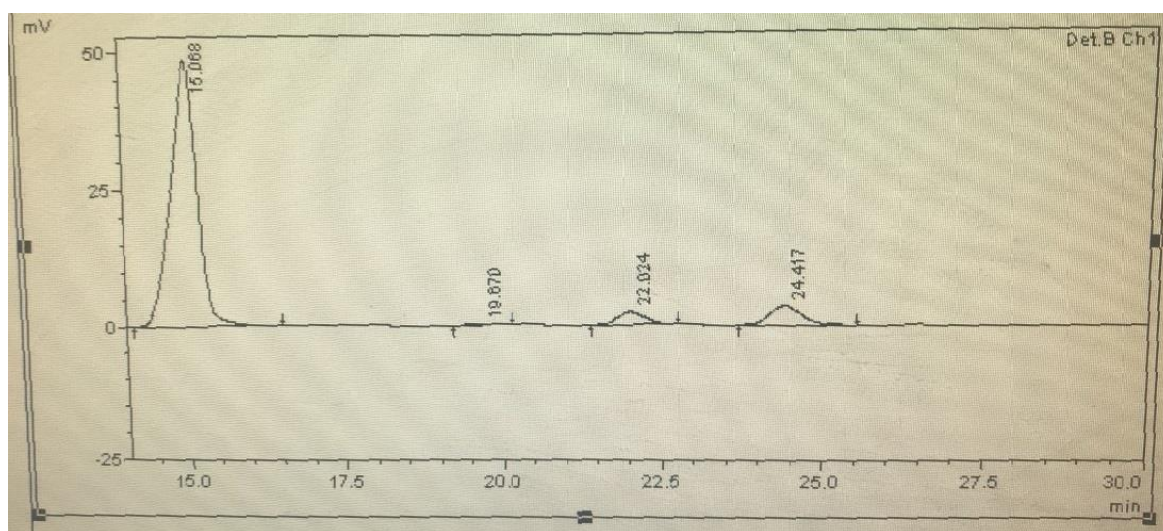


Figure 0.3. HPLC Chromatogram for sucrose. Retention time for sucrose is 15.0 min (August 10th, 2016).

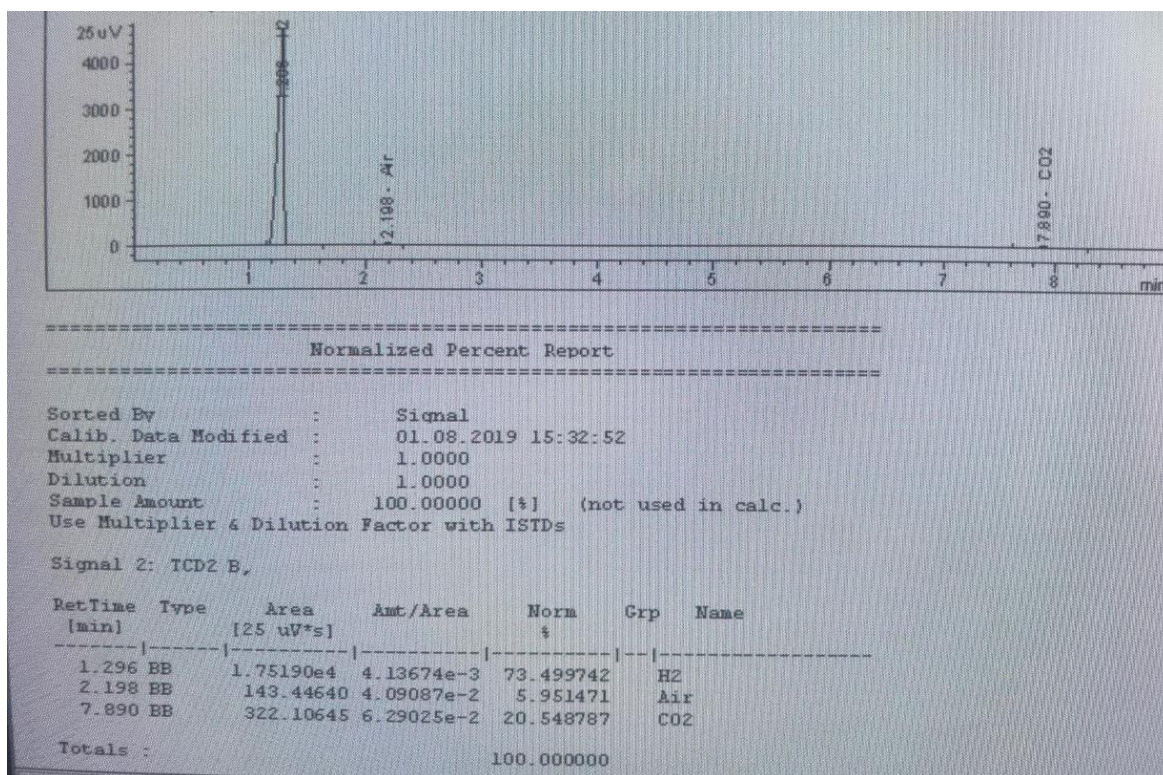


Figure 0.4. GC Chromatogram for produced biogas (August 10th, 2016)

E. Indoor and Outdoor Experimental Data

a. HPLC DATA

Table 0.8. *Daily variation in total and individual organic acids and sugar (glucose, fructose or sucrose) concentrations for indoor and outdoor experiments.*

Run	Day	Lactic Acid (mM)	Formic Acid (mM)	Acetic Acid (mM)	Sugar (mM)	Total Organic Acid
R1 (10 mM fructose)	0	0.79	0.73	0.84	10.00	2.36
	1	1.21	2.04	0.98	3.35	4.22
	2	0.77	2.33	0.27	2.16	3.36
	3	0.77	2.60	0.14	1.48	3.51
	4	0.67	2.62	0.11	1.02	3.40
	5	0.95	2.98	0.17	0.62	4.11
	6	0.59	2.39	0.16	0.38	3.14
	7	0.61	2.43	0.09	0.38	3.13
	8	0.50	2.14	0.16	0.34	2.81
	9	0.52	2.10	0.14	0.32	2.75
R2 (10 mM glucose)	0	1.87	0.00	0.00	10.00	1.87
	1	1.46	2.29	3.55	9.12	7.31
	2	1.86	4.09	3.41	7.01	9.37
	3	1.77	5.41	3.26	4.23	10.44
	4	1.61	5.98	2.60	0.89	10.19
	5	2.11	7.43	2.71	0.09	12.24
	6	1.78	6.74	1.75	0.07	10.27
	7	1.60	6.42	0.43	0.09	8.45
	8	1.18	5.08	0.02	0.07	6.28
	9	1.63	6.21	0.02	0.00	7.85
R3 (30 mM fructose)	0	3.33	3.56	2.15	30.00	9.03
	1	1.80	1.72	1.51	30.00	5.03
	2	2.22	2.09	2.08	27.30	6.39
	3	2.26	1.89	2.45	26.19	6.60
	4	2.20	2.51	1.73	22.26	6.44
	5	1.65	4.01	1.12	13.65	6.78
	6	1.65	4.01	1.12	13.12	6.78
	7	1.53	5.53	0.18	12.22	7.24
	8	1.50	5.41	0.08	8.59	7.00
	9	2.11	6.79	0.25	6.03	9.15

R4 (30 mM glucose)	0	4.74	2.88	1.93	30.00	9.54
	1	3.37	1.29	2.50	29.10	7.16
	2	3.49	2.96	4.86	21.08	11.31
	3	4.33	9.67	7.61	21.72	21.60
	4	4.09	11.73	10.03	20.52	25.86
	5	3.29	10.78	8.22	16.15	22.29
	6	3.35	11.85	9.88	16.74	25.08
	7	2.91	10.38	8.25	13.88	21.55
	8	3.61	11.35	8.16	14.13	23.12
	9	2.84	9.89	7.48	13.37	20.21
R5 (50 mM fructose)	0	0.06	0.05	0.07	50.00	0.19
	1	2.76	3.86	2.50	38.71	9.11
	2	2.77	2.63	2.54	39.49	7.94
	3	1.53	1.19	1.11	40.04	3.82
	4	2.87	2.52	2.85	40.60	8.24
	5	2.65	2.40	2.57	39.06	7.62
	6	2.63	2.26	2.93	36.48	7.83
	7	2.34	1.99	2.39	33.78	6.71
	8	2.02	2.25	1.60	28.58	5.87
	9	2.13	6.84	1.69	22.43	10.66
R6 (50 mM glucose)	0	5.39	4.62	1.80	50.00	11.81
	1	5.26	3.26	3.04	50.93	11.56
	2	5.42	3.27	1.15	49.57	9.83
	3	4.98	3.01	2.27	42.37	10.26
	4	5.05	3.45	2.50	41.12	11.00
	5	4.65	4.02	1.29	38.31	9.95
	6	2.70	4.43	2.14	23.76	9.27
	7	3.97	11.33	2.82	33.02	18.12
	8	2.38	10.55	1.91	32.07	14.84
	9	3.43	12.48	3.26	29.09	19.17
Outdoor (5mM sucrose)	0	0.00	0.00	0.00	5.00	0
	1	0.46	1.39	0.50	4.16	2.4
	2	0.81	5.99	0.77	3.84	7.6
	3	0.11	9.18	0.05	3.33	9.3
	4	0.18	9.98	0.34	3.28	10.5
	5	0.97	6.82	0.29	3.24	8.1
	6	0.29	9.16	0.12	3.23	9.6
	7	0.00	11.86	3.80	3.73	15.7
	8	0.08	8.67	0.99	2.91	9.7

	9	0.37	9.00	0.90	2.92	10.3
	10	0.03	8.79	0.97	2.91	9.8
	11	0.05	8.69	0.89	3.32	9.6
	12	1.10	10.30	2.37	3.37	13.8
	13	0.38	9.30	3.56	3.32	13.2
	14	0.38	8.90	4.03	3.34	13.3
	15	0.16	6.20	3.94	3.33	10.3
	16	0.20	4.87	7.85	2.95	12.9
	17	0.62	5.87	7.04	3.06	13.5

b. UV Spectrophotometer Data

Table 0.9. Daily variation in OD and cell concentration for indoor and outdoor experiments.

	Day	OD1	OD2	OD (avg.)	Cell Conc. gdcw/Lc
R1 (10 mM fructose)	0	0.278	0.290	0.284	0.132
	1	1.034	0.935	0.985	0.458
	2	1.355	1.353	1.354	0.630
	4	1.145	1.110	1.128	0.525
	5	1.157	1.133	1.145	0.533
	6	1.126	1.092	1.109	0.516
	7	1.135	1.080	1.108	0.516
	8	1.101	1.066	1.084	0.504
	9	1.063	1.055	1.059	0.493
	12	1.079	1.011	1.045	0.487
	13	1.010	0.958	0.984	0.458
	14	1.105	1.041	1.073	0.500
R2 (10 mM glucose)	0	0.285	0.268	0.277	0.129
	1	0.816	0.691	0.754	0.351
	2	1.210	1.208	1.209	0.563
	3	1.097	1.034	1.066	0.496
	4	1.064	1.147	1.106	0.515
	5	0.970	1.012	0.991	0.461
	6	0.822	0.900	0.861	0.401
	7	0.844	0.829	0.837	0.389
	8	0.803	0.804	0.804	0.374

	9	0.802	0.778	0.790	0.368
R3 (30 mM fructose)	0	0.256	0.248	0.252	0.117
	1	0.361	0.336	0.349	0.162
	2	0.306	0.294	0.300	0.140
	4	0.358	0.277	0.318	0.148
	5	0.799	0.719	0.759	0.353
	6	1.042	1.274	1.158	0.539
	7	1.121	1.464	1.293	0.602
	8	1.075	1.441	1.258	0.586
	9	1.112	1.421	1.267	0.590
	12	1.230	1.230	1.230	0.573
	13	1.294	1.473	1.384	0.644
	14	1.243	1.505	1.374	0.640
R4 (30 mM fructose)	0	0.314	0.283	0.30	0.139
	1	0.504	0.435	0.47	0.219
	2	0.862	0.846	0.85	0.398
	3	1.186	1.161	1.17	0.546
	4	1.301	1.264	1.28	0.597
	5	1.22	1.203	1.21	0.564
	6	1.221	1.186	1.20	0.560
	7	1.187	1.202	1.19	0.556
	8	1.149	1.141	1.15	0.533
	9	1.094	1.039	1.07	0.497
R5 (50 mM glucose)	0	0.279	0.274	0.277	0.129
	1	0.324	0.346	0.335	0.156
	2	0.294	0.291	0.293	0.136
	4	0.243	0.238	0.241	0.112
	5	0.239	0.226	0.233	0.108
	6	0.216	0.210	0.213	0.099
	7	0.215	0.198	0.207	0.096
	8	0.238	0.209	0.224	0.104
	9	0.702	0.212	0.457	0.213
	12	0.389	0.389	0.389	0.181
	13	1.352	0.468	0.910	0.424
	14	1.436	0.554	0.995	0.463
R6	0	0.313	0.303	0.308	0.143

(50 mM glucose)	1	0.367	0.375	0.371	0.173
	2	0.316	0.355	0.336	0.156
	3	0.323	0.381	0.352	0.164
	4	0.475	0.456	0.466	0.217
	5	0.760	0.744	0.752	0.350
	6	0.843	0.914	0.879	0.409
	7	0.969	0.893	0.931	0.433
	8	1.010	0.983	0.997	0.464
	9	0.931	0.879	0.905	0.421
Outdoor (5 mM sucrose)	0	0.500	0.500	0.500	0.233
	0.5	1.097	1.081	1.089	0.507
	1	1.860	1.900	1.880	0.875
	1.5	2.118	2.100	2.109	0.982
	2	2.262	2.198	2.230	1.038
	2.5	2.473	2.208	2.341	1.090
	3	2.312	2.133	2.223	1.035
	3.5	2.152	2.099	2.126	0.990
	4	2.352	2.118	2.235	1.041
	4.5	2.154	2.256	2.205	1.027
	5	2.117	2.392	2.255	1.050
	5.5	2.102	2.071	2.087	0.971
	6	2.094	2.072	2.083	0.970
	6.5	2.345	2.098	2.222	1.034
	7	2.069	2.144	2.107	0.981
	7.5	2.094	2.084	2.089	0.973
	8	2.097	2.103	2.100	0.978
	8.5	2.118	2.120	2.119	0.987
	9	2.191	2.061	2.126	0.990
	9.5	2.150	2.067	2.109	0.982
	10	2.085	2.103	2.094	0.975
	10.5	2.174	2.080	2.127	0.990
	11	2.122	2.067	2.095	0.975
	11.5	2.102	2.133	2.118	0.986
	12	2.122	2.191	2.157	1.004
	12.5	2.115	2.141	2.128	0.991
	13	2.171	2.096	2.134	0.993
	13.5	2.205	2.081	2.143	0.998

	14	2.163	2.197	2.180	1.015
	14.5	2.188	2.191	2.190	1.019
	15	2.116	2.102	2.109	0.982
	15.5	2.106	2.098	2.102	0.979
	16	2.128	2.092	2.110	0.982
	16.5	2.182	2.205	2.194	1.021
	17	2.279	2.235	2.257	1.051

c. pH Data

Table 0.10. *Daily variation in pH for indoor and outdoor experiments*

Run	Day	pH1	pH2	pH3*	pH (avg.)
R1 (10 mM fructose)	0	7.11	7.12		7.12
	1	6.94	6.96		6.95
	2	6.93	6.92		6.93
	4	6.83	6.83		6.83
	5	6.80	6.80		6.80
	6	6.83	6.82		6.83
	7	6.74	6.79		6.77
	8	6.77	6.80		6.79
	9	6.86	6.88		6.87
	12	7.04	7.12		7.08
	13	6.86	6.87		6.87
	14	6.81	6.80		6.81
R2 (10 mM glucose)	0	7.26	7.31		7.29
	1	6.97	7.02		7.00
	2	6.96	6.95		6.96
	3	6.98	6.98		6.98
	4	6.77	6.81		6.79
	5	6.61	6.60		6.61
	6	6.67	6.62		6.65
	7	6.71	6.76		6.74
	8	6.74	6.70		6.72
	9	6.70	6.64		6.67
R3 (30 mM)	0	6.90	6.89		6.90
	1	6.88	6.94		6.91
	2	6.83	6.84		6.84

fructose)	4	6.76	6.77		6.77
	5	6.65	6.69		6.67
	6	6.42	6.53		6.48
	7	6.17	6.15		6.16
	8	6.11	6.05		6.08
	9	6.01	6.02		6.02
	12	6.09	6.09		6.09
	13	6.10	5.95		6.03
	14	5.95	5.92		5.94
R4 (30 mM glucose)	0	7.00	7.00		7.00
	1	6.93	6.98		6.96
	2	6.69	6.69		6.69
	3	6.56	6.50		6.53
	4	6.32	6.34		6.33
	5	6.26	6.23		6.25
	6	6.16	6.11		6.14
	7	6.25	6.27		6.26
	8	6.38	6.35		6.37
	9	6.28	6.21		6.25
R5 (50 mM fructose)	0	6.70	6.69		6.70
	1	6.69	6.69		6.69
	2	6.65	6.66		6.66
	4	6.65	6.64		6.65
	5	6.65	6.64		6.65
	6	6.61	6.63		6.62
	7	6.56	6.58		6.57
	8	6.56	6.59		6.58
	9	6.61	6.60		6.61
	12	6.81	6.81		6.81
	13	5.85	6.57		6.21
	14	5.84	6.50		6.17
R6 (50 mM glucose)	0	6.92	6.92		6.92
	1	6.91	6.89		6.90
	2	6.81	6.83		6.82
	3	6.75	6.74		6.75
	4	6.64	6.65		6.65
	5	6.42	6.41		6.42
	6	6.38	6.30		6.34
	7	6.22	6.16		6.19

	8	6.07	6.08		6.08
	9	5.99	6.00		6.00
Outdoor (5 mM sucrose)	0	7.50	7.50	7.50	7.5
	0.5	6.88	7.00	7.00	7.0
	1	6.90	6.98	7.05	7.0
	1.5	6.55	6.57	6.59	6.6
	2	6.50	6.57	6.60	6.6
	2.5	6.58	6.60	6.64	6.6
	3	6.54	6.53	6.51	6.5
	3.5	6.64	6.58	6.63	6.6
	4	6.55	6.54	6.55	6.5
	4.5	6.64	6.61	6.61	6.6
	5	6.55	6.55	6.62	6.6
	5.5	6.59	6.51	6.54	6.5
	6	6.60	6.57	6.58	6.6
	6.5	6.60	6.61	6.58	6.6
	7	6.56	6.49	6.62	6.6
	7.5	6.67	6.66	6.60	6.6
	8	6.66	6.63	6.62	6.6
	8.5	6.66	6.64	6.73	6.7
	9	6.62	6.67	6.69	6.7
	9.5	6.72	6.67	6.67	6.7
	10	6.63	6.60	6.72	6.7
	10.5	6.73	6.66	6.69	6.7
	11	6.65	6.63	6.67	6.7
	11.5	6.37	6.36	6.38	6.4
	12	6.42	6.38	6.40	6.4
	12.5	6.46	6.49	6.44	6.5
	13	6.45	6.40	6.44	6.4
	13.5	6.46	6.49	6.44	6.5
	14	6.53	6.53	6.50	6.5
	14.5	6.62	6.52	6.56	6.6
	15	6.59	6.56	6.59	6.6
	15.5	6.65	6.65	6.69	6.7
	16	6.60	6.65	6.62	6.6
	16.5	6.53	6.62	6.58	6.6
	17	6.33	6.36	6.29	6.3

*Only for the outdoor experiment pH3 data was taken.

d. Gas Chromatography Data

Table 0.11. *Biogas production during (a) indoor and (b) outdoor experiments.*

(a)

	Total H ₂ produced (mmol)	Max. H ₂ productivity [mol/(m ³ .h)]
R1 (10 mM fructose)	0.80	0.40
R2 (10 mM glucose)	1.25	0.46
R3 (30 mM fructose)	1.00	0.27
R4 (30 mM glucose)	1.51	0.60
R5 (50 mM fructose)	0.62	0.35
R6 (50 mM glucose)	1.43	0.28

(b)

Day	Daily gas Produced (avg.) (mL)	H ₂ %	Total H ₂ produced (mmol)	H ₂ productivity [mol/(m ³ .h)]
0	0	0.00	0.00	0.000
1	7750	93.60	223.71	0.466
2	6800	82.12	399.80	0.367
3	3800	78.32	500.30	0.209
4	1350	82.50	534.33	0.071
5	100	100.00	537.35	0.006
6	150	100.00	539.12	0.004
7	150	94.13	541.84	0.006
8	500	82.79	552.69	0.023
9	675	100.00	564.23	0.024
10	300	84.84	569.37	0.011
11	100	93.46	569.88	0.001
12	0	0.00	569.88	0.000
13	250	93.17	572.31	0.005
14	125	94.06	573.65	0.003
15	250	91.95	574.63	0.002
16	100	70.76	576.57	0.004
17	10	66.70	576.78	0.000

*The rest of the biogas is CO₂.

e. Weather Station Data

Table 0.12. Data taken from the weather station for the outdoor experiment (8/13/2016).

Time	Temp. (Outside)	Rain	Rate of Rain	Solar Radiation (W/m ²)
12:00:00 AM	28.4	0	0	0
12:05:00 AM	28.4	0	0	0
12:10:00 AM	28.4	0	0	0
12:15:00 AM	28.2	0	0	0
12:20:00 AM	28.1	0	0	0
12:25:00 AM	27.9	0	0	0
12:30:00 AM	27.8	0	0	0
12:35:00 AM	27.7	0	0	0
12:40:00 AM	27.4	0	0	0
12:45:00 AM	27.2	0	0	0
12:50:00 AM	26.8	0	0	0
12:55:00 AM	26.2	0	0	0
1:00:00 AM	25.7	0	0	0
1:05:00 AM	25.3	0	0	0
1:10:00 AM	25	0	0	0
1:15:00 AM	24.9	0	0	0
1:20:00 AM	24.7	0	0	0
1:25:00 AM	24.4	0	0	0
1:30:00 AM	24.1	0	0	0
1:35:00 AM	23.8	0	0	0
1:40:00 AM	23.6	0	0	0
1:45:00 AM	23.3	0	0	0
1:50:00 AM	23	0	0	0
1:55:00 AM	22.7	0	0	0
2:00:00 AM	22.6	0	0	0
2:05:00 AM	22.3	0	0	0
2:10:00 AM	22.1	0	0	0
2:15:00 AM	21.9	0	0	0
2:20:00 AM	21.8	0	0	0
2:25:00 AM	21.7	0	0	0
2:30:00 AM	21.5	0	0	0
2:35:00 AM	21.4	0	0	0
2:40:00 AM	21.2	0	0	0
2:45:00 AM	21.1	0	0	0
2:50:00 AM	20.9	0	0	0
2:55:00 AM	20.8	0	0	0
3:00:00 AM	20.8	0	0	0

3:05:00 AM	20.9	0	0	0
3:10:00 AM	20.9	0	0	0
3:15:00 AM	20.9	0	0	0
3:20:00 AM	20.9	0	0	0
3:25:00 AM	21	0	0	0
3:30:00 AM	21.3	0	0	0
3:35:00 AM	21.6	0	0	0
3:40:00 AM	21.8	0	0	0
3:45:00 AM	21.9	0	0	0
3:50:00 AM	21.9	0	0	0
3:55:00 AM	21.7	0	0	0
4:00:00 AM	21.6	0	0	0
4:05:00 AM	21.6	0	0	0
4:10:00 AM	21.5	0	0	0
4:15:00 AM	21.3	0	0	0
4:20:00 AM	21.2	0	0	0
4:25:00 AM	21.3	0	0	0
4:30:00 AM	21.3	0	0	0
4:35:00 AM	21.2	0	0	0
4:40:00 AM	20.9	0	0	0
4:45:00 AM	20.7	0	0	0
4:50:00 AM	21	0	0	0
4:55:00 AM	21.5	0	0	0
5:00:00 AM	22.1	0	0	0
5:05:00 AM	22.6	0	0	0

8/13/2016	5:10:00 AM	22.6	0	0	0
8/13/2016	5:15:00 AM	22.4	0	0	0
8/13/2016	5:20:00 AM	22.2	0	0	0
8/13/2016	5:25:00 AM	21.9	0	0	0
8/13/2016	5:30:00 AM	21.7	0	0	0
8/13/2016	5:35:00 AM	21.6	0	0	0
8/13/2016	5:40:00 AM	21.4	0	0	0
8/13/2016	5:45:00 AM	21.2	0	0	0
8/13/2016	5:50:00 AM	21.1	0	0	0
8/13/2016	5:55:00 AM	20.9	0	0	0
8/13/2016	6:00:00 AM	20.8	0	0	0
8/13/2016	6:05:00 AM	20.8	0	0	0
8/13/2016	6:10:00 AM	20.7	0	0	0
8/13/2016	6:15:00 AM	20.7	0	0	6
8/13/2016	6:20:00 AM	20.6	0	0	8
8/13/2016	6:25:00 AM	20.5	0	0	12
8/13/2016	6:30:00 AM	20.3	0	0	13
8/13/2016	6:35:00 AM	20.1	0	0	16
8/13/2016	6:40:00 AM	19.8	0	0	19
8/13/2016	6:45:00 AM	19.8	0	0	23
8/13/2016	6:50:00 AM	19.9	0	0	29
8/13/2016	6:55:00 AM	19.9	0	0	33
8/13/2016	7:00:00 AM	19.7	0	0	33
8/13/2016	7:05:00 AM	19.2	0	0	33
8/13/2016	7:10:00 AM	18.7	0	0	37
8/13/2016	7:15:00 AM	18.3	0	0	50
8/13/2016	7:20:00 AM	18	0	0	85
8/13/2016	7:25:00 AM	17.7	0	0	121
8/13/2016	7:30:00 AM	17.6	0	0	198
8/13/2016	7:35:00 AM	17.3	0	0	195
8/13/2016	7:40:00 AM	17.2	0	0	164
8/13/2016	7:45:00 AM	17.1	0	0	153
8/13/2016	7:50:00 AM	17.1	0	0	186
8/13/2016	7:55:00 AM	17.1	0	0	210
8/13/2016	8:00:00 AM	17.1	0	0	195
8/13/2016	8:05:00 AM	16.9	0	0	173
8/13/2016	8:10:00 AM	16.9	0	0	144
8/13/2016	8:15:00 AM	17.1	0	0	155
8/13/2016	8:20:00 AM	17.1	0	0	181
8/13/2016	8:25:00 AM	16.8	0	0	199
8/13/2016	8:30:00 AM	16.6	0	0	210
8/13/2016	8:35:00 AM	16.6	0	0	252
8/13/2016	8:40:00 AM	16.4	0	0	275
8/13/2016	8:45:00 AM	16.3	0	0	254
8/13/2016	8:50:00 AM	16.3	0	0	235
8/13/2016	8:55:00 AM	16.2	0	0	262
8/13/2016	9:00:00 AM	16.3	0	0	288
8/13/2016	9:05:00 AM	16.3	0	0	343
8/13/2016	9:10:00 AM	16.2	0	0	395
8/13/2016	9:15:00 AM	16.2	0	0	437
8/13/2016	9:20:00 AM	16.1	0	0	216
8/13/2016	9:25:00 AM	16.1	0	0	174
8/13/2016	9:30:00 AM	16.2	0	0	191
8/13/2016	9:35:00 AM	16.2	0	0	607
8/13/2016	9:40:00 AM	16.4	0	0	507
8/13/2016	9:45:00 AM	16.6	0	0	281
8/13/2016	9:50:00 AM	16.6	0	0	206
8/13/2016	9:55:00 AM	16.5	0	0	409
8/13/2016	10:00:00 AM	16.3	0	0	171
8/13/2016	10:05:00 AM	16.2	0	0	138
8/13/2016	10:10:00 AM	16.1	0	0	356
8/13/2016	10:15:00 AM	16.1	0	0	677
8/13/2016	10:20:00 AM	16.1	0	0	675

10:25:00 AM	16	0	0	655
10:30:00 AM	16.1	0	0	741
10:35:00 AM	16.2	0	0	343
10:40:00 AM	16.4	0	0	527
10:45:00 AM	16.6	0	0	444
10:50:00 AM	16.7	0	0	483
10:55:00 AM	16.8	0	0	548
11:00:00 AM	17.1	0	0	619
11:05:00 AM	17.4	0	0	610
11:10:00 AM	17.6	0	0	526
11:15:00 AM	17.8	0	0	343
11:20:00 AM	17.9	0	0	257
11:25:00 AM	18.1	0	0	244
11:30:00 AM	18.2	0	0	317
11:35:00 AM	18.4	0	0	298
11:40:00 AM	19	0	0	264
11:45:00 AM	19.8	0	0	224
11:50:00 AM	20.4	0	0	229
11:55:00 AM	21.1	0	0	214
12:00:00 PM	21.6	0	0	212
12:05:00 PM	21.9	0.2	0	272
12:10:00 PM	22.1	0	0	358
12:15:00 PM	22.3	0	0	424
12:20:00 PM	22.7	0	0	383
12:25:00 PM	22.9	0	0	326
12:30:00 PM	22.9	0	0	348
12:35:00 PM	22.9	0	0	441
12:40:00 PM	23.1	0	0	502
12:45:00 PM	23.4	0	0	759
12:50:00 PM	23.9	0	0	442
12:55:00 PM	23.9	0	0	1065
1:00:00 PM	23.7	0	0	392
1:05:00 PM	23.7	0	0	1051
1:10:00 PM	23.9	0	0	350
1:15:00 PM	24.2	0	0	388
1:20:00 PM	24.4	0	0	404
1:25:00 PM	24.6	0	0	452
1:30:00 PM	24.7	0	0	456
1:35:00 PM	25.3	0	0	420
1:40:00 PM	25.7	0	0	565
1:45:00 PM	25.6	0	0	814
1:50:00 PM	25.6	0	0	807
1:55:00 PM	25.7	0	0	821
2:00:00 PM	25.4	0	0	853
2:05:00 PM	25.4	0	0	853
2:10:00 PM	25.9	0	0	326
2:15:00 PM	26.2	0	0	421
2:20:00 PM	26.4	0	0	334
2:25:00 PM	26.7	0	0	392
2:30:00 PM	26.7	0	0	478
2:35:00 PM	26.7	0	0	639
2:40:00 PM	27	0	0	840
2:45:00 PM	27.2	0	0	802
2:50:00 PM	27.2	0	0	784
2:55:00 PM	27.4	0	0	780
3:00:00 PM	27.7	0	0	781
3:05:00 PM	27.9	0	0	813
3:10:00 PM	28.4	0	0	369
3:15:00 PM	28.2	0	0	944
3:20:00 PM	27.8	0	0	966
3:25:00 PM	27.8	0	0	606
3:30:00 PM	27.9	0	0	462
3:35:00 PM	28.3	0	0	540

3:40:00 PM	28.9	0	0	697
3:45:00 PM	29.6	0	0	645
3:50:00 PM	29.6	0	0	320
3:55:00 PM	29.1	0	0	342
4:00:00 PM	29.4	0	0	321
4:05:00 PM	29.8	0	0	344
4:10:00 PM	29.8	0	0	549
4:15:00 PM	30.2	0	0	329
4:20:00 PM	30.3	0	0	282
4:25:00 PM	30.4	0	0	223
4:30:00 PM	30.2	0	0	208
4:35:00 PM	30.2	0	0	207
4:40:00 PM	30.1	0	0	316
4:45:00 PM	30.3	0	0	489
4:50:00 PM	30.3	0	0	397
4:55:00 PM	30.4	0	0	456
5:00:00 PM	30.7	0	0	447
5:05:00 PM	30.7	0	0	454
5:10:00 PM	30.6	0	0	412
5:15:00 PM	30.7	0	0	392
5:20:00 PM	31.1	0	0	340
5:25:00 PM	31.3	0	0	352
5:30:00 PM	31.7	0	0	327
5:35:00 PM	31.8	0	0	315
5:40:00 PM	31.4	0	0	304
5:45:00 PM	31.3	0	0	293
5:50:00 PM	31.8	0	0	277
5:55:00 PM	31.9	0	0	227
6:00:00 PM	31.7	0	0	254
6:05:00 PM	32.1	0	0	235
6:10:00 PM	32.6	0	0	150
6:15:00 PM	32.6	0	0	105
6:20:00 PM	32.6	0	0	67
6:25:00 PM	32.1	0	0	63
6:30:00 PM	32.1	0	0	57
6:35:00 PM	32.7	0	0	64
6:40:00 PM	32.9	0	0	50
6:45:00 PM	32.8	0	0	44
6:50:00 PM	32.9	0	0	58
6:55:00 PM	32.9	0	0	57
7:00:00 PM	32.3	0	0	43
7:05:00 PM	32.1	0	0	30
7:10:00 PM	32.2	0	0	33
7:15:00 PM	32.6	0	0	28
7:20:00 PM	32.5	0	0	17
7:25:00 PM	32.3	0	0	10
7:30:00 PM	32.1	0	0	5
7:35:00 PM	32.1	0	0	0
7:40:00 PM	32.5	0	0	0
7:45:00 PM	32.9	0	0	0
7:50:00 PM	33.1	0	0	0
7:55:00 PM	33.2	0	0	0
8:00:00 PM	33.3	0	0	0
8:05:00 PM	32.8	0	0	0
8:10:00 PM	31.9	0	0	0
8:15:00 PM	31.4	0	0	0
8:20:00 PM	31.1	42401	40.6	0
8:25:00 PM	31	3	57.8	0
8:30:00 PM	30.9	42522	33.2	0
8:35:00 PM	30.8	0.4	42593	0
8:40:00 PM	30.7	0.6	42407	0
8:45:00 PM	30.3	0.2	42405	0
8:50:00 PM	29.7	0.4	4	0

8:55:00 PM	29.2	0	2	0
9:00:00 PM	28.9	0.2	2	0
9:05:00 PM	28.9	0	42461	0
9:10:00 PM	28.9	0	1	0
9:15:00 PM	29	0	0	0
9:20:00 PM	29.6	0	0	0
9:25:00 PM	30.1	0	0	0
9:30:00 PM	30.6	0	0	0
9:35:00 PM	31.2	0	0	0
9:40:00 PM	31.7	0	0	0
9:45:00 PM	32	0	0	0
9:50:00 PM	31.9	0	0	0
9:55:00 PM	31.9	0	0	0
10:00:00 PM	32.1	0	0	0
10:05:00 PM	32.1	0	0	0
10:10:00 PM	32.2	0	0	0
10:15:00 PM	32.2	0	0	0
10:20:00 PM	31.8	0	0	0
10:25:00 PM	31.7	0	0	0
10:30:00 PM	31.5	0	0	0
10:35:00 PM	31.4	0.2	0	0
10:40:00 PM	31.2	0.2	2	0
10:45:00 PM	30.9	0	42522	0
10:50:00 PM	30.7	0.2	42522	0
10:55:00 PM	30.6	0	42401	0
11:00:00 PM	30	0	1	0
11:05:00 PM	29.4	0	0	0
11:10:00 PM	29.3	0.2	0	0
11:15:00 PM	29.4	0	0	0
11:20:00 PM	29.5	0	0	0
11:25:00 PM	29.4	0	0	0
11:30:00 PM	29.3	0	0	0
11:35:00 PM	29.2	0	0	0
11:40:00 PM	29	0	0	0
11:45:00 PM	28.9	0	0	0
11:50:00 PM	28.7	0.2	0	0
11:55:00 PM	28.6	0.2	2	0